ABSTRACT

Bromate is formed by the ozonation of bromide-containing water. Bromate is categorized as a probable human carcinogen. The proposed Disinfectants/Disinfection By-Products (D/DBP) Rule contains an MCL (maximum contaminant level) of 10 µg/L for bromate. The World Health Organization (WHO) has a recommended limit for bromate of 25 µg/L.

In this research, bromate formation was examined on a dynamic basis, in a continuous-flow, completely-mixed ozonation reactor. Bromate formation was investigated in model waters as a function of ozone dose, pH, bromide concentration, total organic carbon concentration, and inorganic carbon concentration. Chemical additions of ammonia, tertiary butyl alcohol (a hydroxyl radical scavenger), and hydrogen peroxide were also examined to assess their impact on bromate formation. The source of organic material for these studies was hydrophobic organic carbon extracted from the Kralingen Plant of Water Supply Company Europoort in Rotterdam in The Netherlands. The extract was provided by KIWA, the sponsors of this research, because of their concern regarding bromate formation in Dutch waterworks employing ozonation.

Synthetic waters with the desired water quality characteristics were ozonated in a 500-mL completely-mixed flow reactor with a hydraulic residence time of ten minutes. Various ozone doses were applied to achieve effluent dissolved ozone residuals of 0.05 to 1.0 mg/L. The effluent was analyzed to determine bromate concentrations corresponding to these ozone residuals. The influent baseline conditions for the experiments were pH 7.0, 2.5 mg/L TOC, 300 µg/L Br^-, and 1 mM carbonate. The range of variations for the water quality parameters included: influent pH from 6.0 to 8.3, total organic carbon concentrations from 0.0 to 5.0 mg/L as C, bromide ion concentrations from 50 to 500 µg/L, and carbonate concentrations from 0.0 to 2.0 mM. The hydraulic residence time was varied from 2.0 to 20 minutes and the gas flow rate was investigated at 100 mL/min and 395 mL/min.

The results of this study indicate that bromate formation increased with increasing pH. For any given ozone dose, the formation of bromate was found to be enhanced with increasing influent Br^- concentration and carbonate concentration. As TOC concentration increased, the organic matter created an ozone demand that resulted in a decreased formation of bromate. The addition of t-butanol provided for both an increase in dissolved ozone residual and an appreciable decrease in bromate production for all ozone doses tested. The impact of ammonia was found to be pH-specific, where ammonia additions decreased bromate formation at a pH of 8.3 while addition of ammonia did not affect bromate formation at pH 7.0. Additionally, as the liquid flow rate increased, dissolved ozone residuals increased, but with lower bromate production. A decrease in the gas flow rate also provided increased dissolved ozone residuals and partial pressures and decreased bromate production.

Effluent ozone residuals and bromate concentrations appeared to follow an exponential increase with increasing ozone dose. Exponential models were fitted to the experimental data for illustrative purposes and were used to discuss the implications of the experimental results to ozonation in practice. The results show that under the best conditions, i.e., warm water temperatures and 0.5 and 2.0-log inactivation of *Giardia* and viruses, respectively, the USEPA's MCL of 10 µg/L for bromate could be met for waters with a wide range of water quality characteristics. When 0.5-log inactivation of *Cryptosporidium* at cold water temperatures are considered, bromate formation significantly exceeds the USEPA's MCL and the WHO's suggested levels for bromate under a number of water quality conditions.

TABLE OF CONTENTS

List of Figures

LIST OF FIGURES (CONTD.)

List of Figures (Contd.)

List of Tables

List of Tables (Contd.)

List of Abbreviations

CT	Concentration x Time
D/DBP	Disinfectants/Disinfection By-Product
OFDW	Organic-Free De-Ionized Water
HAAs	Haloacetic Acids
IC	Ion Chromatography
MCL	Maximum Contaminant Level
NOM	Natural Organic Matter
PQL	Practical Quantitation Limit
SWTR	Surface Water Treatment Rule
t-Butanol	Tertiary Butyl-Alcohol
TIC	Total Inorganic Carbon
TOC	Total Organic Carbon
THM	Trihalomethane
USEPA	United States Environmental Protection Agency
WHO	World Health Organization

ACKNOWLEDGMENTS

I would like to extend my gratitude to Dr. Singer for his academic guidance, as well as for his instruction on this project. I would also like to show appreciation to Dr. DiGiano and Dr. Weinberg for serving on my committee. I am also grateful to Dr. Weinberg for measuring the low bromate concentration samples with the newly developed IC/Spectrophotometric method and graciously providing the explanation for the new method in the text of this report. I am especially grateful for Dr.Weinberg's patience, knowledge, expertise with the IC, etc., and most importantly for his ability to express a positive attitude when we all need it most.

I would like to thank my fellow WRE students, as well as a handful of ARIH students, without whom I would not have made it through my stay here at the University of North Carolina. Your undying support and friendship have been very important to me.

Finally, I would like to thank my friends and family back in Texas. Thanks Jay. Most importantly, I would like to give thanks to my parents who have given me the opportunity, strength, and endless reassurance, confidence, and support to achieve my goals.

CHAPTER 1

INTRODUCTION

Ozone is a growing alternative disinfectant for drinking water treatment in the United States. Chlorine is currently the most widely used disinfectant, but chlorination can produce halogenated by-products, including trihalomethanes (THMs) and haloacetic acids (HAAs). Some of these disinfection by-products (DBPs) are believed to be possible human carcinogens. Ozone can also produce DBPs, which include aldehydes, ketones, and carboxylic acids (Singer, 1990). When bromide is present during ozonation, bromate may be formed as a DBP (Haag and Hoigne, 1983). In the United States, bromate is classified as a probable human carcinogen (a B2 carcinogen), and it is likely that bromate concentrations in drinking water will be regulated in the near future. The 10^{-4} cancer risk level for bromate in drinking water is 5 µg/L (USEPA, 1994). The US Environmental Protection Agency (USEPA) has proposed, in the D/DBP (Disinfectants/Disinfection By-Products) Rule, that bromate have a MCL (maximum contaminant level) of 10 µg/L (USEPA, 1994). This is the current PQL (practical quantitation limit); bromate regulation at lower levels is not yet feasible because routine analytical methods at lower levels of detection are not yet available. The World Health Organization (WHO) has set a provisional guideline for bromate at 25 µg/L (WHO, 1993).

The presence of the bromide ion in drinking water sources is associated with salt water intrusion and human activities such as the spreading of salts on roads during the winter, the use of methyl bromide and ethylene dibromide for the fumigation of crops and soil, and as additives in leaded gasoline (Siddiqui et al., 1995). The average and median bromide ion concentrations in the US are 61 µg/L and 42 µg/L, respectively (Amy et al., 1993). Bromide ion concentrations were found to be in the range of 10-240 µg/L in Dutch waters (Kruithof and Meijers, 1993). At these levels, upon ozonation, the bromide ion concentrations are sufficient to form bromate above the proposed 10 µg/L limit (Shukiary

et al., 1994). Thus, bromate is a formidable concern when there are both measurable levels of bromide in the source water and ozone is the method of disinfection.

The first theory regarding bromate formation from ozone hypothesized that during ozonation, bromide was oxidized by dissolved molecular ozone to hypobromite ion, which further reacted with molecular ozone to produce bromate (Haag and Hoigne, 1983). This mechanism did not account for the contribution of hydroxyl radicals which are formed by ozone decomposition (Yates and Stenstrom, 1993; von Gunten and Hoigne, 1994). Newer theories suggest that bromate can also be formed through secondary pathways where both ozone and hydroxyl radicals react with bromide (von Gunten and Hoigne, 1994).

In examining the formation of bromate, most studies have been conducted on a site-specific basis or under batch or semi-batch ozonation conditions. Although these studies have provided a basic understanding of the chemistry of bromate formation, their applicability to other locations as well as to continuous-flow ozone contactors is limited. Therefore, it is important to gain a more practical and a conceptual knowledge of the formation and control of bromate in continuous-flow contactors. Conditions for the formation and control of bromate are especially acute in The Netherlands where the raw drinking water sources contain relatively high bromide ion concentrations (Kruithof and Meijers, 1993).

This work examined the formation of bromate in a bench-scale, continuous-flow completely-mixed ozone reactor by varying ozone dose and water quality parameters such as influent bromide ion concentration, pH, total organic carbon (TOC) concentration, and total inorganic carbon (TIC) concentration. Conditions which influence mass transfer, e.g., gas flow rate and liquid flow rate, were also investigated. Model solutions of known chemical composition were used in this study. The source of organic carbon for these studies was hydrophobic organic carbon extracted from the Kralingen Plant of Water Supply Company Europoort in Rotterdam in The Netherlands. This work also examined methods to control the formation of bromate by varying pH, or by introducing hydrogen peroxide, tertiary butyl alcohol (a hydroxyl radical scavenger), or ammonia. Bromate concentrations were analyzed using two different ion

chromatographic (IC) techniques, the direct injection and IC/spectrophotometric methods. As noted above, the measurement of bromate is impeded by the capability to detect bromate using standard, routine analytical methods. Use of the direct injection IC method allowed for the detection of bromate at concentrations down to 10 µg/L. With the use of the IC/spectrophotometric technique developed by Weinberg and Yamada (1997), bromate concentrations as low as 0.2 µg/L could be detected. The experimental results from the bench-scale, continuous-flow studies are discussed with regard to their applicability to ozonation in practice.

CHAPTER 2

LITERATURE REVIEW AND THEORY

2.1 CHEMISTRY OF OZONE

Ozone is the most effective disinfectant in water treatment practice. It is a very strong oxidant as well, having an oxidation potential E° of 2.07 V in acidic solution and 1.23 V in basic solution (Snoeyink and Jenkins, 1980). The primary disadvantage associated with the use of ozone is its instability and inability to produce a persistent disinfectant residual. Ozone readily decomposes in aqueous solution. The decomposition of ozone is initiated by an increase in pH (introduction of OH^- ions) and accelerated by many types of organic compounds (substrates) which may act as promoters of a radical type of chain reaction (Hoigne, 1988). Ozone decomposition leads to the formation of hydroxyl radicals ($OH^{\cdot}$). The rate of disinfection with ozone is proportional to the concentration of molecular ozone in solution. Because ozone is unstable in aqueous solution, the effectiveness of ozone as a disinfectant is dependent upon the rate at which it decomposes.

There are two pathways used to describe the behavior of ozone as an oxidant: the direct reaction pathway involving molecular ozone or the indirect pathway incorporating hydroxyl radicals. Figure 2.1 illustrates ozone decomposition and the two pathways by which ozone reacts with substrates. The direct reaction of molecular ozone with substrates forms oxidation by-products. When the ozone decomposes to hydroxyl radicals, the radicals then react further with impurities or substrates, which then form stable products or other radicals ($R^{\cdot}$). Organic radicals ($R^{\cdot}$) may act as either initiators, promoters, or inhibitors of the radical chain process (Staehelin and Hoigne, 1985). The radical chain initiators react with ozone to commence a new chain of radical reactions.

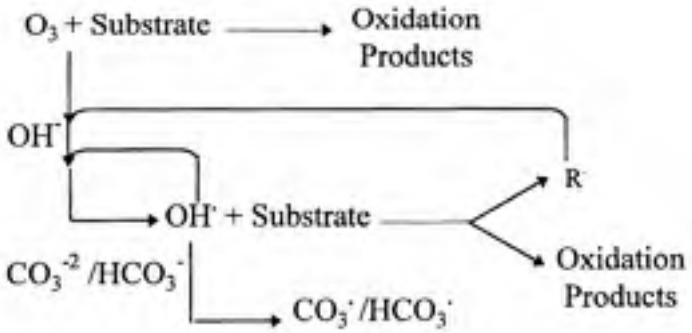

FIGURE 2.1 SCHEMATIC ILLUSTRATION OF REACTIONS INVOLVING AQUEOUS OZONE
(Adapted from Aieta et al., 1988)

In Figure 2.1, the hydroxide ion (OH^-) acts as the initiator of the chain reactions. Other initiators include hydrogen peroxide (H_2O_2) and ultraviolet (UV) light, both of which are used in advanced oxidation processes (AOPs) to increase the hydroxyl radical concentration (Singer, 1990). Promoter radicals are radicals which perpetuate the decomposition of ozone; examples include both the bromide ion and organic matter. Contrasting the promoters are the inhibitors. Inhibitors, such as bicarbonate and carbonate or tertiary-butyl alcohol, delay ozone decomposition by scavenging the hydroxyl radical. Therefore, waters with increased levels of inhibitors can retain a higher level of molecular ozone than waters with low levels of inhibitors (Staehelin and Hoigne, 1985). Table 2.1 further details the decomposition of aqueous ozone to the hydroxyl radical, as initiated by the hydroxide ion.

TABLE 2.1 REACTIONS OF AQUEOUS OZONE
(Staehelin and Hoigne, 1985)

REACTION/EQUATION	RATE OR ACIDITY CONSTANTS	EQN. NUMBER
$O_3 + OH^- \rightarrow O_2^{\cdot-} + HO_2^\cdot$	70 $M^{-1}s^{-1}$	2.1
$HO_2^\cdot \rightarrow O_2^{\cdot-} + H^+$	$pK_a = 4.8$	2.2
$O_2^{\cdot-} + O_3 \rightarrow O_3^{\cdot-} + O_2$	1.6×10^9 $M^{-1}s^{-1}$	2.3
$O_3^{\cdot-} + H^+ \rightarrow HO_3^\cdot$	5.2×10^{10} $M^{-1}s^{-1}$	2.4
$HO_3^\cdot \rightarrow HO^\cdot + O_2$	1.1×10^5 $M^{-1}s^{-1}$	2.5
$HO^\cdot + O_3 \rightarrow HO_2^\cdot + O_2$	2.0×10^9 $M^{-1}s^{-1}$	2.6

2.2 Reactions of Ozone with Organic Matter

Ozone reacts with organic matter to produce many organic by-products. Such by-products include aldehydes, carboxylic acids, organic peroxides, and ketoacids (Singer, 1994). Figure 2.2 illustrates the reactions of ozone with natural organic matter (NOM). In the presence of bromide, ozone reacts with NOM, to produce brominated disinfection by-products. The brominated organic by-products include bromoform, bromoacetic acids, bromoacetonitrile, bromohydrins, and cyanogen bromide, where bromoform and the bromoacetic acids are classified as probable human carcinogens (USEPA, 1994). It is expected that there are many other unidentified brominated by-products.

In natural waters, bromide competes with natural organic matter (NOM) for both ozone and hydroxyl radicals. In waters with low bromide concentrations, ozone reacts with NOM to a greater degree. Thus, organic matter exerts an ozone demand. As bromide concentrations increase, bromo-substituted organic by-products increase, especially at lower pH values (Shukiary et al, 1994). NOM varies with natural water sources; thus, distinct types of NOM may react differently upon ozonation. It is known that bromine is a more potent halogenating agent than chlorine; therefore speciation of the by-products depends on the nature and concentration of the organic matter, as well as the bromide concentration.

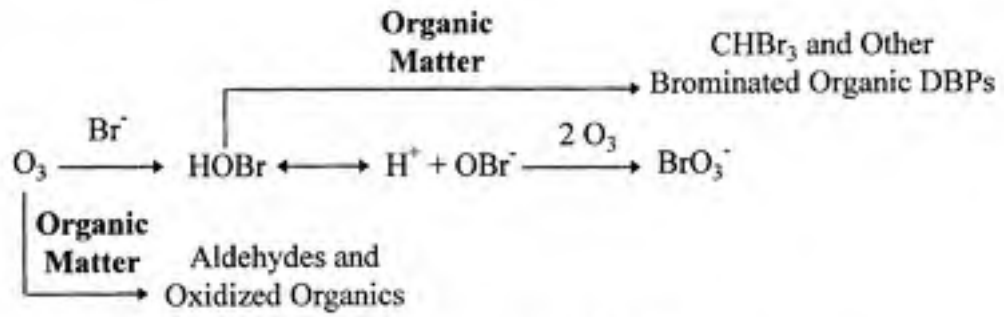

Figure 2.2 Reactions of Ozone and Organic Matter
(Adapted From Krasner et al., 1993; Haag and Hoigne, 1983)

2.3 Reaction of Ozone and Bromide

The reactions controlling the direct interaction of molecular ozone with bromide are shown in Figure 2.3. Further details of the reactions are shown in Table 2.2. Molecular ozone oxidizes the bromide ion (Br^-) to produce hypobromite ion (OBr^-) (See Eqn 2.7). The hypobromite ion further reacts with ozone to form bromite (BrO_2^-) as in Eqn 2.9, then to form bromate (BrO_3^-), shown in Eqn. 2.10. Hypobromous acid (HOBr) has an acidity constant of $10^{-8.8}$ at 20°C. The formation of bromate is dependent on the $HOBr/OBr^-$ ratio, and therefore the reactions are pH-dependent. At lower pH values, where HOBr dominates the speciation of oxidized bromine, reaction with organic matter to produce brominated organic by-products tends to dominate over the formation of bromate.

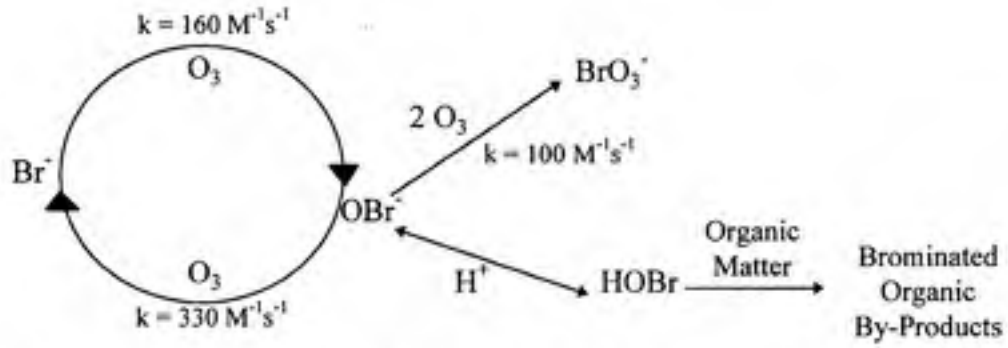

Figure 2.3 Reactions of Ozone with Bromide and Hypobromite
(Adapted from Haag and Hoigne, 1983)

Table 2.2 Reactions Involved in Bromate Formation

Reaction/Equation	Rate or Acidity Constants	Reference	Eqn. Number
$O_3 + Br^- \rightarrow O_2 + OBr^-$	$160\ M^{-1}s^{-1}$	Taube, 1942; Haag and Hoigne, 1983	2.7
$O_3 + OBr^- \rightarrow 2O_2 + Br^-$	$330\ M^{-1}s^{-1}$	Haag and Hoigne, 1983	2.8
$O_3 + OBr^- \rightarrow BrO_2^- + 2O_2$	$100\ M^{-1}s^{-1}$	Haag and Hoigne, 1983	2.9
$O_3 + BrO_2^- \rightarrow BrO_3^-$	$>10^5\ M^{-1}s^{-1}$	Haag and Hoigne, 1983	2.10
$HOBr + H_2O \leftrightarrow OBr^- + H_3O^+$	$pK_a = 8.8$	Haag and Hoigne, 1983	2.11
$HOBr + O_3 \rightarrow BrO_2^- + 2O_2 + H^+$	$<1.3 \times 10^{-2}\ M^{-1}s^{-1}$	Haag and Hoigne, 1983	2.12

2.4 Hydroxyl Radical Chemistry

Various pulse radiolysis studies have examined the reactions of hydroxyl radicals with bromide ions and bromide radicals (Zehavi and Rabani, 1972). Figure 2.4 displays the multiple pathways by which bromate is formed. The first pathway shown is the direct pathway in which molecular ozone (O_3) oxidizes bromide (Br^-) to the hypobromite ion (OBr^-) and then to bromate (BrO_3^-). A second pathway for bromate formation is where molecular ozone oxidizes bromide to the hypobromite ion; this is followed by hydroxyl radical ($OH^\cdot$) oxidation of hypobromite to the bromite radical ($BrO_2^\cdot$) which disproportionates to the bromite ion, BrO_2^-. The bromite ion is oxidized further by molecular ozone to form bromate. In the third pathway, the bromide ion is first oxidized by a hydroxyl radical to form a bromide radical ($Br^\cdot$) which is further oxidized by molecular ozone to form the radical form of the hypobromite ion ($OBr^\cdot$). The pathway continues to form bromate through disproportionation and the subsequent reactions discussed above in the second pathway.

Detailed reactions which describe the indirect pathway for the reaction of ozone with bromide are shown in Table 2.3. There is no evidence for bromate formation in a system where bromide and hydroxyl radicals are the only initial reactants. Hypobromite is needed as an initial reactant with the hydroxyl radical, as in Eqn. 2.19; the hypobromite ion is only formed by the reaction of bromide with molecular ozone (von Gunten and Hoigne, 1994).

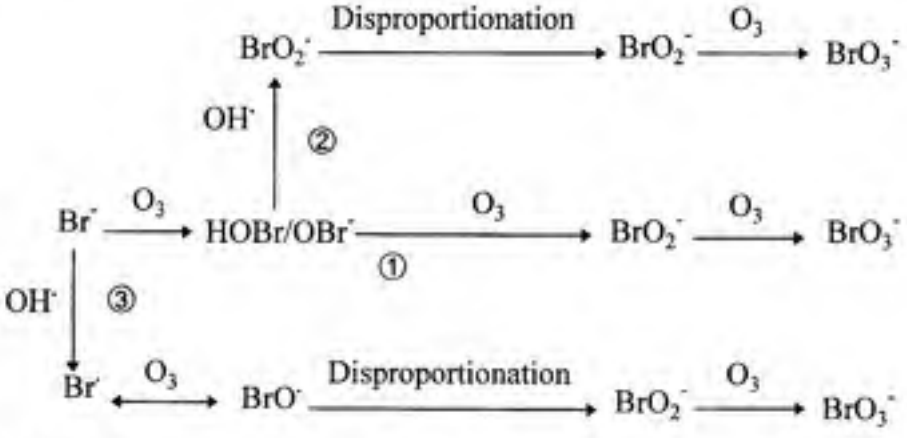

Figure 2.4 Hydroxyl Radical and Direct Pathways of Bromate Formation
(Adapted from Song et al., 1997)

TABLE 2.3 HYDROXYL RADICAL REACTIONS FOR BROMATE FORMATION

REACTION/EQUATION	RATE OR ACIDITY CONSTANTS	REFERENCE	EQN. NUMBER
$Br^- + OH^\cdot \leftrightarrow BrOH^-$	$\rightarrow 1.1 \times 10^{10}\ M^{-1}s^{-1}$ $\leftarrow 3.3 \times 10^{7}\ s^{-1}$	Zehavi and Rabani, 1972 Zehavi and Rabani, 1972	2.13
$BrOH^- \rightarrow OH^- + Br^\cdot$	$\rightarrow 4.2 \times 10^{6}\ s^{-1}$ $\leftarrow 3.3 \times 10^{7}\ s^{-1}$	Zehavi and Rabani, 1972 Zehavi and Rabani, 1972	2.14
$Br^- + Br^\cdot \rightarrow Br_2^-$	$1.0 \times 10^{10}\ M^{-1}s^{-1}$	Zehavi and Rabani, 1972	2.15
$Br_2^- + Br_2^- \rightarrow Br_3^- + Br^-$	$2.0 \times 10^{9}\ M^{-1}s^{-1}$	von Gunten and Hoigne, 1994	2.16
$Br_3^- \rightarrow Br_2 + Br^-$	1.23	Sutton and Downes, 1965	2.17
$Br_2 + H_2O \rightarrow Br^- + HOBr + H^+$	8.24	Sutton and Downes, 1965	2.18
$OH^\cdot + OBr^- \rightarrow BrO^\cdot + OH^-$	$4.5 \times 10^{9}\ M^{-1}s^{-1}$	Buxton and Elliot, 1986	2.19
$OH^\cdot + HOBr \rightarrow H_2O + BrO^\cdot$	$2.0 \times 10^{9}\ M^{-1}s^{-1}$	von Gunten and Hoigne, 1994	2.20
$2BrO^\cdot + H_2O \rightarrow BrO_2^- + BrO^- + 2H^+$	$4.9 \times 10^{7}\ M^{-1}s^{-1}$	von Gunten and Hoigne, 1994	2.21
$BrO_2^- + OH^\cdot \rightarrow BrO_2^\cdot + OH^-$	$2.0 \times 10^{9}\ M^{-1}s^{-1}$	von Gunten and Hoigne, 1994	2.22
$2BrO_2^\cdot \leftrightarrow Br_2O_4$	$\rightarrow 1.4 \times 10^{9}\ M^{-1}s^{-1}$ $\leftarrow 7.0 \times 10^{7}\ M^{-1}s^{-1}$	von Gunten and Hoigne, 1994	2.23
$Br_2O_4 + OH^- \rightarrow BrO_3^- + BrO_2^- + H^+$	$7.0 \times 10^{8}\ M^{-1}s^{-1}$	von Gunten and Hoigne, 1994	2.24

2.5 INFLUENCE OF INORGANIC CARBON ON REACTIONS WITH OZONE

It is known that hydroxyl radical scavengers, such as bicarbonate and carbonate and tertiary-butyl alcohol, are effective inhibitors of the chain reaction in Figure 2.1, and thereby help maintain a molecular ozone residual. As shown in Figure 2.4, in waters without high concentrations of hydroxyl radicals, a molecular ozone residual is necessary for the final oxidation of bromite to bromate (von Gunten and Hoigne, 1994). Thus, waters with higher inorganic carbon concentrations would be expected to yield higher bromate concentrations than waters with lower inorganic carbon concentrations, given similar doses.

However, if the hydroxyl radicals are scavenged, bromate formation via the hydroxyl radical pathway will be interrupted. Yet, recent studies by von Gunten and Hoigne (1994) and Westerhoff et al. (1994) have shown that carbonate radicals formed

may act as secondary oxidants to oxidize the hypobromite ion (OBr^-) to bromite (BrO_2^-) to bromate through radical bromine species. Therefore, appreciable differences in bromate production may be seen between non-carbonate scavengers, such as tertiary-butyl alcohol, and bicarbonate and carbonate hydroxyl radical scavengers. An illustration of the secondary oxidant pathway of the carbonate species is presented in Figure 2.5, shown by the shaded region. These reactions are further detailed in Table 2.4.

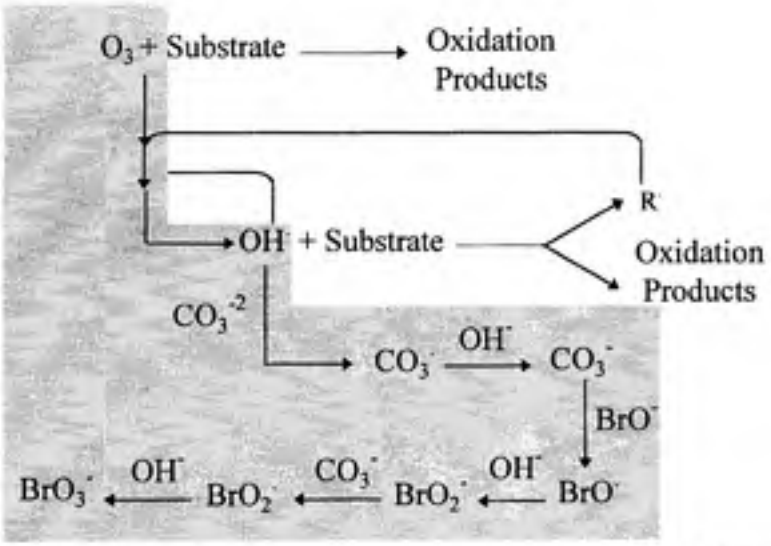

FIGURE 2.5 SCHEMATIC ILLUSTRATION OF REACTIONS INVOLVING CARBONATE OXIDATION (Adapted from Aieta et al., 1988; von Gunten and Hoigne, 1994)

TABLE 2.4 BROMATE FORMATION FROM CARBONATE OXIDATION
(von Gunten and Hoigne, 1994)

REACTION/EQUATION	RATE OR ACIDITY CONSTANTS	EQN. NUMBER
$HCO_3^- \rightarrow CO_3^{2-} + H^+$	$pK_a = 10.3$	2.25
$CO_3^{2-} + HO^\cdot \rightarrow CO_3^{-\cdot} + OH^-$	$3.9 \times 10^8\ M^{-1}s^{-1}$	2.26
$HCO_3^- + OH^\cdot \rightarrow OH^- + HCO_3^\cdot$	$8.5 \times 10^6\ M^{-1}s^{-1}$	2.27
$HCO_3^\cdot \rightarrow CO_3^{-\cdot} + H^+$	$pK_a = 9.6$	2.28
$CO_3^{-\cdot} + OBr^- \rightarrow BrO^\cdot + CO_3^{2-}$	$4.3 \times 10^7\ M^{-1}s^{-1}$	2.29
$CO_3^{-\cdot} + BrO_2^- \rightarrow BrO_2^\cdot + CO_3^{2-}$	$1.1 \times 10^8\ M^{-1}s^{-1}$	2.30

With the above discussions relating to the molecular ozone and hydroxyl radical mechanisms, it is evident that under drinking water treatment conditions, molecular ozone plays an important role for the oxidation steps within the hydroxyl radical mechanism. It is apparent that pH affects both the decomposition of ozone and hydroxyl radical formation, as well as the speciation of hypobromous acid and hypobromite ion. The relative rate and extent of hypobromous acid formation from ozone is influenced by the bromide concentration. The effect of NOM is important, too; NOM impacts the formation of oxidation by-products and brominated organics, and inhibits the formation of hydroxyl radicals. Furthermore, inorganic carbon can both scavenge hydroxyl radicals and act as a secondary oxidant. The complex chemistry associated with ozone and the subsequent formation of bromate is further depicted in Figure 2.6.

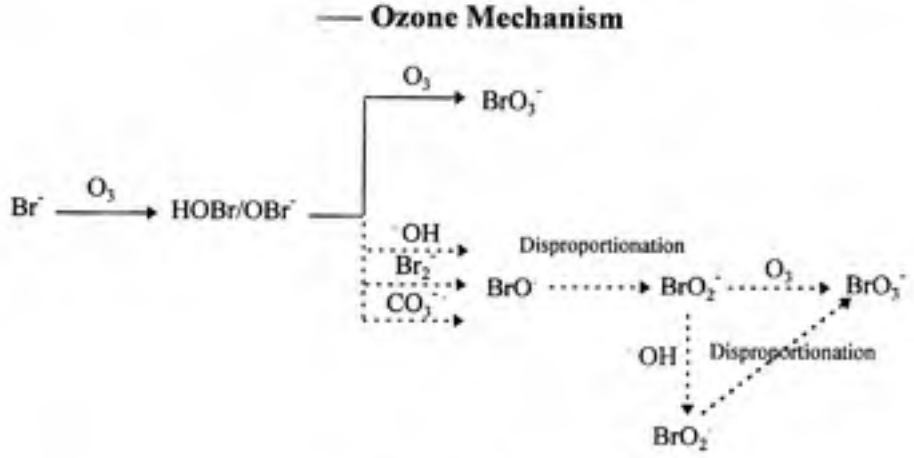

FIGURE 2.6 COMPARISON OF MOLECULAR OZONE AND $OH^{\cdot}$ RADICAL MECHANISMS
(Adapted from von Gunten and Hoigne, 1994)

2.6 OCCURRENCE, HEALTH EFFECTS, AND REGULATION OF BROMATE

Bromide ion in drinking water is not a direct public health risk. However, as shown in previous discussions, its presence can lead to the formation of disinfection by-products (DBPs), such as bromate, when ozone is used as the disinfectant. Sources of the bromide ion in raw drinking water include the infiltration of sea water, spreading of salt

on roadways in the winter, and the leaching of agricultural runoff, fertilizers, and other anthropogenic bromide emissions (Siddiqui, 1995; von Gunten, 1994).

Bromide ion concentrations have been found in raw drinking water sources at levels ranging from a few micrograms per liter to as high as several milligrams per liter. In a survey of 35 U.S. drinking water utilities, Krasner et al. (1989) found that the influent bromide levels ranged from 10 µg/L to 3.0 mg/L. One of the 35 utilities investigated also reported pronounced seasonal variations in the influent bromide ion concentration. Kruithof and Meijers (1993) found ranges of 10-240 µg/L for bromide ion concentrations in Dutch waters. Thus, with these reported concentrations of bromide ion and the use of ozone as an alternative disinfectant, there is the possible danger of producing high levels of bromate in finished drinking water.

Bromate is classified as a possible human carcinogen in drinking water (USEPA, 1994). This finding is based on the research of Kurokawa (1986), which found that bromate caused the formation of renal tumors in laboratory rats. The 10^{-4} cancer risk level is equivalent to a 5 µg/L concentration of bromate in drinking water (USEPA 1994). However, the ability of water quality analytical laboratories to routinely measure bromate concentrations below 5 µg/L is not possible, to date. Therefore, the World Health Organization (WHO) included bromate limits in its guidelines at a proposed level of 25 µg/L (WHO, 1993). The USEPA has proposed a MCL for bromate of 10 µg/L (USEPA, 1994). The proposed MCL for bromate is also the current industry-wide practical quantitation level (PQL) of 10 µg/L. Thus, bromate regulation at levels lower than the PQL would not be feasible due to the analytical limitations.

The two primary analytical methods for bromate analysis are spectrophotometric techniques and electroconductivity detection through ion chromatography. Ion chromatography (IC) is a method which separates, identifies, and quantifies ions; historically, it is the predominant analytical technique for bromate ion measurement. Several researchers have developed methods which have improved the quantification of bromate at low concentrations. Hautman and Bolyard (1992), Vander Der Jagt et al. (1993), and Weinberg (1994), have all quantified bromate at minimum reporting levels

(MRLs) as low as 1 µg/L with the application of IC techniques. Gordon et al. (1994) developed a non-ion chromatographic method using the oxidizing ability of bromate at a low pH to colorize chlorpromazine. Yamada and Weinberg (1997) have developed an IC/spectrophotometric method which enables detection as low as 0.2 µg/L bromate. Often these methods are complex and require great care; until water treatment plant laboratories can routinely utilize these methods for analysis of bromate at lower concentrations, the MCL will remain at the current PQL of 10 µg/L.

2.7 Control of Bromate Formation: Theory and Practice

There are three potential methods for controlling bromate levels in drinking water. These include limitation of ozone contact time, pH depression, and the addition of ammonia or hydrogen peroxide. Limiting the ozone contact time is a simple method of reducing bromate formation. Roustan et al. (1996) found that, as the hydraulic residence time increased, bromate formation increased. The model they developed also investigated bromate formation in two types of reactors: the plug flow reactor (PFR) and the completely mixed flow reactor (CMFR). In both reactors, as the hydraulic residence times increased, bromate formation increased. The PFR formed less bromate at all residence times investigated; thus, the PFR would be more efficient in controlling the amount of bromate formed. The other methods of controlling bromate formation are discussed in the following sections.

2.7.1 Effect of pH Adjustment

Depression of the pH before ozonation is a viable method for minimizing bromate formation. As the pH is depressed, equilibrium shifts the HOBr/OBr^- couple (pK_a=8.8) to be primarily in the form of hypobromous acid (HOBr). This was shown earlier in Figure 2.3. Thus, the rate of bromate formation is reduced because ozone reacts slowly with hypobromous acid to form bromate, compared to its reaction with the hypobromite (OBr^-) ion. Also, ozone residuals are more stable at lower pH values which allows for the

application of lower ozone doses that would be required at higher pH levels in order to achieve the same CT disinfection credit. Krasner et al. (1993) showed that as ozonation pH decreased from 8.0 to 6.0, bromate production also decreased. A few disadvantages associated with lowering the pH of ozonation include the potential increase in the formation of brominated organic by-products due to the increased reactivity of aqueous bromine with natural organic matter (Siddiqui and Amy, 1993), the cost of acid for high-alkalinity waters, and the subsequent need to adjust pH after ozonation for corrosion control (Siddiqui et al., 1995).

2.7.2 Effect of Ammonia

Another method of reducing bromate formation is through the addition of ammonia. Ammonia reacts with the hypobromous acid produced by the oxidation of bromide to form monobromamine. The use of ammonia for this purpose is pH-dependent due to the dissociation of the ammonium ion (pK_a=9.3) and hypobromous acid (pK_a=8.8) at pH values of interestin drinking water. Yamada (1993) and Siddiqui et al. (1995) both observed that the higher the pH value, the greater the effect of ammonia in lowering bromate formation in organic-free water. This effect is not long-lasting; ozone reacts with monobromamine and oxidizes it to nitrate, thereby regenerating the bromide ion which again can react with ozone to produce HOBr/OBr^-. Hence, ammonia effectively controls bromate formation until all of the ammonia is oxidized, thereby delaying the formation of bromate (Siddiqui et al, 1995). A schematic illustration of these reactions is shown in Figure 2.7; a list of the relevant reactions is shown in Table 2.5. At high ammonia concentrations, the elimination of ammonia through ozonation of monobromamine becomes the rate-limiting step (see Reaction 2.34). This could introduce a considerable time-lag for overall bromate formation (von Gunten and Hoigne, 1992), but would require the use of high ozone doses to achieve target disinfection requirements (Krasner et al., 1993).

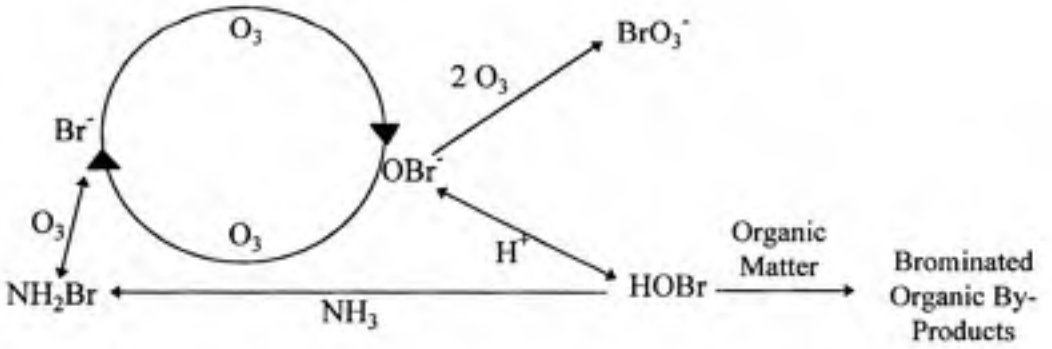

FIGURE 2.7 SCHEMATIC ILLUSTRATION OF REACTIONS OF OZONE, BROMIDE, AND AMMONIA (Adapted from Haag and Hoigne, 1994)

TABLE 2.5 REACTIONS BETWEEN AMMONIA AND BROMIDE
(Wajon and Morris, 1982)

REACTION/EQUATION	RATE OR ACIDITY CONSTANTS	EQN. NUMBER
$HOBr + NH_3 \rightarrow NH_2Br + H_2O$	$7.5 \times 10^7\ M^{-1}s^{-1}$	2.31
$NH_4^+ + H_2O \leftrightarrow NH_3 + H_3O^+$	$pK_a = 9.3$	2.32
$3O_3 + NH_2Br \rightarrow 2H^+ + NO_3^- + Br^-$	$40\ M^{-1}s^{-1}$	2.33

2.7.3 EFFECT OF HYDROGEN PEROXIDE

Hydrogen peroxide has been widely used with ozone to remove pesticides, and geosmin and other taste and odor compounds in drinking water (Siddiqui et al, 1995). Hydrogen peroxide has also been suggested as a potential control mechanism for bromate. However, this proposed use of hydrogen peroxide as a method of reducing bromate formation is not clearly understood. Hydrogen peroxide is a known catalyst for ozone decomposition, as shown in Figure 2.1. It is a weak acid, having an acidity constant of $10^{-11.6}$, as shown in Eqn. 2.35 in Table 2.6 (Staehelin and Hoigne, 1982). In its acid form, hydrogen peroxide reacts with ozone, producing hydroxyl radicals that catalyze the decomposition of ozone. As hydrogen peroxide consumes ozone, the available ozone used to produce HOBr/OBr^- is decreased. However, the hydroxyl radicals can also lead to the formation of bromate (Staehelin and Hoigne, 1982), as shown

in Figures 2.4 and 2.6. Therefore, the results of hydrogen peroxide addition and bromate formation are mixed due to the combination of pathways for bromate formation.

TABLE 2.6 REACTIONS BETWEEN HYDROGEN PEROXIDE AND OZONE
(Staehelin and Hoigne, 1982)

REACTION/EQUATION	RATE OR ACIDITY CONSTANTS	EQN. NUMBER
$H_2O_2 \leftrightarrow HO_2^- + H^+$	$pK_a = 11.6$	2.34
$HO_2^- + O_3 \rightarrow O_2^- + O_2 + OH^-$	$5.5 \times 10^6\ M^{-1}s^{-1}$	2.35

von Gunten et al. (1996) concluded that in a combined disinfection process with both ozone and hydrogen peroxide, bromate formation increased with a constant ozone residual and bromate formation decreased when the ozone dose was held constant, compared to cases with no addition of hydrogen peroxide. Other researchers, Siddiqui and Amy (1993) and Krasner et al. (1993), also reported increases in bromate concentrations when ozone was used with hydrogen peroxide. Yet, Kruithof and Meijers (1993) reported decreases in the formation of bromate upon the addition of hydrogen peroxide. Despite differences in these results and the complexity of the chemistry, it is also important to remember that hydrogen peroxide addition results in the depletion of molecular ozone which hinders the ability to achieve adequate CT disinfection credit.

CHAPTER 3

MATERIALS AND METHODS

This study was designed to examine the effect of various water quality and treatment parameters on the formation of bromate in a bench-scale, continuous-flow, completely-mixed ozonation reactor. The water quality parameters that were investigated included influent bromide ion concentration, pH, total organic carbon (TOC) concentration, and total inorganic carbon (TIC) concentration. The use of tertiary butyl alcohol as a radical scavenger and the effect of variable gas and liquid flow rates were explored, as well. For each set of conditions, the synthetic waters were ozonated to obtain various ozone residuals in order to ascertain the corresponding bromate production under those conditions. The addition of ammonia and hydrogen peroxide were researched as possible methods for the control of bromate formation.

3.1 PREPARATION OF GLASSWARE

Glassware for general use was soaked in detergent (Alconox, Inc., New York, N.Y.) overnight, rinsed with tap water, and soaked in a 10% nitric acid bath for at least four hours. Glassware was then rinsed with organic-free, de-ionized water (OFDW) (Dracor Water Systems, Durham, N.C.) three times. The Dracor water system includes a 1.0 µm pre-filter which is followed by 0.5 ft^3 of activated carbon for removal of chlorine and organic material. The activated carbon is then followed by two mixed-bed deionizers which contain macroreticular resins capable of removing any remaining organics. Volumetric glassware was air-dried and non-volumetric glassware and 40 mL vials used for sample collection were oven-dried at 100°C. The teflon-coated septa and vial caps were soaked in a detergent bath overnight and rinsed with OFDW before being oven-dried at 85°C. Volumetric flasks used for liquid-phase ozone determinations were cleaned in the same manner as the 40 mL vials and then were allowed to air-dry.

3.2 Preparation of Model Waters

Several parameters were investigated to study their effect on the formation of bromate. Table 3.1 lists the various parameters and variations studied, as well as the source of all chemical reagents.

Table 3.1 Water Quality Parameters Examined

Parameter	Variations	Source
Bromide	50, 100, 300*, 500 µg/L	NaBr (EM Science, Gibbstown, N.J.)
pH	6.0, 6.5, 7.0*, 7.5,	KH_2PO_4 (BDH Lab. Supplies, Poole, England) + NaOH (Mallinckrodt AR, Paris, KY.)
	8.3	H_3BO_3 (EM Science, Gibbstown, N.J.) + NaOH
TOC	0.0, 2.5*, 5.0 mg/L as C	Extracted NOM from KIWA
TIC	0.0, 1.0*, 2.0 mM Carbonate	$NaHCO_3$; Mallinckrodt AR, Paris, KY.
Ammonia	0.0*, 1:1 molar ratio (N:Br)	NH_4Cl; Baker & Adamson, Morristown, N.J.
t-Butyl Alcohol (TBA)	0.0*, 5:1 molar ozone dose (TBA:O_3)	EM Science, Gibbstown, N.J.
Hydrogen Peroxide	0.0*, 0.5:1 mass ratio (mg H_2O_2:mg O_3)	Mallinckrodt AR, Paris, KY.

* Denotes baseline conditions

Stock solutions of bromide, inorganic carbon, t-butanol, ammonia, and hydrogen peroxide were prepared with OFDW. A 2 mM borate buffer was used to buffer the pH at 8.3. A 1 mM phosphate buffer was used to buffer the pH at the other pH's examined (6.0, 6.5, 7.0, 7.5). Prior to experimentation, representative concentrations of all buffers were analyzed ion chromatographically to ensure that the buffer concentrations did not diminish the ability to accurately detect the concentrations of bromate.

Model waters were prepared by first adding the buffer, and then adding the bromide, TOC, TIC, and, if appropriate, ammonia. The OFDW was then added after adjusting the pH as needed with 0.1 M NaOH or 0.1 M HCl/0.1 N H_2SO_4 (Fisher Scientific Co., Pittsburgh, PA). Model waters were prepared either daily or a day or two before each experimental run. The baseline synthetic water, as noted by the asterisk in Table 3.1, had the following water quality characteristics: pH 7.0, 300 µg/L Br^-, TOC

concentration of 2.5 mg/L as C, and 1.0 mM carbonate. Tertiary butyl-alcohol, ammonia, and hydrogen peroxide were not included in the baseline scenario.

3.3 Source of Organic Carbon

The dissolved organic carbon for these experiments was hydrophobic organic material extracted from the Kralingen Plant of Water Supply Company Europoort in Rotterdam, The Netherlands. This material was chosen because this facility is interested in using ozone, but the source of water has a relatively high bromide ion concentration. The natural organic matter was collected by KIWA, the sponsor of this research effort. The organic material was extracted using an XAD-8 extraction procedure modeled after the method of Thurman and Malcolm (Harrington, 1997).

First, the necessary quantity of XAD-8 resin was obtained from the supplier (Rohm and Haas Corp., Philadelphia, PA.) and cleaned to remove residual impurities from the manufacturing process. The cleaning process included first soaking the resin in 0.1 N NaOH for 24 hours, decanting the residue, and then re-soaking in NaOH. The resin was then cleaned by Soxhlet-extraction in sequence with methanol, acetonitrile, diethyl ether, and methanol, where each solvent was used for 24 hours. The cleaned resin was stored in methanol. Next, a glass column (3.0 ft long with an outside diameter of 3.5 in.) was packed with the resin with a bed volume of 3.0 L and then rinsed, in a sequential manner, with OFDW, 0.1 N NaOH, OFDW, and 0.1 N HCl. All NaOH and HCl solutions were prepared with OFDW and reagent-grade chemicals. Upon completion of these steps, the column was shipped to KIWA for the extraction of organic carbon. Dr. Greg Harrington performed this preparation.

Source water from the plant was pumped through a cartridge (honeycomb) filter with a 1.0 µm nominal pore size to remove any gross particulate material. The filtered water was stored in a reservoir from which it was pumped to the XAD column. Before application to the column, the water was acidified to pH 2.0 with a 1.0 N HCl solution. Pumping of the acid solution and the raw and filtered waters was performed using

peristaltic pumps. Figure 3.1 shows a process flow diagram for the extraction procedure which was designed by Dr. Greg Harrington.

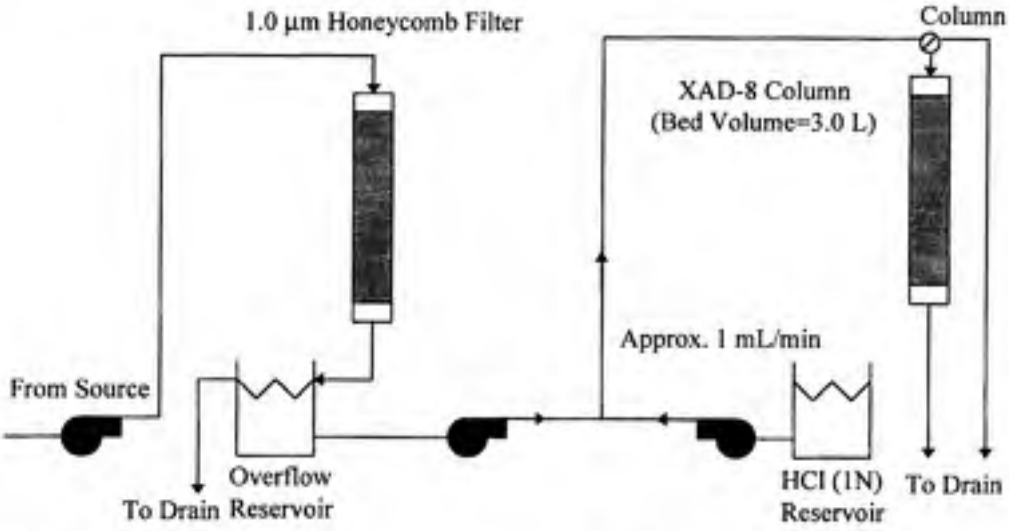

FIGURE 3.1 SCHEMATIC OF XAD-8 EXTRACTION SYSTEM

The flow rate through the column was two bed volumes per hour or 100 mL/min. This flow rate, as well as the effluent pH, was monitored several times a day for process control purposes. Adjustments were made to the flow rate or acid feed whenever the effluent pH deviated from pH 2.0 by more than 0.1 pH unit. Both the influent and effluent TOC concentrations were monitored several times per week. The influent and effluent TOC concentrations were approximately 3.2-3.5 mg/L and 2.1-2.4 mg/L, respectively. The column was run until the required amount of organic carbon was collected. The shut-down criteria was based on the amount of organic carbon needed for experimentation and on an assumed carbon loss of 40% through elution and post-elution workup. The extraction period began on July 25, 1996 and ended on August 10, 1996.

Once the extraction was complete, the column was shipped to the University of North Carolina (UNC). In transport to UNC, the column was broken, but the resin with its adsorbed organic matter was recovered by KIWA and slurried with a pH 2.0 aqueous solution into a 5L glass vessel. Upon receipt of the 5L vessel at the University of North Carolina, the mixture was placed into a new glass column (same dimensions as the

previous column). The mixture was placed into the column with care to ensure the slurry was firmly packed and that there were no pockets of air in the column. The mixture was then rinsed for one hour with one bed volume of OFDW to remove chloride. Hydrophobic organic material was then eluted from the column with 0.1 N NaOH at a flow rate of one bed volume per hour. The eluate was collected in 500 - 2000 mL fractions and the TOC concentration of each fraction was analyzed. Ten of the twelve most concentrated fractions were saved and combined for experimental use; this provided approximately 2.3 g of organic carbon.

The next step was to remove sodium and other cationic species from the solution by cation exchange. The concentrated organic solution was passed through a column containing a 400-mL empty bed volume of AG-MP-50 cation exchange resin in hydrogen form (BioRad Laboratories, Hercules, CA.). The flow rate was maintained at one bed volume per hour and the effluent pH was monitored to confirm the lack of breakthrough. The final pH of the eluate was 3.0. The final TOC concentration of the organic extract was approximately 180 mg/L. The eluate was stored in a refrigerator at 4°C for the subsequent ozonation experiments.

3.4 Experimental Procedure

Ozonation experiments were carried out in a 500-mL glass, gas-washing bottle with both an influent liquid port and an effluent sampling port to provide a continuous-flow reactor, as shown in Figure 3.2. Ozone was generated from oxygen by a Model 200 Sanders Ozonizer (Uetze/Eltze, Germany). The baseline gas flow rate was adjusted to 395 mL/min with a rotameter (Cole Parmer, Chicago, IL.). The influent gas-phase ozone concentration was varied by changing the power setting on the generator. Partial pressures of ozone ranged from 0.0002 atm to 0.0045 atm. The baseline liquid flow rate was adjusted to 50 mL/min with a Masterflex peristaltic pump (Cole Parmer, Chicago, IL.). This provided a theoretical hydraulic residence time of 10 minutes within the reactor. No means of external mixing was provided; all mixing of the reactor contents was induced by the applied gas.

Figure 3.3 displays a schematic of the entire experimental set-up. All tubing was

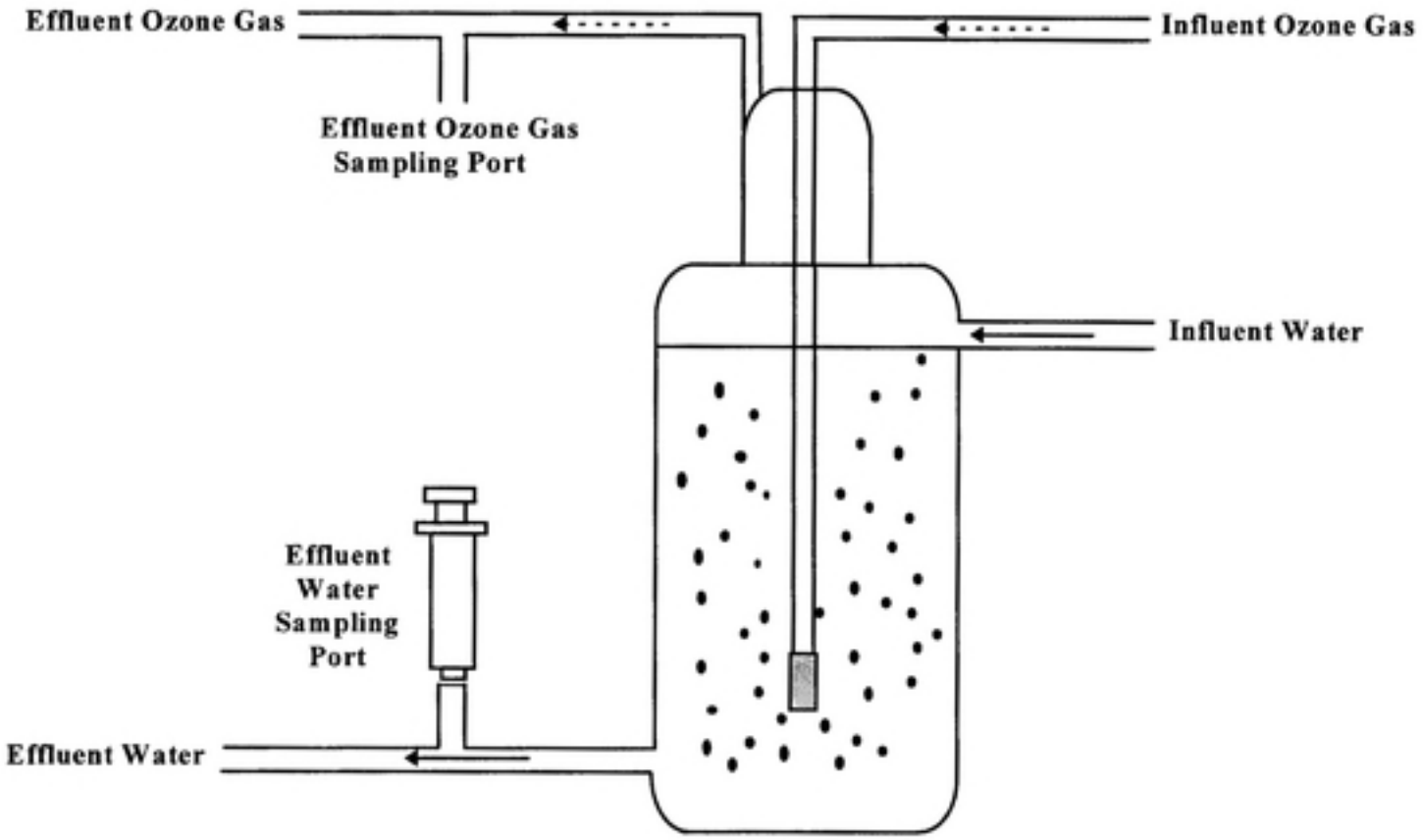

FIGURE 3.2 SCHEMATIC OF CONTINUOUS-FLOW OZONE REACTOR

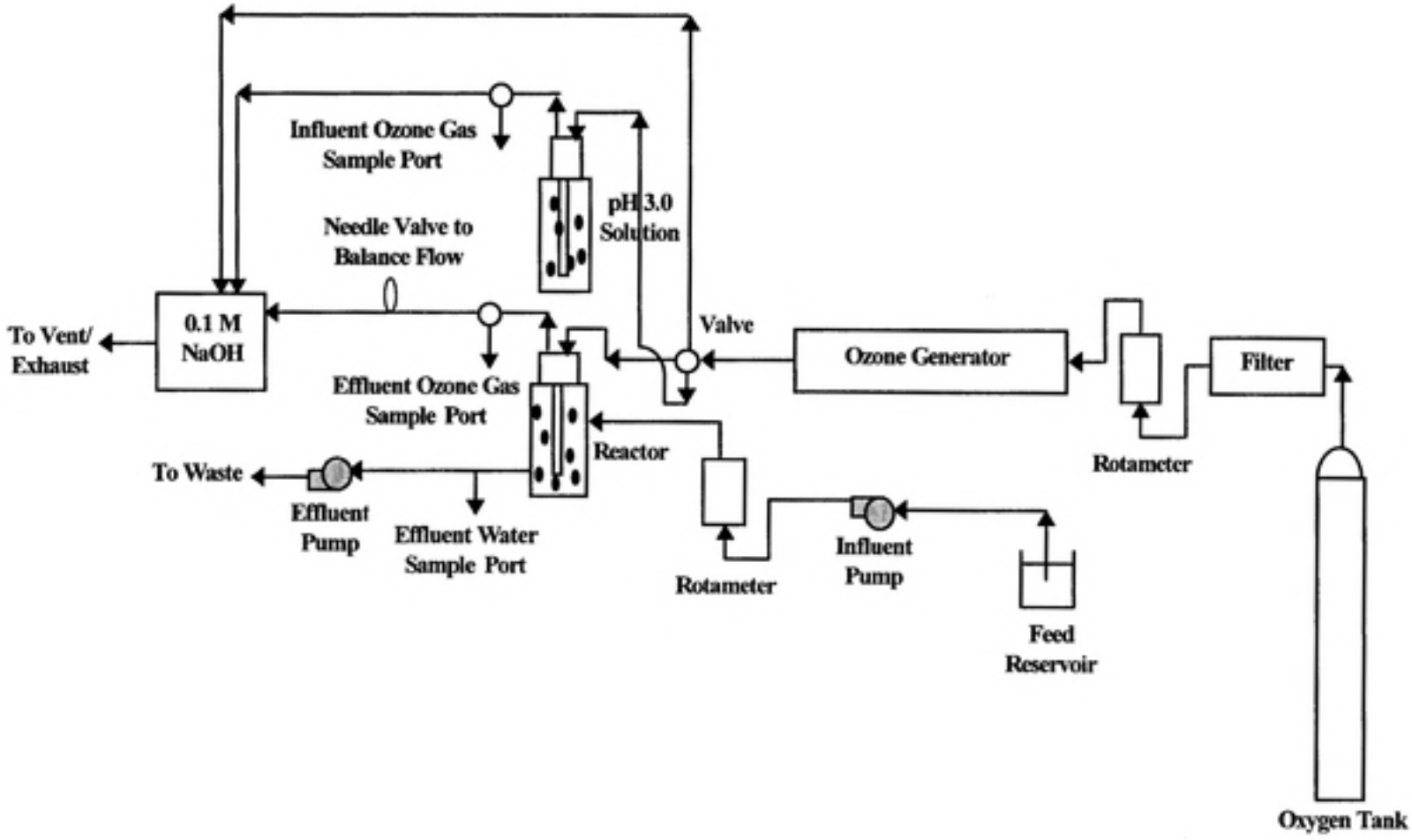

FIGURE 3.3 SCHEMATIC OF EXPERIMENTAL SET-UP

made of teflon and all valves and Swage-Lok connections were made of stainless steel. As the model water was being pumped into the reactor, influent gas-phase concentrations were obtained by diverting the gas stream to a 500-mL gas-washing bottle filled with pH 3.0 OFDW. At pH 3.0, the solution was considered to be non-reactive and, therefore, auto-decomposition of ozone was assumed to be negligible. When steady-state was reached, after approximately twenty minutes, effluent gas from the pH 3.0 gas-washing bottle was collected in a 1-cm quartz cell and analyzed for ozone immediately. Measurements were repeated until several readings, spaced five minutes apart, were within 10% of each other. Once the influent gas-phase ozone concentration was determined, the gas stream was directed back to the reactor, which was already filled with the model water. A needle valve was used to balance the gas stream flow between both sides (the pH 3.0 solution and the reactor) of the system. Therefore, when the gas stream was directed back to the ozonation reactor, the pressure in the system remained constant. Thus, the ozone concentration measured in the pH 3.0 solution could be assumed to be equal to the influent gas-phase concentration to the reactor. The influent gas-phase concentration was also verified by repeating the above procedure at the end of an experiment to ensure that the gas-phase concentration throughout the experiment remained constant. These concentrations were always within 5% of each other.

When the ozonation reactor was filled with the model water, a second Masterflex pump (Cole Parmer, Chicago, IL.) was used to pump the water out of the reactor. The flow rates into and out of the reactor were balanced to maintain a constant volume in the reactor. After three hydraulic residence times, the system was verified to be at steady-state. Appendix A shows an example verification of steady-state for both the gas- and liquid-phase ozone concentrations. It was also assumed that the liquid phase was completely mixed based on the high gas-liquid flow ratio, hydraulic residence time, geometry of the reactor, and earlier experiments with a similar set-up (Hull, 1992; Harrington, 1994).

After verifying that steady-state had been reached, effluent samples for ozone gas-phase analysis and dissolved ozone analysis were taken for two hydraulic residence times. Effluent gas from the reactor was collected in a 1-cm quartz cell and analyzed for

ozone immediately. Samples were collected in duplicate, once per residence time, for two residence times after steady-state was reached. An effluent dissolved sample for ozone analysis, usually 40 to 45 mL, was taken by withdrawing water from the sampling port with a glass syringe. The sample was immediately added to a 50-mL volumetric flask which contained 5.0 to 10.0 mL of indigo reagent II (potassium indigotrisulfonate, Aldrich Chemical Co., Milwaukee, WI.). Indigo rapidly decolorizes ozone and is used here to measure the dissolved ozone concentration; the indigo reagent II is applicable in a range of 0.05 mg/L to 0.5 mg/L of dissolved ozone when 5 mL is added. The flask was carefully filled to the mark to avoid loss of ozone by volatilization. The quenched sample was then analyzed in a 1-cm cell at the end of the experiment.

Samples for bromate analysis were taken in triplicate after steady-state had been reached. The liquid samples were taken from the effluent sampling port with a glass syringe and teflon tubing. The bromate samples were immediately sparged with ultra-high purity (UHP) nitrogen gas (99.998%) for approximately ten minutes to purge the samples of any dissolved ozone residual. After sparging, the samples were stored in a 5°C refrigerator and analyzed for bromate within six weeks of collection. Samples for pH measurements were also taken from the effluent sampling port with the glass syringe.

The analytical methods for determination of the ozone and bromate concentrations are discussed in the next section.

3.5 Analytical Methods

The analytical methods for this study required the measurement of ozone concentrations in both the liquid and gas phases and bromate. Spectrophotometric methods were used to quantify ozone concentrations; gas-phase ozone concentrations were measured by ultraviolet (UV) spectroscopy, while dissolved ozone concentrations were measured by visible spectroscopy using the indigo colorimetric procedure (Standard Method 4500-O_3 APHA, AWWA, and WEF, 1989). Bromate analysis involved two ion chromatographic (IC) procedures, the direct injection and IC/spectrophotometric techniques. The direct injection IC procedure was utilized for bromate samples with

concentrations greater than 10 µg/L utilized (Method 300.0 USEPA, 1993). Bromate samples with concentrations less than 10 µg/L were measured with an IC/spectrophotometric technique developed by Weinberg and Yamada (1997).

3.5.1 Ozone

All gas- and liquid-phase ozone measurements were made with a Spectronic 1201 spectrophotometer (Milton Roy Co., Rochester, N.Y.).

3.5.1.1 Gas-Phase Ozone

The analytical method for both the influent and effluent gas-phase ozone concentrations was direct UV spectroscopy. Ozone gas samples were collected in a 1-cm quartz cell and analyzed immediately on the spectrophotometer at a wavelength of 253.7 nm. Ozone concentrations were determined according to Beer's Law:

$$O_{3_g}\left(\frac{mg}{L}\right) = \frac{\Delta Abs_{253.7} \times 48{,}000 \frac{mg\ O_3}{mol}}{\varepsilon \times l} \qquad \text{Eqn. 3.1}$$

where $\Delta Abs_{253.7}$ = Absorbance of sample at 253.7 nm - absorbance of blank at 253.7 nm
(where the absorbance of blank air tended to be about 0.030)

ε = extinction coefficient = 3000 M^{-1} cm^{-1} at 253.7 nm
(Bader and Hoigne, 1981)

l = path length =1 cm

3.5.1.2 Liquid-Phase Ozone

Liquid-phase ozone concentrations were analyzed using the indigo colorimetric method (Standard Method 4500-O_3 APHA, AWWA, and WEF, 1989). At the end of an experiment, the quenched samples were analyzed in a 1-cm cell at a wavelength of 600 nm. The dissolved ozone residuals were calculated according to Beer's Law:

$$O_{3_{aq}}\left(\frac{mg}{L}\right) = \frac{\Delta Abs_{600} \times V_t}{0.42 \times V_s \times l} \qquad \text{Eqn. 3.2}$$

where ΔAbs_{600} = Absorbance of blank indigo solution - absorbance of sample at 600 nm
(where the absorbance of the blank tended to be about 0.290)

V_t = Total volume (mL) = Sample volume (V_s) + indigo reagent = 50.0 mL

V_s = Sample volume (mL) = 40.0 -45.0 mL

l = Path length, 1 cm

0.42 = Conversion factor (L/(cm-mg))

A calibration curve was prepared to verify the applicability of the Eqn. 3.2. A sample calibration curve and discussion of this procedure is shown in Appendix A.

3.5.2 BROMATE

Bromate concentrations were measured with a Dionex Ion Chromatograph (Model 4500i, Sunnyvale, CA.). Eluents were prepared from reagent-grade boric acid and analytical grade sodium hydroxide. The eluents were vacuum-filtered through a 0.45-µm nylon filter (Alltech Assoc., Deerfield, IL.) and purged with UHP helium for at least ten minutes to remove carbon dioxide and dissolved carbonate. A 25 mM sulfuric acid regenerant was used. OFDW used for dilution of the eluents was also sparged for at least ten minutes.

3.5.2.1 DIRECT INJECTION PROCEDURE

When bromate samples were expected to contain levels higher than 10 µg/L, the direct injection method of ion chromatography was utilized (Method 300.0 USEPA, 1993). The system, as shown in Figure 3.4, consisted of a 150 µL injection loop, an AG-9 guard column, and an AS-9 analytical column (Dionex IonPac, Sunnyvale, CA.). Two different programs for bromate analysis, one program was used for bromate calibration curve analysis and the other was used for bromate sample analysis. This did not impact sample analysis because the eluent concentrations used in both analyses was the same and therefore the detention time for bromate was the same in both programs. A 24 mM H_3BO_3/6 mM NaOH eluent at a flow rate of 1.5 mL/min was used to obtain bromate detection at a retention time of approximately 2.6 minutes. After 8.0 minutes, a gradient elution was used, where the eluent concentration was gradually increased to 120 mM

H_3BO_3/30 mM NaOH for four minutes; this was done to remove any remaining ions on the analytical column. After four minutes at the high eluent concentration, the eluent concentration gradually was returned to 24 mM H_3BO_3/6 mM NaOH eluent concentration through gradient elution in the next five minutes. An example program used in the analysis is shown in Appendix B. Figure 3.5 is an illustration of a typical direct injection chromatogram.

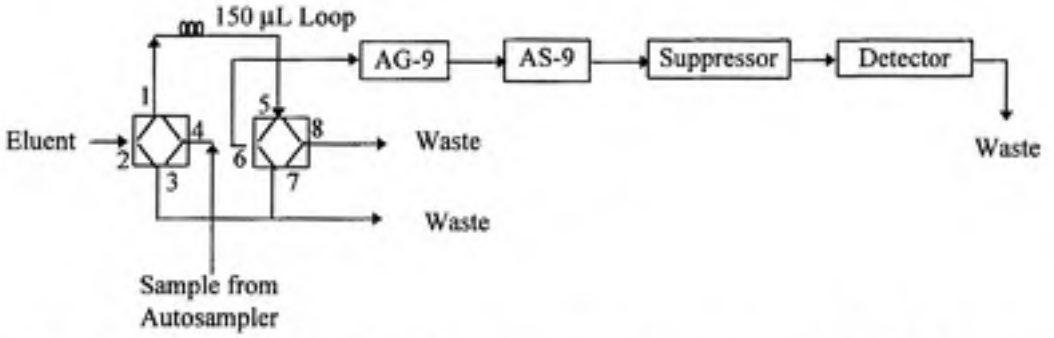

FIGURE 3.4 SCHEMATIC OF DIRECT INJECTION ION CHROMATOGRAPHY PLUMBING

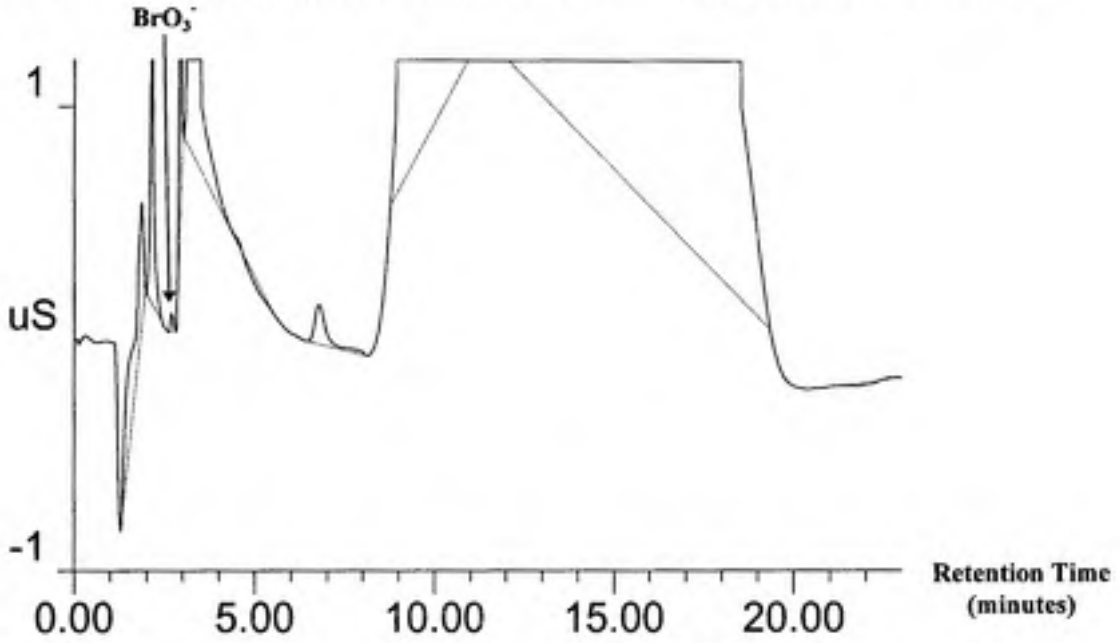

FIGURE 3.5 ILLUSTRATIVE CHROMATOGRAM FOR DIRECT INJECTION ION CHROMATOGRAPHY

Before measurement on the ion chromatograph, each sample was manually passed through a 0.2 µm non-sterile, nylon syringe filter (Nalgene, Rochester, N.Y.) and two

AgCl OnGuard sample pre-treatment cartridges (Dionex, Sunnyvale, CA.) to remove particulates and excess chloride. The retention time for chloride is close to the retention time for bromate. Therefore, if the concentration of chloride in a sample is excessive, the chloride peak can obscure the bromate peak.

The calibration standards for the direct injection procedure were prepared from a 100 mg/L $KBrO_3$ (Mallinckrodt AR, Paris, KY), prepared every two months, in OFDW prior to each analysis. Calibration curves consisted of at least five calibration points analyzed in duplicate. The range of calibration was 0-250 µg/L. Linear responses were exhibited over the entire range with a minimum R-squared value of 0.993. A typical direct injection calibration curve is shown in Figure 3.6. All bromate concentrations were based on the area responses from the ion chromatograph.

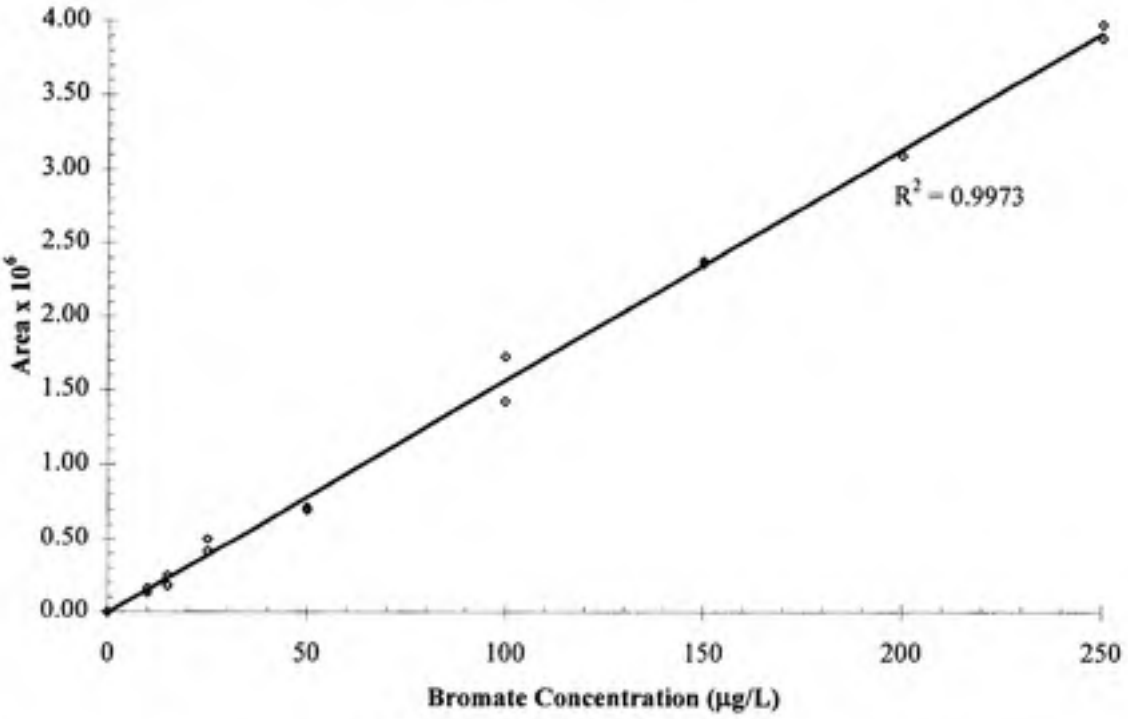

FIGURE 3.6 ILLUSTRATIVE CALIBRATION CURVE FOR DIRECT INJECTION ION CHROMATOGRAPHY

A method detection limit (MDL) was calculated to determine if the PQL of 10 µg/L could be achieved by the instrument and analyst. The PQL is usually five times the

MDL and represents a practical and routinely achievable detection limit with a relatively good certainty than any reported value is reliable (Standard Method 1030-E APHA, AWWA, and WEF, 1989). The MDL was determined according to the Environmental Protection Agency's DBP/ICR (Preliminary) Analytical Methods Manual (1995). A MDL was calculated for bromate in both OFDW as well as a matrix with OFDW and a NOM solution with a TOC concentration of 2.5 mg/L as C. Ten replicates of 10 µg/L were analyzed in the TOC matrix and eight replicates of 10 µg/L were analyzed in the OFDW standard. The following equation was applied to obtain the MDL:

$$MDL = t \times s \qquad \text{Eqn.3.3}$$

where t = student t value for n-1 degrees of freedom (n = number of replicates) at the 99% confidence level

s = standard deviation of the replicates

The direct injection MDL was determined to be 2.08 µg/L in the OFDW and 5.81 µg/L in the TOC matrix. The MDLs were found to be less than the PQL of 10 µg/L; five times the MDL in OFDW is approximately 10 µg/L, the expected PQL. Bromate calibration concentrations were obtained in the OFDW; therefore, the PQL was selected to be the minimum reporting level (MRL) for all samples analyzed using the direct injection procedure. Also, because of the difference found between the two MDLs, samples obtained for bromate analysis were also spiked with known concentrations of bromate. This was done to ensure that the use of calibration standards made in OFDW were appropriate to use in obtaining bromate concentrations from the synthetic water samples. All spike recoveries in this research primarily ranged between 80% and 120%.

Appendix C contains more detailed information on the method evaluation and development for the IC.

3.5.2.2 IC/Spectrophotometric Method

Bromate samples with concentrations less than 10 µg/L were analyzed by the IC/spectrophotometric procedure (Weinberg and Yamada, 1997). The new ion

chromatographic method successfully determines bromate in drinking water at practical quantitation limits of 0.2 µg/L. Sample pre-treatment is not required. Sensitivity of detection is enhanced by conversion of the eluting bromate into the tribromide ion by a post-column reaction with bromide under acidic conditions. Spectrophotometric detection of the tribromide ion is at 267 nm. All results were quality-assured and spike recoveries were in the range 94-110%. The method is applicable to a wide range of waters containing high levels of ions and organic carbon.

The diagram shown in Figure 3.7 illustrates the general layout of the method. The hardware consisted of a ternary gradient pump for supplying the mobile phase (carbonate/bicarbonate) across the guard and analytical columns (AG12 and AS12, respectively). The sulfuric acid regenerant is supplied to the suppressor pneumatically by use of helium pressure. The reagent generator is another anion membrane suppressor whose reagents are also supplied with the help of helium head pressure. In the case of the driving species (sodium bromide), the flow rate is controlled by use of a single-piston pump with pulse dampener. Conductivity (CDM-2) and UV (VDM-2) detectors are placed in series with a reaction coil inserted after the T-junction which introduces the active species for derivatization into the column's effluent stream. The reaction coil is placed in a heating block. A six-port pressure-operated slider valve provides the switching mechanism to place the sample loop contents into the mobile phase stream. All hardware components were supplied by the Dionex Corporation (Sunnyvale, CA). The major safety considerations with the use of high pressure ion chromatography systems apply. Setting the operational maximum and minimum pressure range in a reasonably narrow band will stop the mobile phase flow if there are any sudden leaks or restrictions in the flow.

All reagents used in this work were ACS grade or higher, assayed at >99.5% purity and supplied by Fluka Chemical Corp. (Ronkonkoma, N.Y.) or Fisher Scientific (Fairlawn, N.J.). OFDW was used to prepare mobile-phases, dilutions of reagents, and synthetic waters. Mobile phases were filtered through 0.45 µm glass fiber filters prior to use, and then degassed with UHP helium.

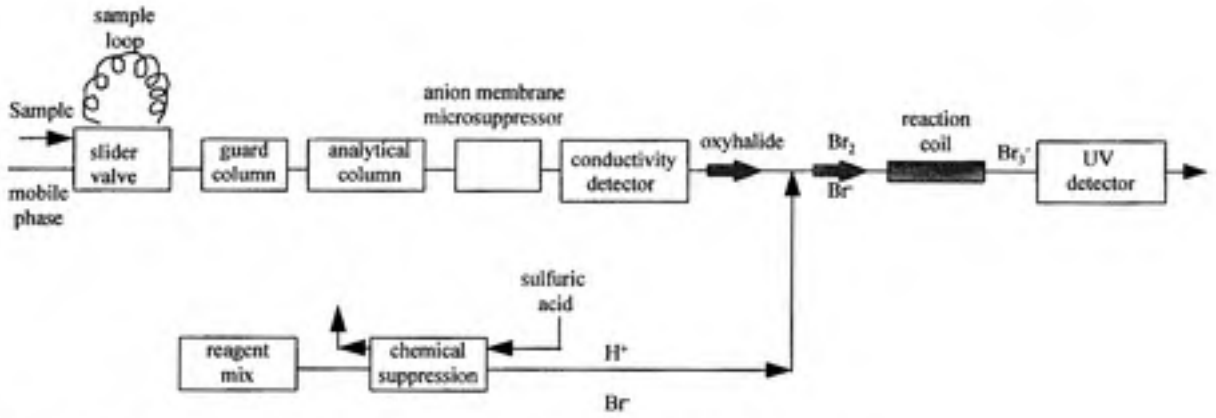

FIGURE 3.7 SCHEMATIC OF IC/SPECTROPHOTOMETRIC SYSTEM

Dr. Howard Weinberg used this method to measure all the samples in this research with bromate concentrations below 10 µg/L.

3.5.3 OTHER MEASUREMENTS

3.5.3.1 pH

All pH measurements were made with an Accumet Model 10 pH-meter (Fisher Scientific, Pittsburgh, PA.). The pH electrode was stored in a pH 7.0 electrode solution and the pH meter was calibrated weekly with both pH 10.0 and pH 4.0 standard solutions.

3.5.3.2 TOC CONCENTRATION

All TOC concentration measurements were made with a TOC-5000 Carbon Analyzer (Shimadzu, Columbia, MD.). The calibration standards for the TOC analysis were made from dilutions of a 1000 mg/L as C standard solution of potassium hydrogen phthalate (KHP) (Kanto Chemical Co., Inc., Tokyo, Japan) in OFDW prepared prior to each analysis. Calibration curves consisted of three calibration points analyzed in duplicate with a range of 2.0 to 10.0 mg/L as C.

CHAPTER 4

RESULTS AND DISCUSSION

The basis of this study was to investigate the effects of water quality variables on bromate formation in a dynamic, continuous-flow system. Ozonations were performed on synthetic waters in a completely-mixed, continuous-flow ozonation reactor. The composition of the synthetic waters and experimental conditions were adjusted to examine the effects of pH, bromide concentration, inorganic carbon concentration, organic carbon concentration, variable gas and liquid flow rates, and the addition of tertiary butyl alcohol (a hydroxyl radical scavenger), ammonia, and hydrogen peroxide on bromate formation. The transferred ozone doses (mg O_3/Liter of solution) were calculated by subtracting the measured ozone concentration in the reactor off-gas (effluent) from the applied gas-phase ozone concentration (influent), as shown below:

$$\text{Ozone Dose}\left(\frac{\text{mg}}{\text{L}}\right) = \left[\text{Influent Ozone}\left(\frac{\text{mg O}_3}{\text{L gas}}\right)\right] \times \left[\frac{\text{Gas Flowrate}\left(\frac{\text{mL}}{\text{min}}\right)}{\text{Liquid Flowrate}\left(\frac{\text{mL}}{\text{min}}\right)}\right] - \left[\text{Effluent Ozone}\left(\frac{\text{mg O}_3}{\text{L gas}}\right)\right] \times \left[\frac{\text{Gas Flowrate}\left(\frac{\text{mL}}{\text{min}}\right)}{\text{Liquid Flowrate}\left(\frac{\text{mL}}{\text{min}}\right)}\right] \quad \text{Eqn.4.1}$$

The complete set of data for these experiments is reported in Appendix D.

4.1 EFFECT OF pH

The effect of pH on the formation of bromate at various ozone doses was studied by varying the influent pH and the applied ozone dose under baseline conditions (300 µg/L influent Br^- concentration, 1 mM carbonate concentration, 2.5 mg/L total organic carbon concentration). The pH's examined included 6.0, 6.5, 7.0, 7.5, 8.3; the pH 8.3 solution was buffered with a 2 mM boric acid buffer and the other pH's were buffered

with a 1 mM phosphate buffer. Figures 4.1a and b display the baseline (pH 7.0) results. The pattern shows that as ozone dose increases, dissolved ozone residual and effluent bromate concentration increase, too, in an exponential manner.

For purposes of convenience and subsequent comparisons, several mathematical relationships were examined to find a relationship which best described the results. An exponential relationship was found to represent the data most accurately. Figures 4.2a and 4.2b show the pH 7.0 results with the fitted exponential model. It is evident that the exponential model is a fairly good representation of the data; the R-squared values for the model curves were 0.93 and 0.74 for Figures 4.2a and b, respectively.

All subsequent curves shown in this chapter were created using an exponential model of the form:

$$Y = ae^{(bX)} \qquad \text{Eqn.4.2}$$

where Y = Effluent Ozone Residual (mg/L) or Bromate Concentration (µg/L)

X = Ozone Dose (mg/L)

The curves are shown for illustrative purposes only. They do not have any mechanistic or theoretical meaning, and they apply only to ranges over which the data were fitted. However, in order to more accurately represent theory, the positive intercept "a" in the above equation was subtracted from the model curves to force the curves to go through the origin (0,0). To ensure that this alteration did not modify the goodness of fit for the model curve, a comparison was made between the R-squared value calculated by the best-fit line and the R-squared value calculated by the equation which goes through the origin. For the pH 7.0 results, the best-fit R-squared values, as stated above, were found to be 0.93 and 0.74 for the ozone residual and bromate models, respectively. For the pH 7.0 results with the lines forced through the origin, the R-squared values were found to be 0.89 and 0.73 for the respective ozone residual and bromate models. Thus, forcing the model through the origin did not drastically affect the goodness of fit of the model curves. Hence, all calculations for comparison purposes in this report are made from the

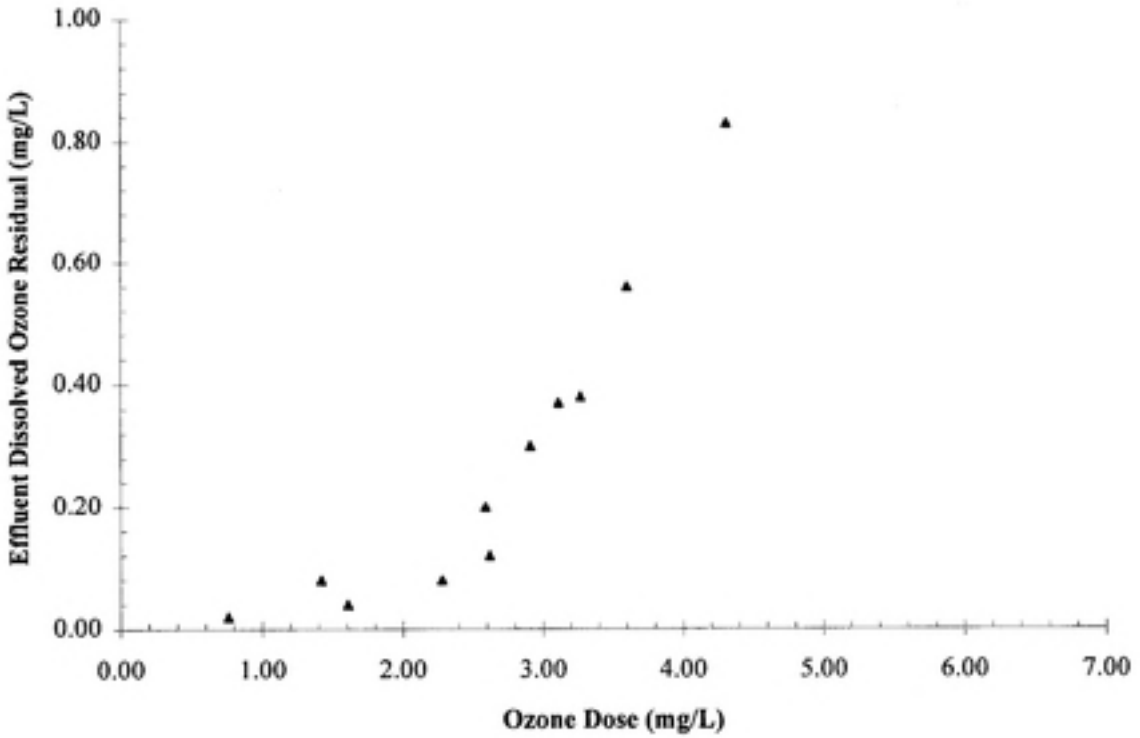

FIGURE 4.1 (A) EFFECT OF OZONE DOSE ON EFFLUENT OZONE RESIDUAL AT pH 7.0

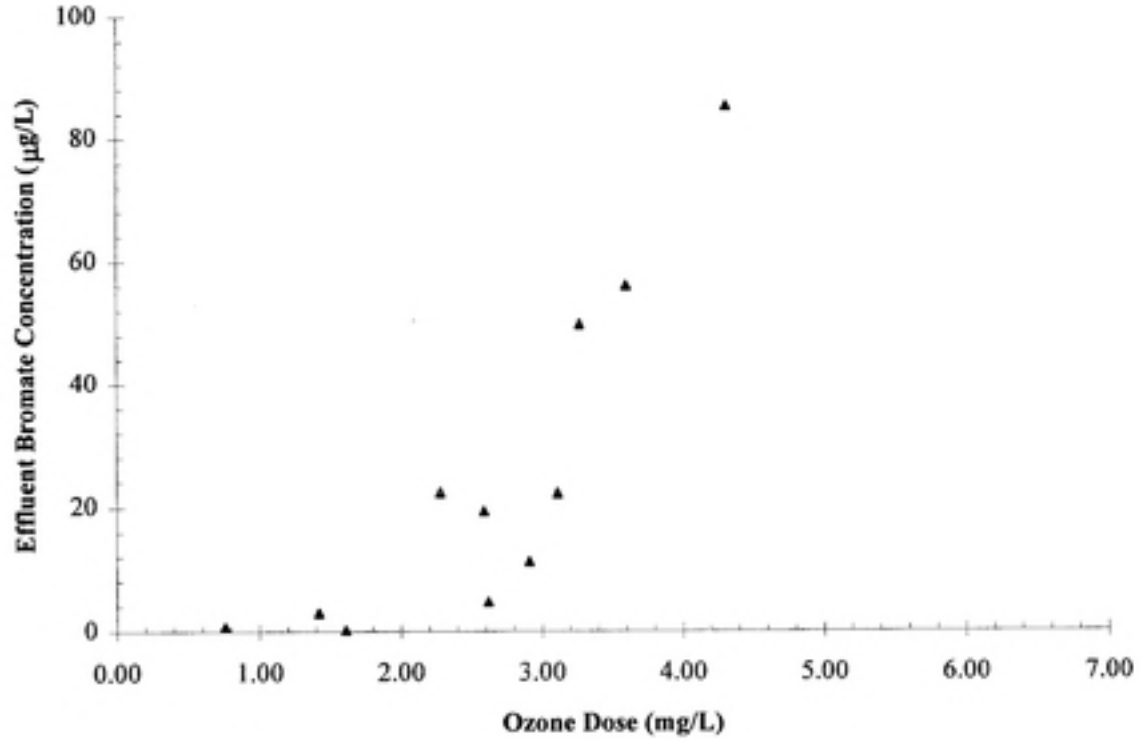

FIGURE 4.1 (B) EFFECT OF OZONE DOSE ON BROMATE FORMATION AT pH 7.0
(300 µg/L Br^-, 1mM carbonate, 2.5 mg/L TOC)

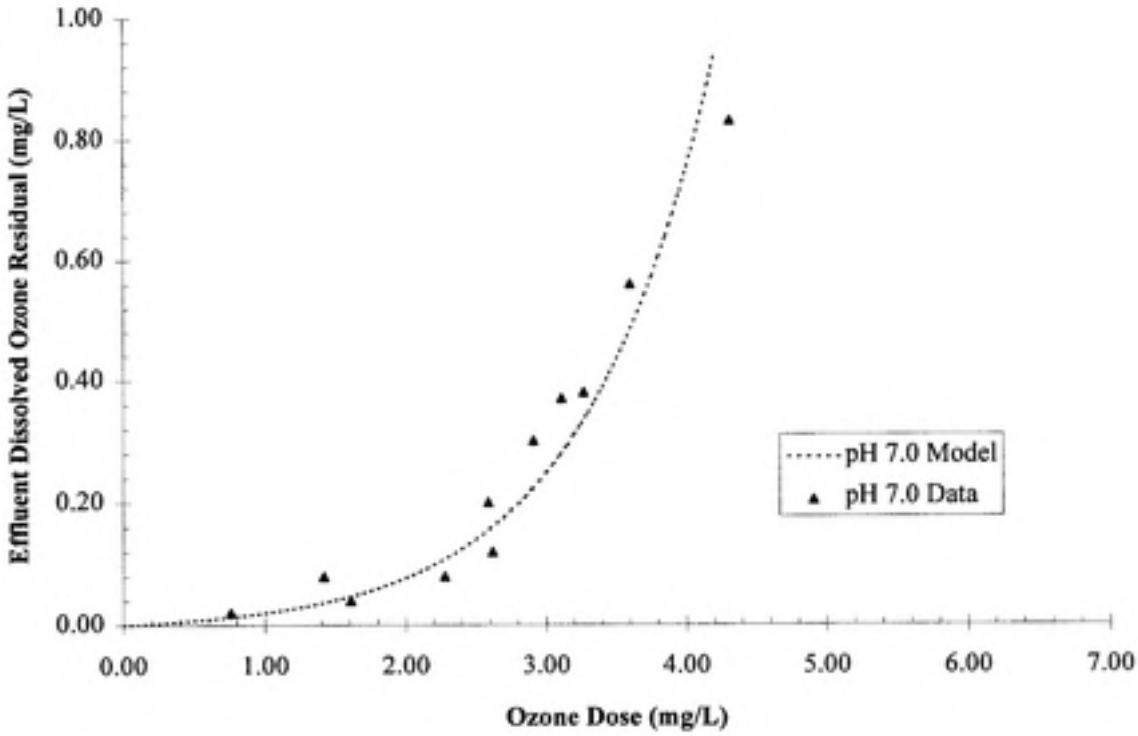

FIGURE 4.2 (A) EXPONENTIAL MODEL ILLUSTRATING EFFECT OF OZONE DOSE ON EFFLUENT OZONE RESIDUAL AT pH 7.0

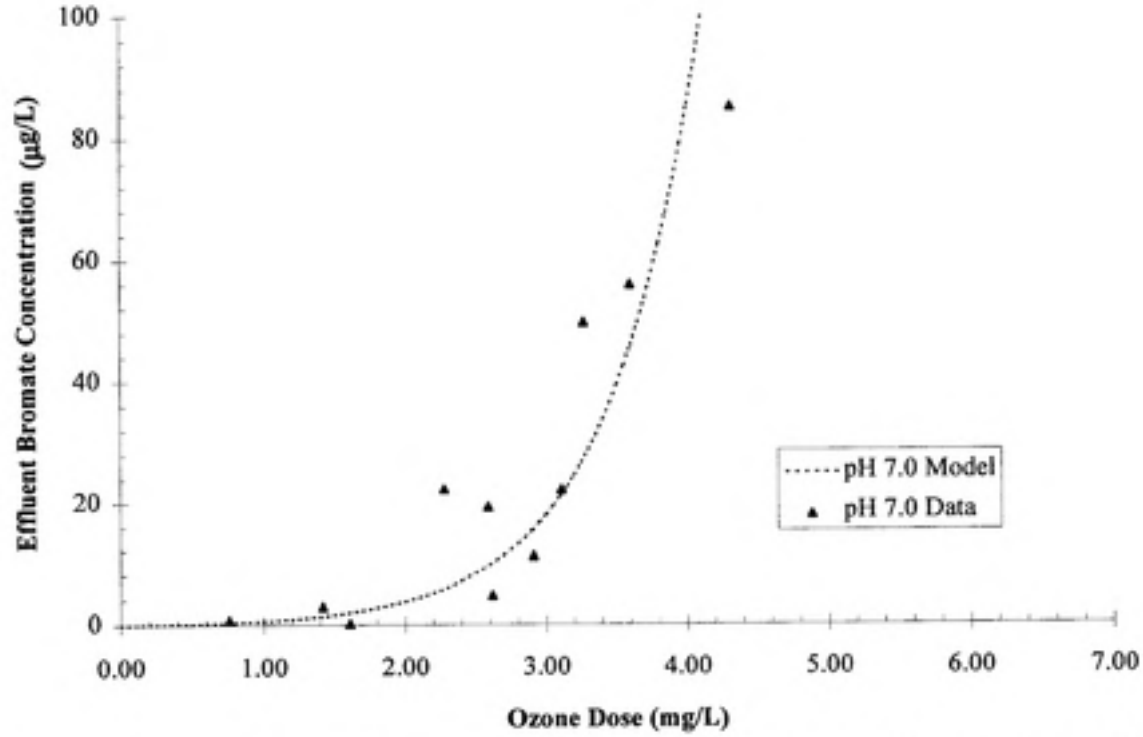

FIGURE 4.2 (B) EXPONENTIAL MODEL ILLUSTRATING EFFECT OF OZONE DOSE ON BROMATE FORMATION AT pH 7.0 (300 µg/L Br^-, 1 mM carbonate, 2.5 mg/L TOC)

original best-fit exponential model trendlines, i.e., the model equations given in subsequent tables where the positive intercept "a" is not subtracted.

Figure 4.3a shows that for a variety of pH values between pH 6.0 and 8.3, the dissolved ozone residual tends to increase with a decrease in pH, for any transferred ozone dose. As pH increases, more ozone is required to reach any given ozone residual. This is due to the increased rate of ozone decomposition at higher pH values. Table 4.1 displays the corresponding best-fit equations (without the positive intercept "a" subtracted) and R-squared values for each pH value tested. The experimental for the effluent ozone residuals appear to be fairly similar data at pH's 6.0, 6.5, and 7.0. Statistical analysis of the ozone residual results showed no significant difference for the pH values of 6.0, 6.5, and 7.0, at the α=0.05 level. Therefore, a single exponential model is plotted through these data.

In Figure 4.3b, bromate formation does not appear to be dependent on pH, aside from the pH 6.0 data which does not appear to follow an exponential trend, especially at higher ozone doses. Statistical analysis indicated that there was no significant difference among the results at the different pH values examined for bromate formation. Both the individual and combined exponential model equations are shown in Table 4.1. The individual pH exponential equations are shown because they are used for comparison purposes elsewhere in this chapter. Statistical analysis of the results are shown in Appendix E.

TABLE 4.1 MODEL EQUATIONS FOR EFFECT OF PH ON OZONE RESIDUAL AND BROMATE FORMATION

	Ozone Residual (mg/L)		Bromate Formation (µg/L)	
pH*	Equation	R^2	Equation	R^2
6.0	$0.0172e^{1.0116x}$	0.94	$0.5664e^{0.9967x}$	0.49
6.5	$0.0021e^{1.7166x}$	0.99	$0.0055e^{2.5281x}$	0.95
7.0	$0.0099e^{1.0864x}$	0.93	$0.1747e^{1.5494x}$	0.74
7.5	$0.0339e^{0.6525x}$	0.93	$0.8017e^{1.1058x}$	0.84
8.3	$0.0145e^{0.6343x}$	0.80	$0.6235e^{1.0857x}$	0.87
6.0, 6.5, 7.0	$0.0182e^{0.9489x}$	0.74	-	-
6.0-8.3	-	-	$0.2754e^{1.3137x}$	0.77

* The individual pH 7.0 equations shown here are the "baseline" equations used throughout the chapter.

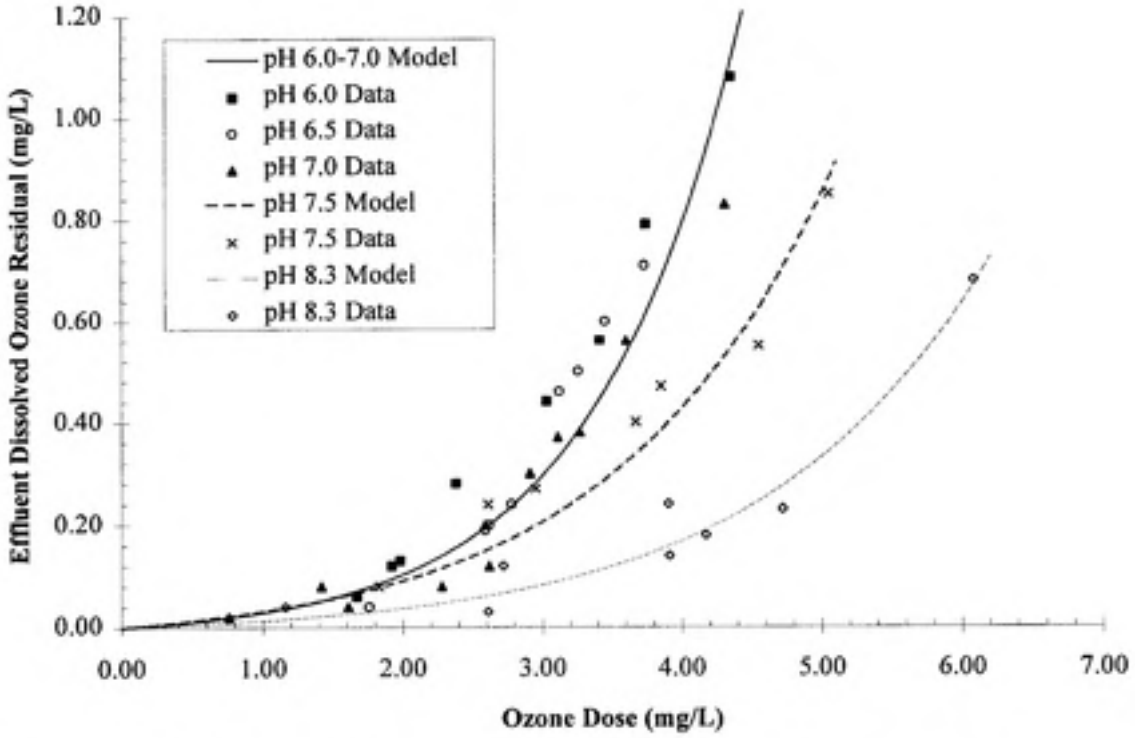

FIGURE 4.3 (A) EFFECT OF VARIABLE pH ON EFFLUENT OZONE RESIDUAL

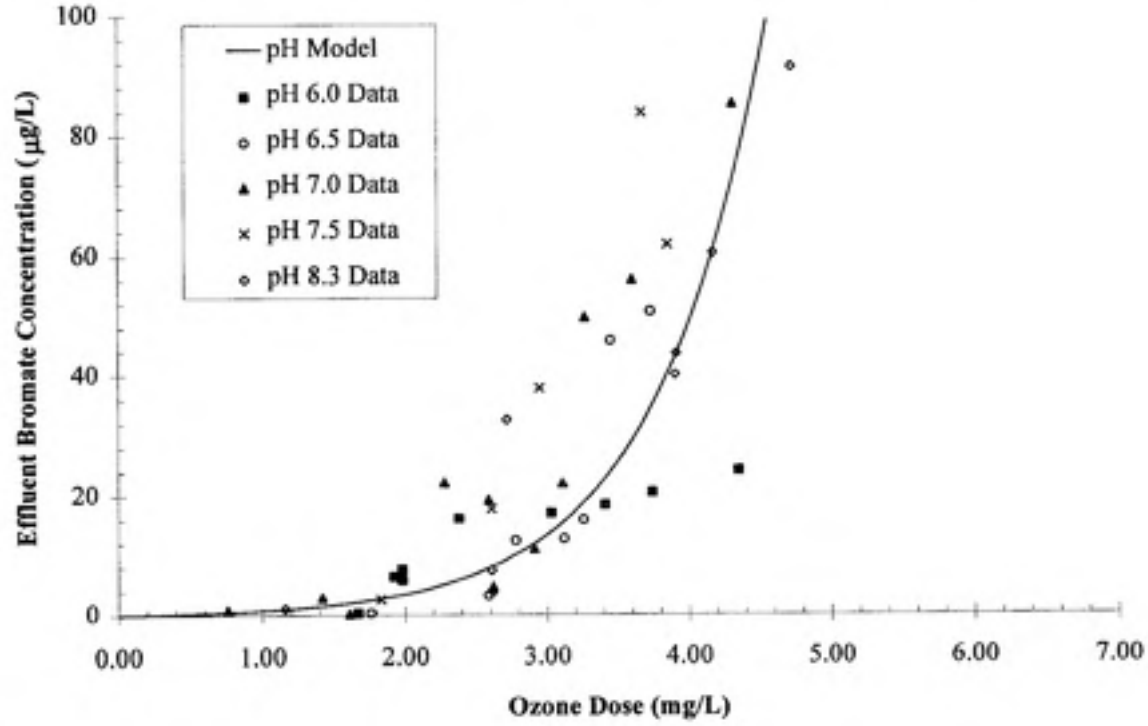

FIGURE 4.3 (B) EFFECT OF VARIABLE pH ON BROMATE FORMATION
(300 µg/L Br^-, 1 mM carbonate, 2.5 mg/L TOC)

Table 4.2 shows a comparison between the two extreme pH values examined. For two target ozone residuals of 0.2 mg/L and 0.4 mg/L, Table 4.2 shows that the required ozone doses and corresponding bromate formation were calculated to be higher for pH 8.3 than for pH 6.0. Even though the exponential curves at pH 8.3 and 6.0 are not statistically different for bromate formation (see Figure 4.3b), the increased bromate formation at pH 8.3 is due to the increased ozone doses required to reach a specified ozone residual at pH 8.3. For all ozone doses tested at pH 6.0, even for those producing dissolved ozone residuals as high as 1.0 mg/L, the effluent bromate concentration was measured to be less than the WHO's recommended limit of 25 µg/L.

TABLE 4.2 EFFECT OF PH 6.0 AND 8.3 ON THE CALCULATED BROMATE FORMATION FOR TWO TARGET OZONE RESIDUALS

pH	Target Ozone Residual 0.2 mg/L		Target Ozone Residual 0.4 mg/L	
	Required Ozone Dose (mg/L)	Corresponding Bromate Conc. (µg/L)	Required Ozone Dose (mg/L)	Corresponding Bromate Conc. (µg/L)
6.0	2.5	7.4	3.3	19
8.3	4.1	57	5.2	>100

The results for the effect of pH and ozone dose on the formation of bromate contradict the findings of Siddiqui and Amy (1993) who found bromate concentrations that in a semi-batch reactor almost tripled with a constant ozone dose where the pH was increased from 6.0 to 8.5. These results are consistent with the results of Harrington (1994) who reported that in a completely mixed flow reactor (CMFR), an increase in pH required an increase in ozone dose to achieve a target ozone residual. Harrington also reported that bromate formation was not dependent on pH in a continuous-flow system for pH's of 7.0 and 8.5.

4.2 Effect of Influent Br^- Concentration

The effect of influent Br^- concentration was investigated by varying the Br^- concentration at 50, 100, 300, and 500 µg/L under the baseline conditions of 2.5 mg/L TOC, pH 7.0, and 1 mM carbonate. The bromide concentrations examined are representative of those found in drinking water sources. The results are shown in Figures 4.4a and b. Figure 4.4a shows that as ozone dose increases, the effluent dissolved ozone residual increases in an exponential manner, independent of the influent bromide concentration. This agrees with the findings of Harrington (1994) who conducted similar CMFR experiments. The results in Figure 4.4a can be fit by a single exponential relationship, as shown in Figure 4.5a.

The results in Figure 4.4b, indicate that bromate concentration does appear to be dependent on influent Br^- concentration, as expected. The results in Figure 4.5b show that for the lower influent bromide concentrations (i.e., 50 and 100 µg/L), there was not a statistically significant difference in the effluent bromate concentration results, at the α=0.05 level. Therefore, a single exponential curve was fit to both sets of results. This was also true for the two higher bromide concentrations of 300 and 500 µg/L, i.e., there was no statistical difference in the effluent bromate concentration results. Hence, a single exponential curve was also fit to the higher bromide concentration results. Table 4.3 shows the equations for the exponential model curves.

Table 4.3 Model Equations for Influent Br^- Variations

	Ozone Residual (mg/L)		Bromate Formation (µg/L)	
Influent Br^- (µg/L)	Equation	R^2	Equation	R^2
50, 100	$0.0129e^{1.0790x}$	0.91	$0.0831e^{1.3974x}$	0.84
300, 500	$0.0129e^{1.0790x}$	0.91	$0.2029e^{1.5183x}$	0.74

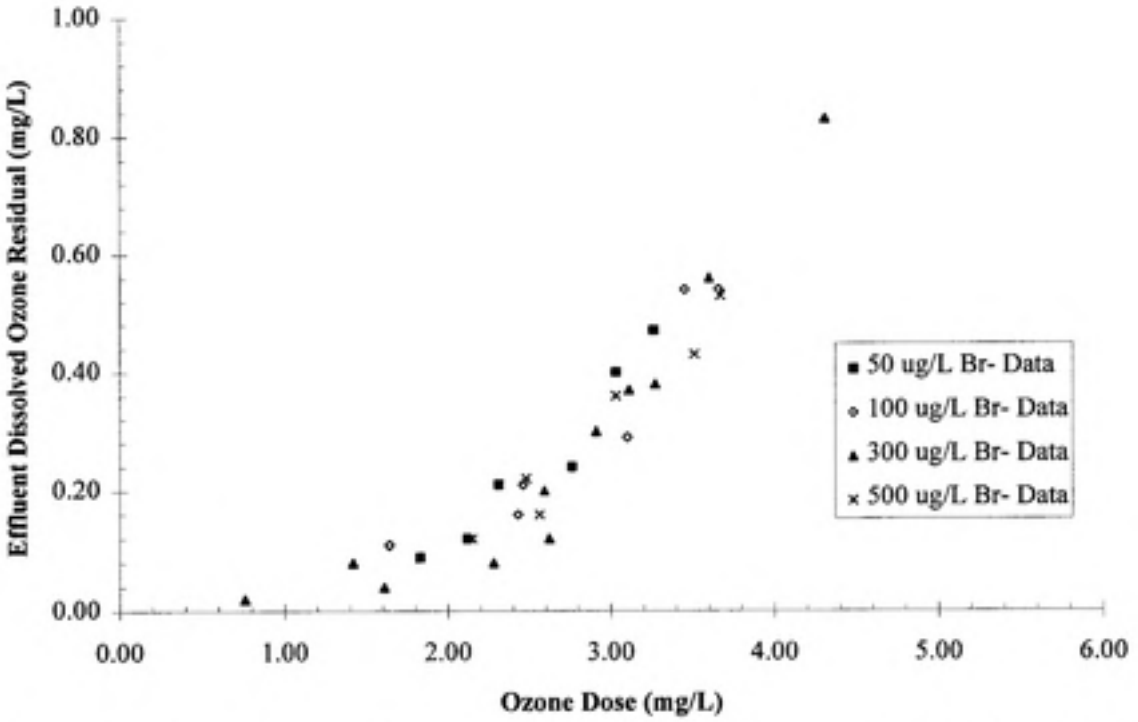

FIGURE 4.4 (A) EFFECT OF OZONE DOSE ON EFFLUENT OZONE RESIDUAL FOR VARIOUS INFLUENT Br^- CONCENTRATIONS

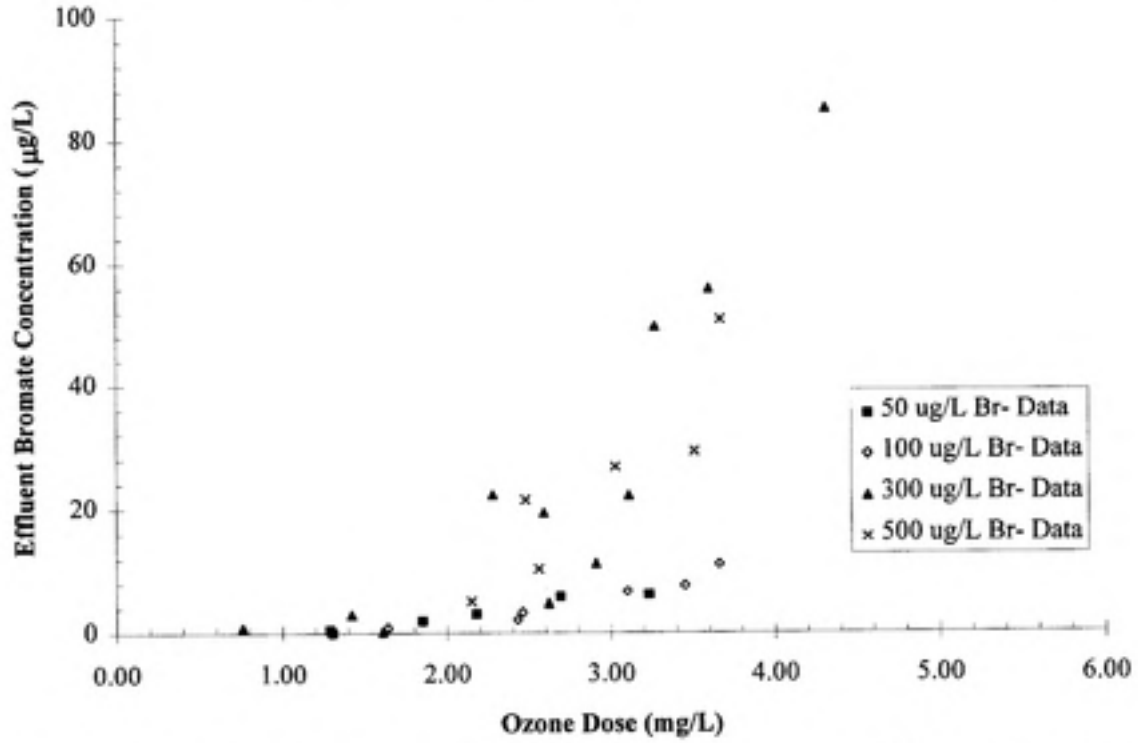

FIGURE 4.4 (B) BROMATE FORMATION FOR VARIOUS INFLUENT Br^- CONCENTRATIONS
(pH 7.0, 1 mM carbonate, 2.5 mg/L TOC)

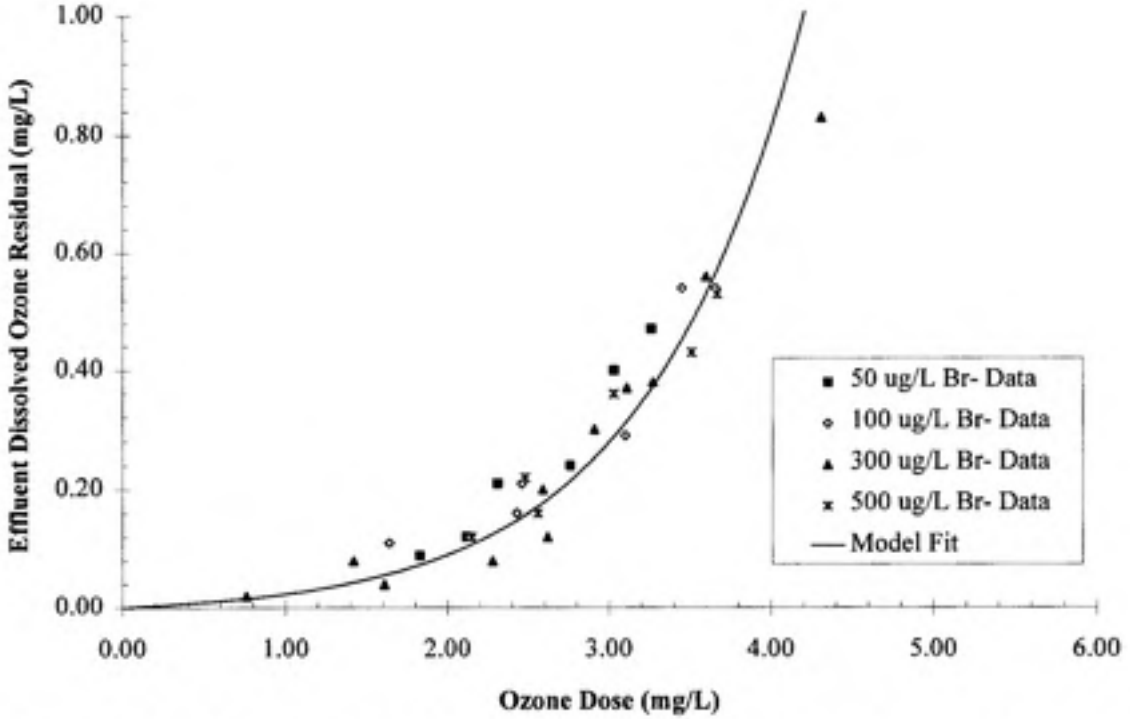

FIGURE 4.5 (A) EXPONENTIAL MODEL ILLUSTRATING EFFECT OF OZONE DOSE ON EFFLUENT OZONE RESIDUAL FOR VARIOUS INFLUENT Br^- CONCENTRATIONS

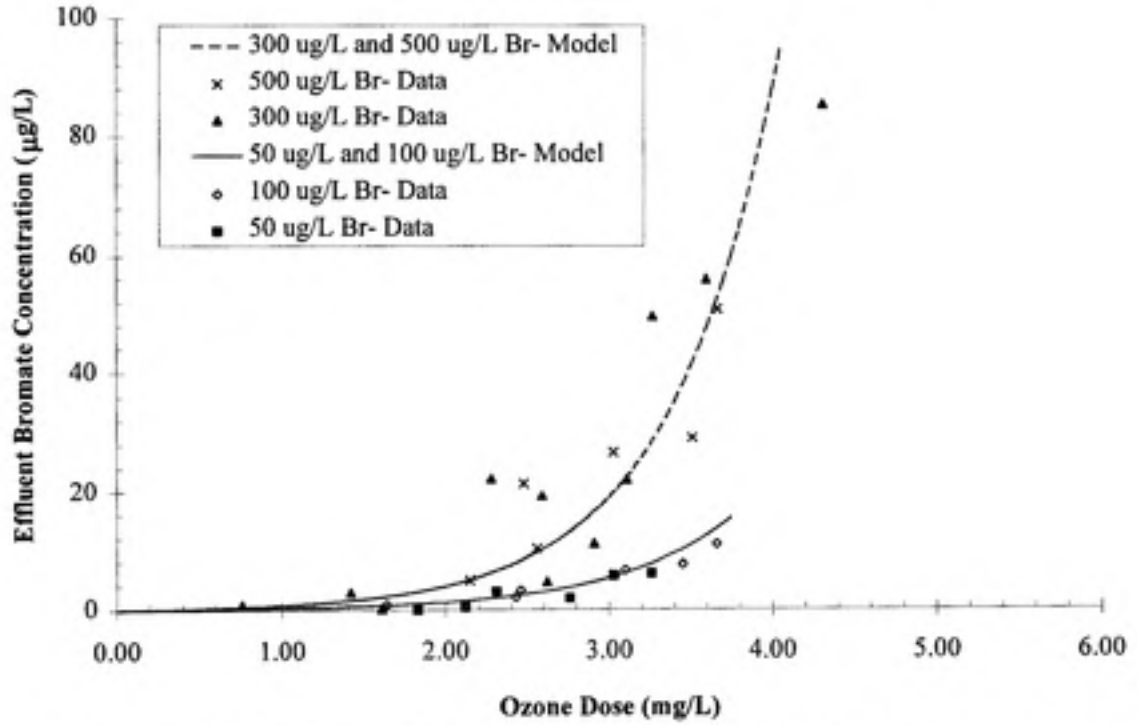

FIGURE 4.5 (B) EXPONENTIAL MODEL ILLUSTRATING BROMATE FORMATION FOR VARIOUS INFLUENT Br^- CONC. (pH 7.0, 1 mM carbonate, 2.5 mg/L TOC)

The results in Figures 4.5a and b show that for a constant ozone dose, bromate concentration increases as bromide concentration increases. For a target ozone residual of 0.4 mg/L, corresponding to an ozone dose of 3.3 mg/L, the 50/100 µg/L influent Br^- concentration formed only 8.4 µg/L of bromate in contrast to the 31 µg/L of bromate formed when the influent Br^- concentrations were 300/500 µg/L. These results agree with theory which indicates the concentration of hypobromite, which leads to the formation of bromate, should increase with increases in bromide ion concentration. The implications of influent bromide concentration on bromate formation are discussed further in Section 4.9 with respect to disinfection credit.

4.3 Effect of TOC Concentration

TOC concentrations of 0.0, 2.5, and 5.0 mg/L as C were investigated to assess the effect of organic carbon on effluent ozone residual and bromate formation. The baseline synthetic water conditions were pH 7.0, 1 mM carbonate concentration, and 300 µg/L Br^-. Figures 4.6a and b display the results and the corresponding fitted exponential model curves for the TOC concentrations examined, and Table 4.4 gives the equations for the model curves. Although the model fit for the 0.0 mg/L TOC case is not a very good fit, the same model format was used for consistency and for purposes of comparison. Figure 4.6a shows that the required ozone dose to achieve measurable ozone residuals increased with an increase in TOC concentration, as expected. Organic carbon exerts an ozone demand which promotes the consumption of ozone. Therefore, as organic carbon concentration increases, more ozone is required to achieve a dissolved ozone residual. For a TOC concentration of 5.0 mg/L, an ozone dose of more than 4.5 mg/L was necessary to achieve a measurable dissolved ozone residual, whereas for the 0.0 mg/L TOC case, an ozone residual as high as 0.30 mg/L was achieved at a 0.80 mg/L ozone dose.

For any ozone dose, bromate formation increases with decreasing TOC concentration, as shown in Figure 4.6b. Thus, at a constant ozone dose, the solutions

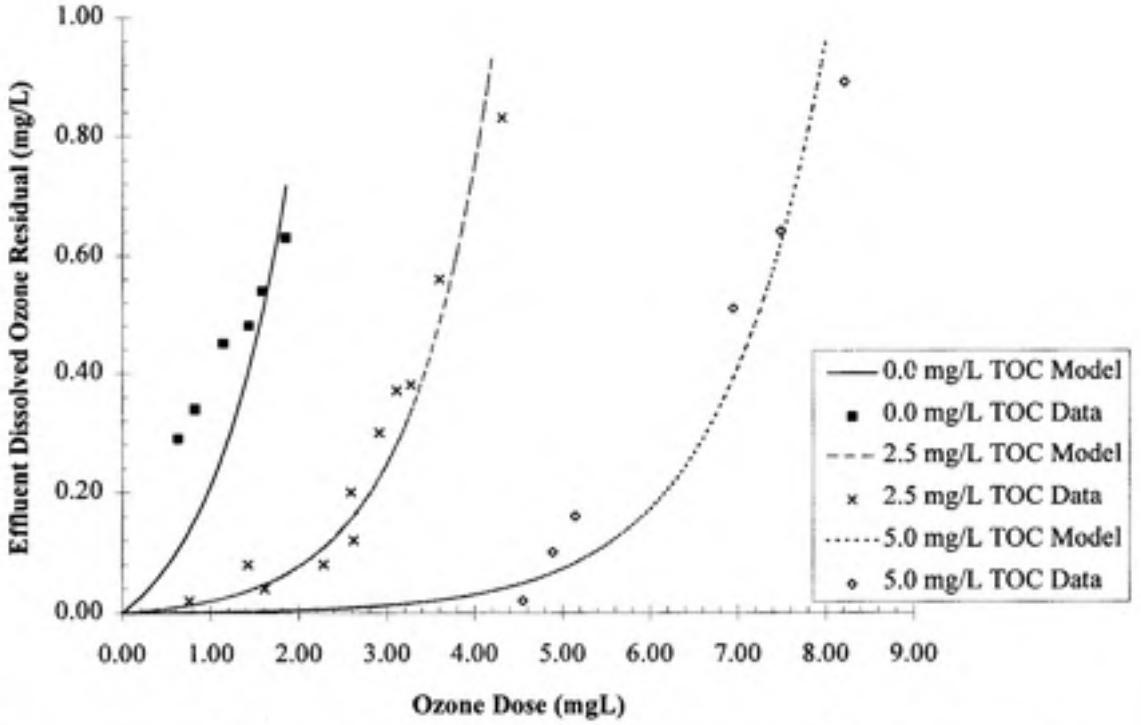

FIGURE 4.6 (A) EFFLUENT OZONE RESIDUAL FOR VARIOUS TOC CONCENTRATIONS

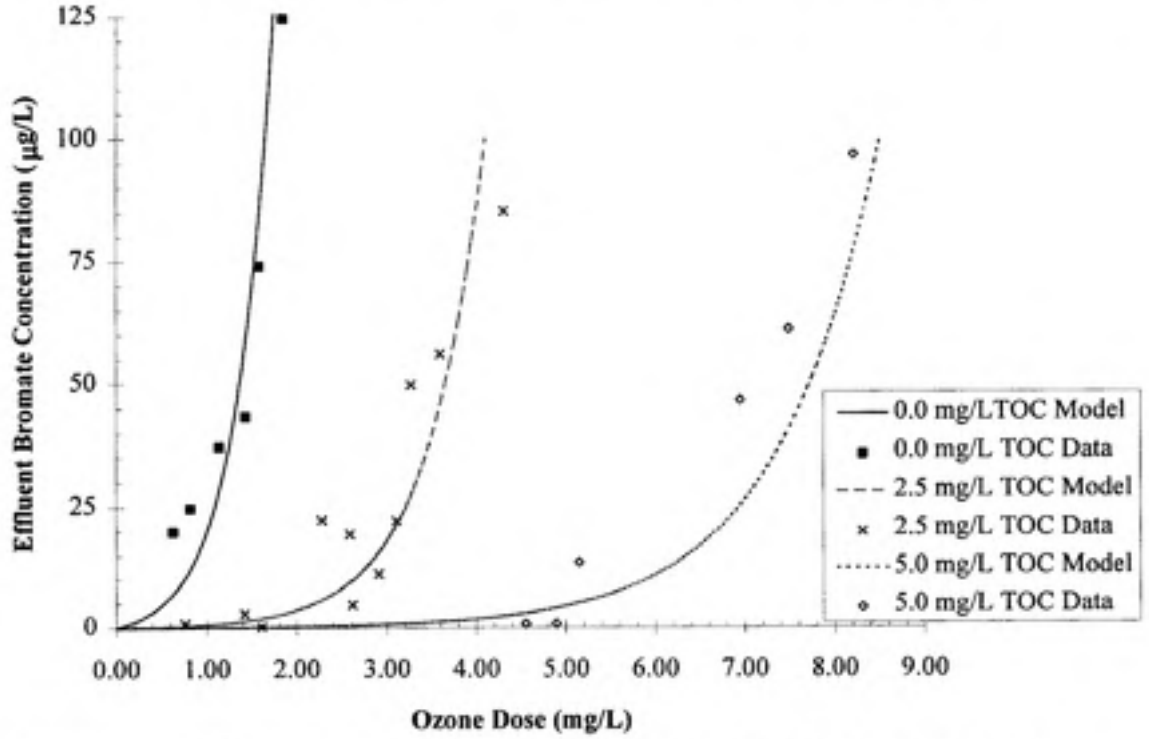

FIGURE 4.6 (B) BROMATE FORMATION FOR VARIOUS TOC CONCENTRATIONS
(pH 7.0, 1 mM carbonate, 300 µg/L Br^-)

with lower organic carbon concentrations exert less of an ozone demand and therefore more ozone is available to react with the bromide ion to form bromate.

TABLE 4.4 MODEL EQUATIONS FOR TOC CONCENTRATIONS

	Ozone Residual (mg/L)		Bromate Formation (µg/L)	
TOC Conc. (mg/L)	Equation	R^2	Equation	R^2
0.0	$0.1000e^{1.1347x}$	0.22	$2.0000e^{2.3851x}$	0.50
2.5	$0.0099e^{1.0864x}$	0.93	$0.1747e^{1.5494x}$	0.74
5.0	$0.0010e^{0.8590x}$	0.85	$0.0551e^{0.8831x}$	0.75

Bromate concentrations were greatest in the synthetic water in the absence of organic matter. Table 4.5 presents a comparison for two target ozone residuals, 0.2 mg/L and 0.5 mg/L, for TOC concentrations of 0.0 mg/L, 2.5 mg/L, and 5.0 mg/L, using the exponential model equations shown in Table 4.5 and illustrated in Figures 4.6a and b. For the lower ozone residual, bromate formation is approximately the same for all TOC concentrations, but at the high target dissolved ozone residual, bromate formation increases as the TOC concentration decreases.

TABLE 4.5 EFFECT OF TOC CONCENTRATION ON CALCULATED BROMATE FORMATION FOR TWO TARGET OZONE RESIDUALS

	Target Ozone Residual 0.2 mg/L		Target Ozone Residual 0.5 mg/L	
TOC Conc. (mg/L)	Required Ozone Dose (mg/L)	Corresponding Bromate Conc. (µg/L)	Required Ozone Dose (mg/L)	Corresponding Bromate Conc. (µg/L)
0.0	0.6	8.6	1.4	59
2.5	2.8	13	3.6	47
5.0	6.2	13	7.2	33

The differences in bromate formation are relatively small and appear to be insensitive to organic carbon concentration at lower effluent dissolved ozone residuals but, in general, bromate concentrations tend to increase with a decrease in TOC concentration. These results are in contrast to those of Najm and Krasner (1995) who found, for flow-through reactor, that for a constant influent bromide concentration, an increase in TOC concentration produced an increase in bromate concentration. Natural

organic matter (NOM) competes with the bromide ion for reaction with molecular ozone. The NOM consumes the ozone which can alter the hydroxyl radical yield in the system. This will affect both the direct and indirect pathways for bromate formation. These results suggest that the increase in organic matter consumed more hydroxyl radicals, thereby decreasing the extent of bromate production.

4.4 Effect of Inorganic Carbon Concentration

The formation of bromate as a result of varying inorganic carbon concentrations was examined at pH 7.0, 2.5 mg/L TOC, 300 µg/L Br^-, and 0.0, 1.0, and 2.0 mM carbonate concentrations. Figures 4.7a and b show the results for the various inorganic carbon concentrations examined. At the α=0.05 level, there is no significant difference in either the bromate or ozone residual results for 1 and 2 mM carbonate; therefore one curve was fit through these two data sets. The equations for the trendlines are shown in Table 4.6.

Table 4.6 Model Equations for Inorganic Carbon Concentrations

	Ozone Residual (mg/L)		Bromate Formation (µg/L)	
Carbonate Conc. (mM)	Equation	R^2	Equation	R^2
0	$0.0126e^{0.8324x}$	0.77	$0.0182e^{1.4539x}$	0.83
1, 2	$0.0124e^{1.0296x}$	0.89	$0.2246e^{1.514x}$	0.75

In Figure 4.7a, it appears that in the presence of carbonate species, i.e., bicarbonate and carbonate ions, both of which are hydroxyl radical scavengers, ozone residuals increased for any applied ozone dose compared to water in the absence of carbonate species. This is due to the scavenging of hydroxyl radicals by the carbonate species, which decelerates ozone decomposition and promotes the persistence of a higher effluent dissolved ozone residual. In Figure 4.7b, in the absence of carbonate, measurable bromate concentrations were not detected until ozone doses greater than 3.3 mg/L, with a fairly flat bromate formation response curve with increasing ozone dose. In contrast, a dramatic increase in bromate formation was observed at an ozone dose above 2.5 mg/L in the presence of inorganic carbon and the bromate formation curve was relatively steep in

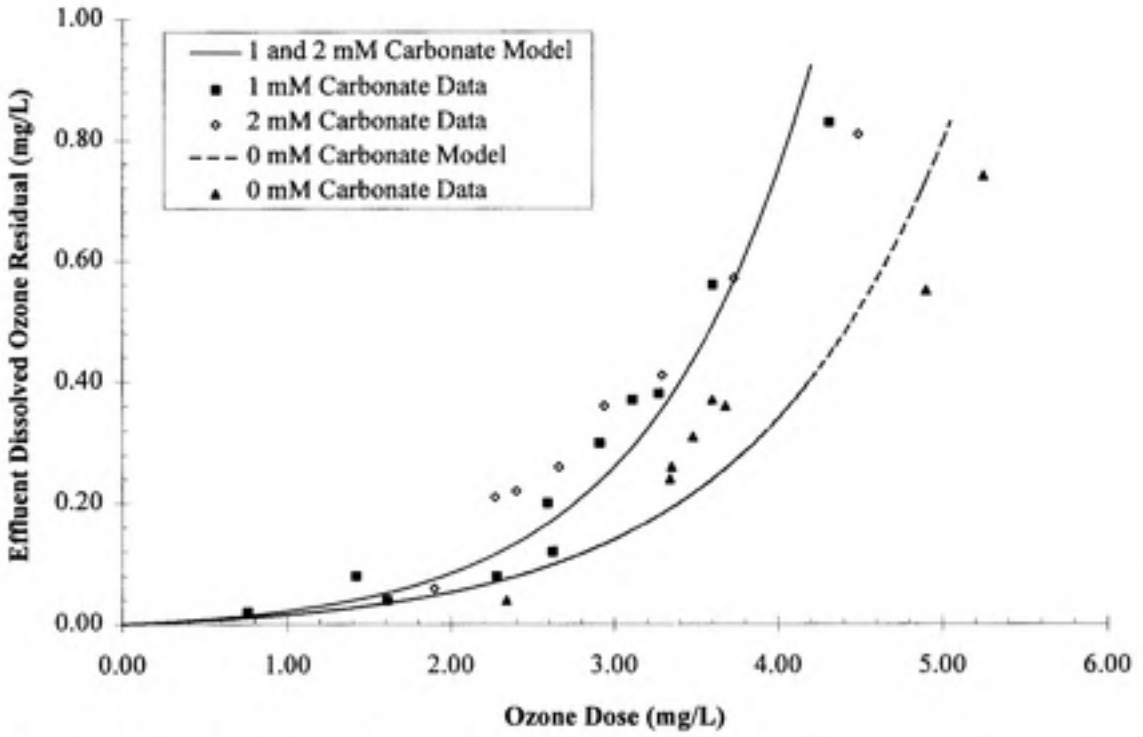

FIGURE 4.7 (A) EFFLUENT OZONE RESIDUAL FOR VARIOUS INORGANIC CARBON CONCENTRATIONS

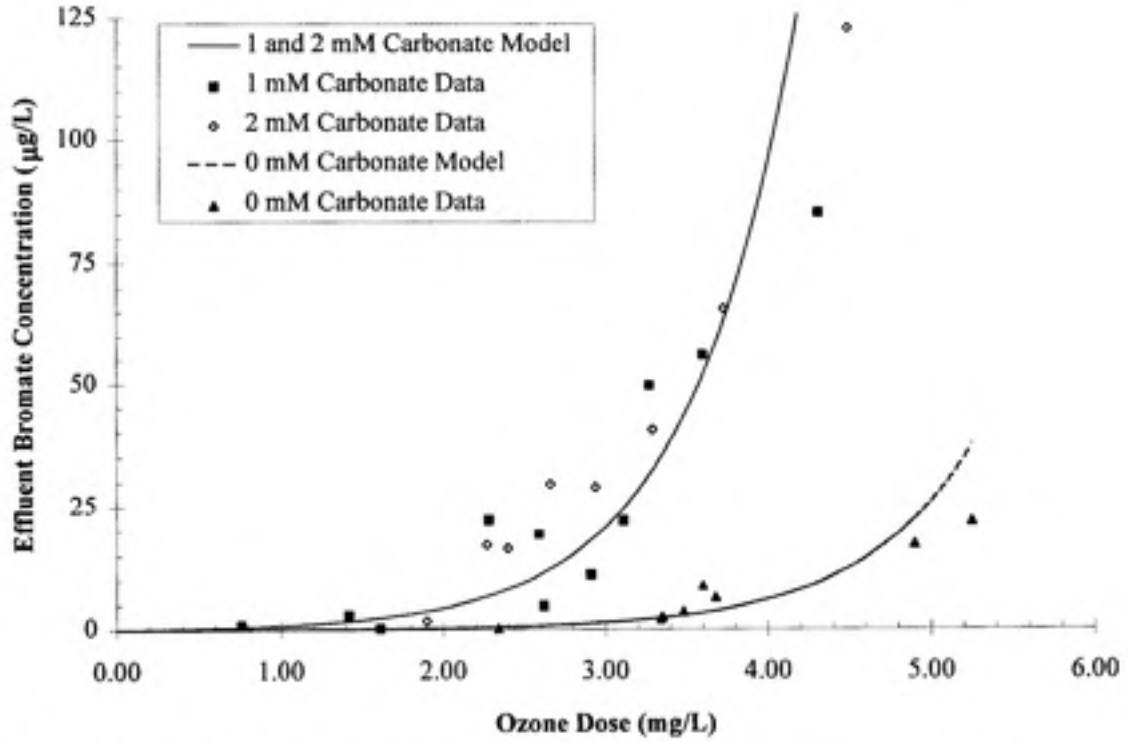

FIGURE 4.7 (B) BROMATE FORMATION FOR VARIOUS INORGANIC CARBON CONCENTRATIONS (pH 7.0, 2.5 mg/L TOC, 300 µg/L Br^-)

comparison. This is further illustrated by the results in Table 4.7. For two target ozone residuals of 0.2 mg/L and 0.4 mg/L, the calculated bromate formation was approximately five times greater with carbonate species present compared to bromate formation in the absence of inorganic carbon. Table 4.7 also shows that without inorganic carbon present, greater ozone doses are required to achieve the target ozone residuals, compared to the lower required ozone doses for the waters with inorganic carbon present. All ozone doses examined without carbonate species present produced bromate concentrations below 25 µg/L, the WHO suggested limit, even with dissolved ozone residuals as high as 0.7 mg/L. Croue et al. (1995) reported that the addition of inorganic carbon increased bromate formation in a treated drinking water (Temp. 20°C, 2.0 mg/L aquatic fulvic acid, 200 µg/L Br^-) at pH 6.4 in a continuous-flow system. These findings are consistent with those reported here.

TABLE 4.7 CALCULATED BROMATE FORMATION FOR VARIOUS CARBONATE CONCENTRATIONS

Carbonate Conc. (mM)	Target Ozone Residual 0.2 mg/L		Target Ozone Residual 0.4 mg/L	
	Required Ozone Dose (mg/L)	Corresponding Bromate Conc. (µg/L)	Required Ozone Dose (mg/L)	Corresponding Bromate Conc. (µg/L)
0	3.3	2.3	4.2	8.3
1, 2	2.7	13	3.4	37

Although it has been suggested that carbonate species act as hydroxyl radical scavengers to slow down the formation of bromate, these results show that bromate production is enhanced by the presence of the carbonate species. As stated in Chapter 2, recent theories by Westerhoff et al. (1994) indicate that the carbonate radicals produced from scavenging the hydroxyl radicals play a role in bromate production. Therefore, it appears that these results agree with that theory.

4.5 Effect of t-Butanol Addition

Tertiary butyl-alcohol (t-butanol), a well-known hydroxyl radical scavenger (von Gunten and Hoigne, 1994), was investigated to determine its effect on the formation of bromate. The effect of t-butanol was examined at pH 7.0, 2.5 mg/L TOC, 1 mM carbonate, 300 µg/L Br^-, and a 5:1 molar ratio of t-butanol to applied ozone dose. Figure 4.8 shows an increase in ozone residual with t-butanol as compared to the same synthetic water in the absence of t-butanol. In addition to acting as a hydroxyl radical scavenger, the t-butanol also appeared to produce smaller bubbles during ozonation. Therefore, the measured increase in dissolved ozone residual could be due to increased mass transfer from the decrease in bubble size and/or to the radical scavenging properties of the t-butanol. Table 4.8 shows the ozone residual equations for the t-butanol results.

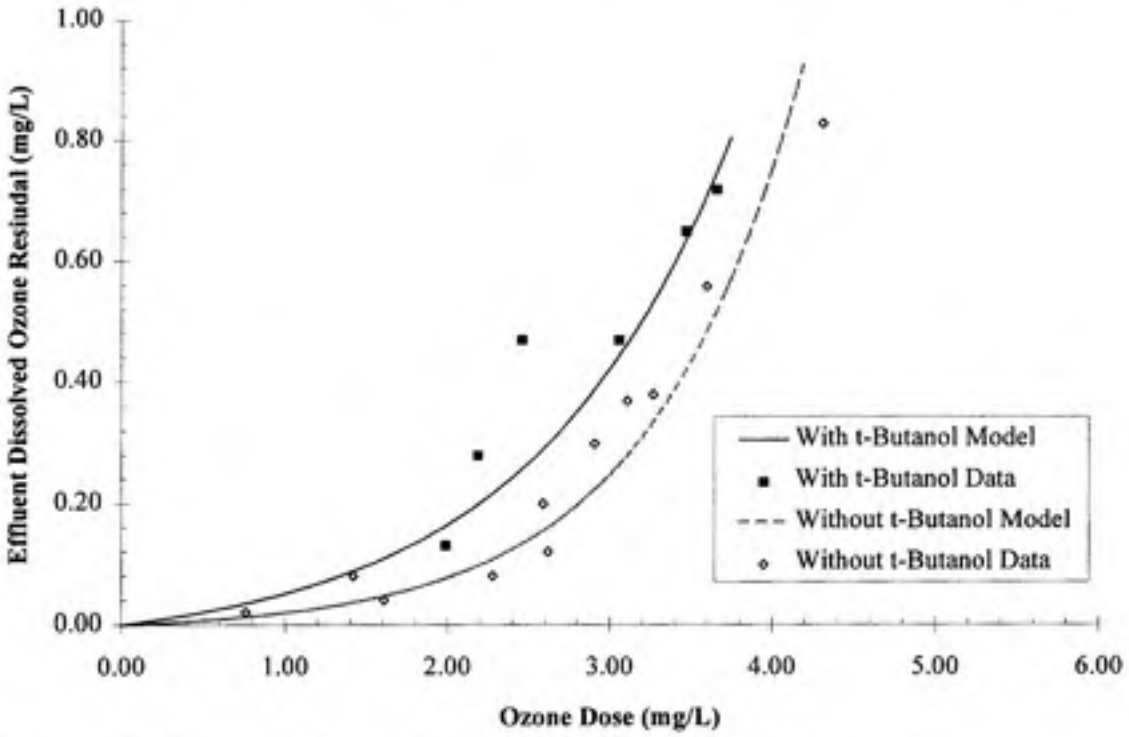

Figure 4.8 Effluent Ozone Residual With t-Butanol Addition
(pH 7.0, 2.5 mg/L TOC, 300 µg/L Br^-, 1 mM total carbonate)

TABLE 4.8 MODEL EQUATIONS FOR T-BUTANOL ADDITION

	Ozone Residual (mg/L)	
T-Butanol Addition	**Equation**	**R^2**
With	$0.0405e^{0.811x}$	0.78
Without	$0.0099e^{1.0864x}$	0.93

Table 4.9 displays the dramatic decrease in bromate formation due to the addition of t-butanol. Most of the samples with t-butanol addition had effluent bromate concentrations less than 0.2 µg/L, the detection limit for bromate, even at dissolved ozone residuals greater than 0.6 mg/L. Therefore, the presence of a hydroxyl radical scavenger like t-butanol, appears to be an effective method for controlling bromate formation.

TABLE 4.9 EFFECT OF T-BUTANOL ADDITION ON BROMATE FORMATION

With t-Butanol			Without t-Butanol		
Transferred Ozone Dose (mg/L)	**Ozone Residual (mg/L)**	**Bromate Conc. (µg/L)**	**Transferred Ozone Dose (mg/L)**	**Ozone Residual (mg/L)**	**Bromate Conc. (µg/L)**
2.0	0.1	<0.2	0.8	0.02	0.8
2.2	0.3	<0.2	1.4	0.08	3.0
2.5	0.5	<0.2	1.6	0.04	0.2
3.1	0.5	<0.2	2.3	0.08	22
3.5	0.7	<0.2	2.6	0.1	5.0
3.7	0.7	0.4	2.6	0.2	19
			2.9	0.3	11
			3.1	0.4	22
			3.3	0.4	50
			3.6	0.6	56
			4.3	0.8	86

Westerhoff et al. (1994) made a comparison under batch conditions between the use of t-butanol and carbonate as radical scavengers compared to ozonation without a radical scavenger. They found that both scavengers doubled the half-life of ozone. They reported bromate concentrations of 44 µg/L in the absence of a scavenger, 181 µg/L with the addition of carbonate, and 4 µg/L with the addition of t-butanol. Thus, the carbonate species are a less effective radical scavenger for bromate control than t-butanol; the

ineffectiveness of the carbonate species was attributed to the ability of the carbonate radical to act as a secondary oxidant in the formation of bromate (Westerhoff et al., 1994). This is not the case with t-butanol. The findings reported here under continuous-flow conditions, are consistent with those findings and that interpretation.

4.6 Effect of Variable Gas and Liquid Flow Rates

Mass transfer effects were investigated by varying the baseline gas and liquid flow rates of 395 mL/min and 50 mL/min, respectively. The baseline gas flow rate was chosen based on the balance of pressure in the system, as well as the intent to produce bubble sizes and concentrations similar to those found in ozone contactors used in practice. The liquid flow rate was chosen to model representative hydraulic residence times used in practice.

The variation in gas flow rate was examined at 100 mL/min and 395 mL/min; the results with the corresponding exponential model curves are presented in Figures 4.9a and b. The equations for the model curves are shown in Table 4.10. Although the fit of the exponential model for the 100 mL/min ozone residual data is not as good for the other models, it was used for consistency and comparison purposes.

Table 4.10 Model Equations for Various Gas Flow Rates

	Ozone Residual (mg/L)		Bromate Formation (µg/L)	
Flow Rate (mL/min)	Equation	R^2	Equation	R^2
100	$0.1136e^{1.2983x}$	0.59	$5.251e^{1.3313x}$	0.92
395	$0.0099e^{1.0864x}$	0.93	$0.1747e^{1.5494x}$	0.74

Figure 4.9a shows that an increase in the effluent dissolved ozone residual was observed with a decrease in gas flow rate. These results are contrary to what would intuitively be expected. The decrease in the gas flow rate would be expected to increase the bubble size and decrease the number of bubbles in the reactor at any time, both of which should decrease the mass transfer of ozone to the solution. However, at the lower gas flow rate, the gas stream has a longer contact time with the plates in the ozone generator resulting in an increase in the partial pressure of ozone in the applied gas. This

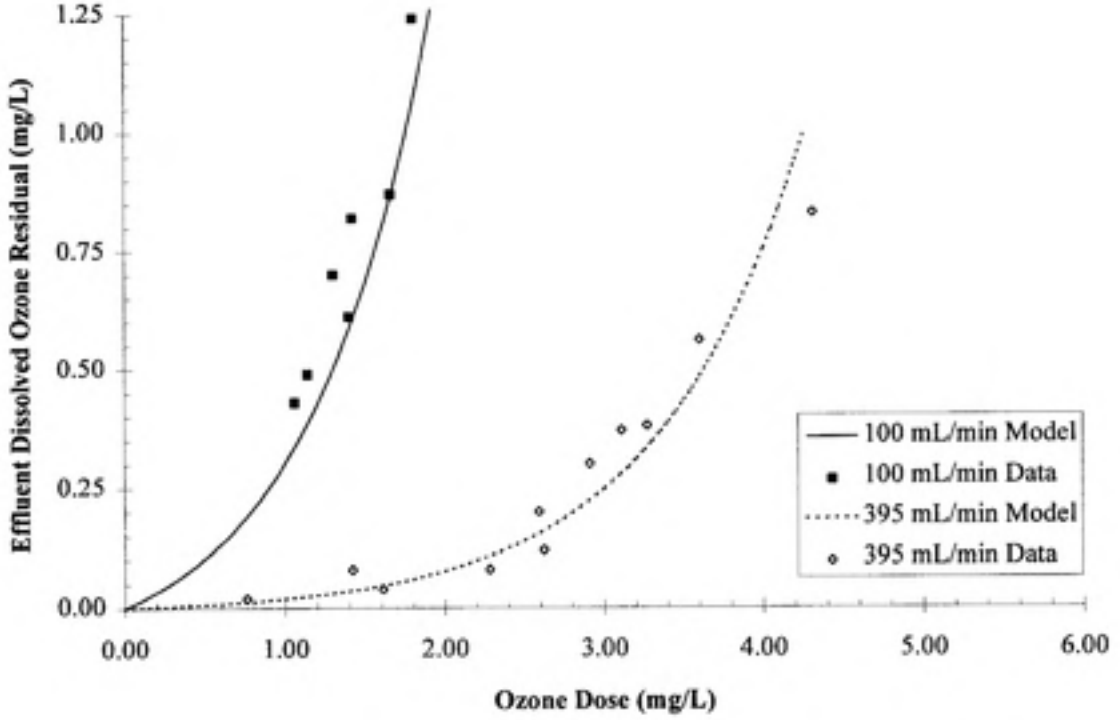

FIGURE 4.9 (A) EFFLUENT OZONE RESIDUAL FOR VARIOUS GAS FLOW RATES

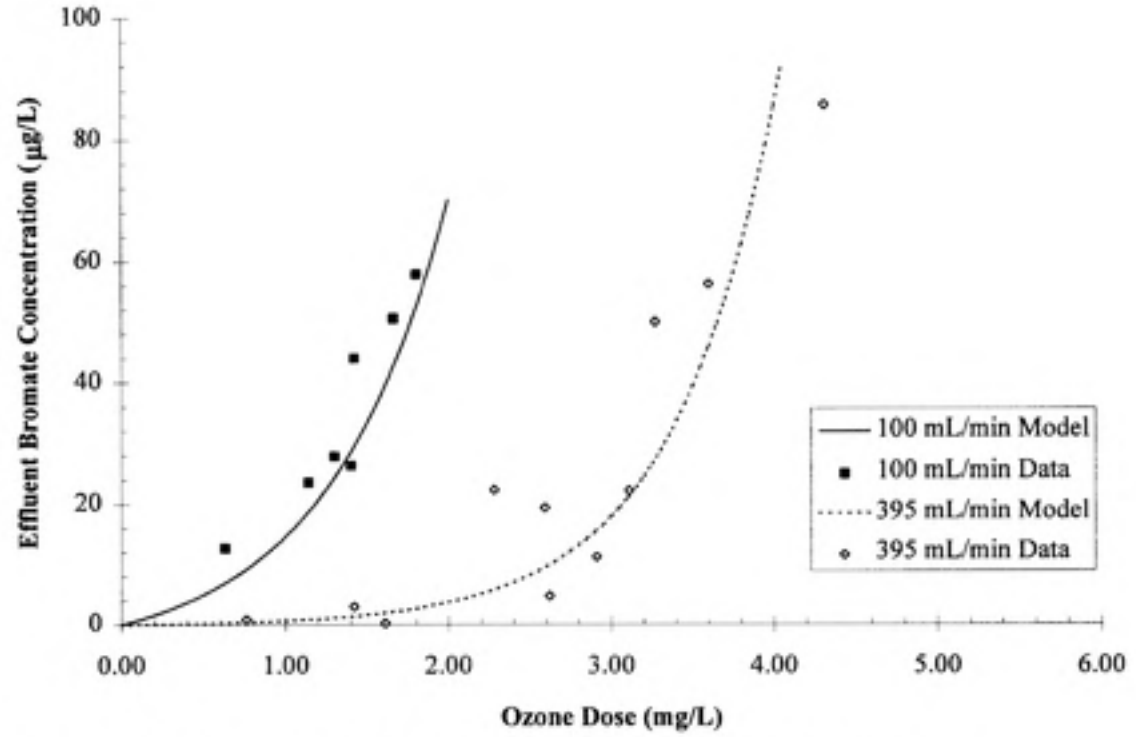

FIGURE 4.9 (B) BROMATE FORMATION FOR VARIOUS GAS FLOW RATES

(pH 7.0, 2.5 mg/L TOC, 300 µg/L Br^-, 1 mM carbonate)

increases the driving force for more ozone to be transferred into the system during the same ten minute hydraulic residence time. This is demonstrated in Table 4.11 by the increased ozone concentration in the influent gas stream at the lower gas flow rate. Table 4.11 provides some of the results obtained for the same power settings on the ozone generator for each flow rate. For the lower flow rate, the influent ozone gas concentrations and partial pressures are all higher than for the baseline flow rate conditions. Also, gas was transferred twice as efficiently at the 100 mL/min flow rate than at the 395 mL/min flow rate. From the results in Figure 4.9a, the increase in the partial pressure of ozone in the gas stream seems to dominate over the lower gas flow rate.

TABLE 4.11 SYSTEM CHARACTERISTICS FOR VARIOUS GAS FLOW RATES

Q_g=100 mL/min			
Setting	**Cg, in (mg/L)**	**PO_3 (atm)**	**Transfer Eff. (%)**
1	2.1	0.0010	26
2	3.0	0.0014	28
3	3.8	0.0018	26
4	4.1	0.0019	30
5	5.8	0.0027	26
Q_g=395 mL/min			
Setting	**Cg, in (mg/L)**	**PO_3 (atm)**	**Transfer Eff. (%)**
1	0.6	0.0003	15
2	1.2	0.0006	15
3	2.0	0.0009	16
4	2.7	0.0013	14
5	3.0	0.0014	14

Figure 4.9b shows the formation of bromate for the two gas flow rates. For any target ozone residual, bromate formation decreased with a decrease in gas flow rate. For example, at a dissolved ozone residual of 0.4 mg/L, an ozone dose of only 1.0 mg/L was required at a gas flow rate of 100 mL/min and the corresponding bromate concentration was 19 µg/L. In comparison, for the same target ozone residual, an ozone dose of 3.4 mg/L was required at a gas flow rate of 395 mL/min and the corresponding bromate concentration was 34 µg/L.

The various liquid flow rates examined included the baseline flow rate of 50 mL/min, as well as flow rates of 25, 150, and 250 mL/min. Table 4.12 gives the corresponding hydraulic residence times (HRTs) for each flow rate. The data for all of the flow rates examined is shown in Table 4.13.

TABLE 4.12 LIQUID FLOW RATES EXAMINED AND THEIR CORRESPONDING HRTS

Flow rate (mL/min)	Hydraulic Residence Time (min)
25	20
50	10
150	3.3
250	2

The data show that for each applied ozone dose, residual ozone concentrations increased, as flow rate increased. Again, these results differ from expectations. One would expect that with increasing liquid flow rate, a decrease in dissolved ozone residuals would be observed because the water is in contact with the ozone for less time. Yet, the transfer efficiencies in Table 4.13 exhibit the same trend as the ozone residuals, i.e., as liquid flow rate increased, overall ozone transfer efficiencies increased, too. For example, for a transferred ozone dose of approximately 2.6 mg/L, as shown by the shaded areas in Table 4.13, the transfer efficiency increased from 14% to 24% as the liquid flow rate increased from 25 mL/min to 250 mL/min. Therefore, the increased mixing conditions in the reactor at increased liquid flow rates apparently allowed for more mass transfer of ozone into the liquid phase, resulting in higher dissolved ozone residuals. Also, it may be that the transfer of ozone into the liquid phase is a faster reaction than the subsequent reaction of ozone with TOC or Br^-. Thus, at the shorter HRTs, there was enough time for ozone to be transferred into the liquid phase and to create a dissolved ozone residual, but not enough time for the ozone to react with the TOC or Br^-, thereby resulting in the formation of less bromate, as shown in the following figures.

TABLE 4.13 TRANSFER EFFICIENCIES FOR VARIOUS LIQUID FLOW RATES

	Q_l=25 mL/min			Q_l=250 mL/min	
Ozone Dose (mg/L)	Ozone Residual (mg/L)	Transfer Eff. (%)	Ozone Dose (mg/L)	Ozone Residual (mg/L)	Transfer Eff. (%)
2.8	0.2	14	0.9	0.01	43
3.4	0.3	13	1.2	0.03	25
3.9	0.3	8.2	2.1	0.3	24
4.3	0.5	11	2.6	0.5	24
4.6	0.5	9.2	2.7	0.6	24
5.3	0.8	6.5	2.8	0.8	19
	Q_l=50 mL/min			Q_l=150 mL/min	
Ozone Dose (mg/L)	Ozone Residual (mg/L)	Transfer Eff. (%)	Ozone Dose (mg/L)	Ozone Residual (mg/L)	Transfer Eff. (%)
0.8	0.02	15	1.0	0.02	40
1.4	0.08	15	1.3	0.02	32
1.6	0.04	31	1.6	0.01	40
2.3	0.08	23	1.6	0.08	19
2.6	0.1	26	1.6	0.04	17
2.6	0.2	16	2.2	0.2	28
2.9	0.3	14	2.6	0.5	21
3.1	0.4	19	2.8	0.7	17
3.3	0.4	14	3.3	0.9	15
3.6	0.6	12			
4.3	0.8	11			

Figures 4.10a and b present the results for all the flow rates examined. The model equations for each of the liquid flow rates are shown in Table 4.14. At the α=0.05 level, a significant difference was not found in the results for the ozone residuals and bromate concentrations for the 150 mL/min and 250 mL/min flow rates; therefore, a single model curve was fit through those data points. In Figure 4.10a and b, it is evident that at a constant ozone dose, the dissolved ozone residual and bromate production increase as liquid flow rate increases.

Figures 4.11a and b show the results and model curves for the 25 mL/min and 150/250 mL/min experiments. The results show that, for any target dissolved ozone residual, the formation of bromate increases with an increased hydraulic residence time or decreased flow rate. For example, to achieve an ozone residual of 0.4 mg/L, the lower flow rate required a 4.2 mg/L ozone dose which produced 48 µg/L of bromate, whereas at 150/250 mL/min, an ozone dose of only 2.6 mg/L was required to achieve the same residual, forming only 12 µg/L of bromate. Because the ozone is in contact with the water for a longer time at the lower flow rate, there is more reaction time for bromate to form.

Although a decrease in bromate formation with an increase in ozone residual was observed under the increased liquid flow rate conditions, it is important to note that disinfection, and the ability to gain disinfection credit, is compromised with lower hydraulic residence times.

TABLE 4.14 MODEL EQUATIONS FOR VARIOUS LIQUID FLOW RATES

	Ozone Residual (mg/L)		Bromate Formation (µg/L)	
Liquid Flow Rate (mL/min)	Equation	R^2	Equation	R^2
25	$0.0325e^{0.6021x}$	0.99	$1.4878e^{0.8349x}$	0.96
50	$0.0099e^{1.0864x}$	0.93	$0.1747e^{1.5494x}$	0.74
150, 250	$0.0019e^{2.0616x}$	0.89	$0.0269e^{2.3536x}$	0.92

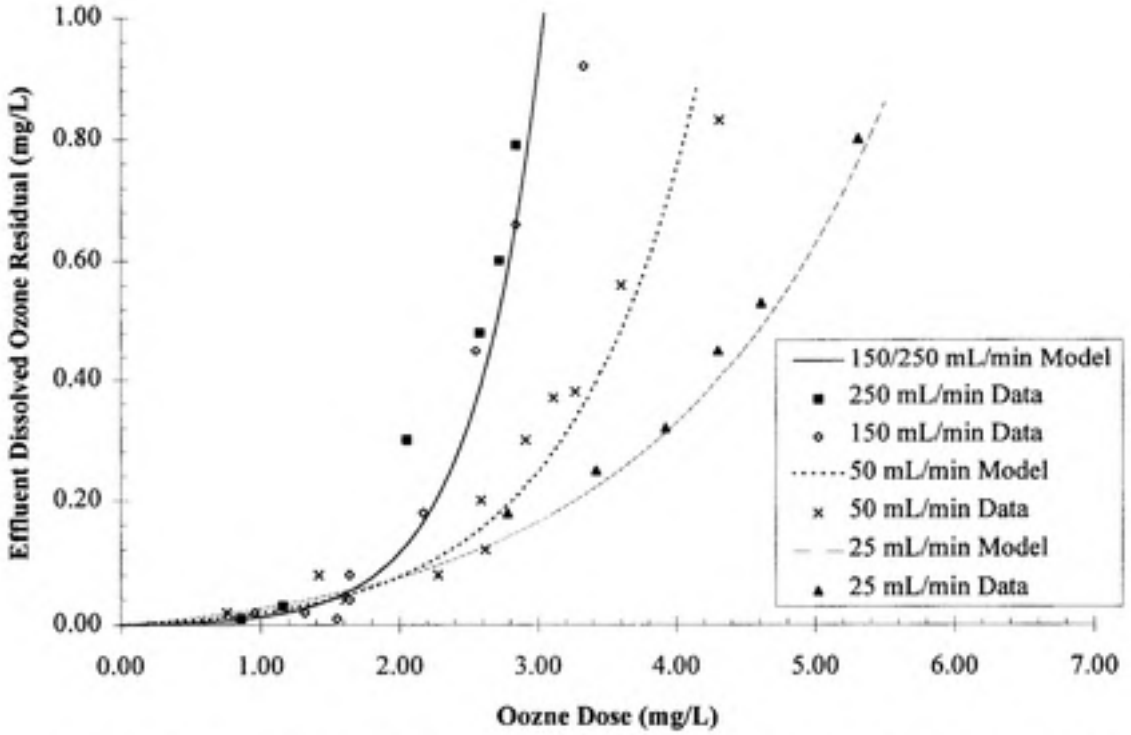

FIGURE 4.10 (A) EFFLUENT OZONE RESIDUAL FOR VARIOUS LIQUID FLOW RATES

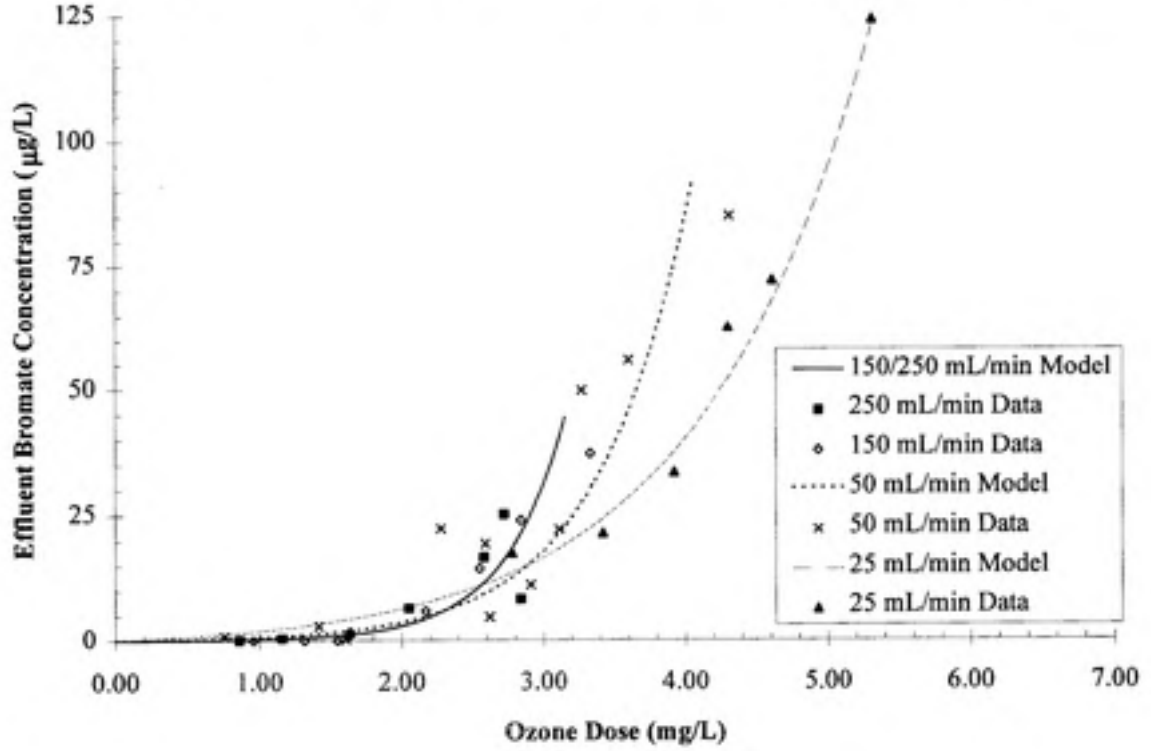

FIGURE 4.10 (B) BROMATE FORMATION FOR VARIOUS LIQUID FLOW RATES
(pH 7.0, 2.5 mg/L TOC, 300 µg/L Br^-, 1 mM carbonate)

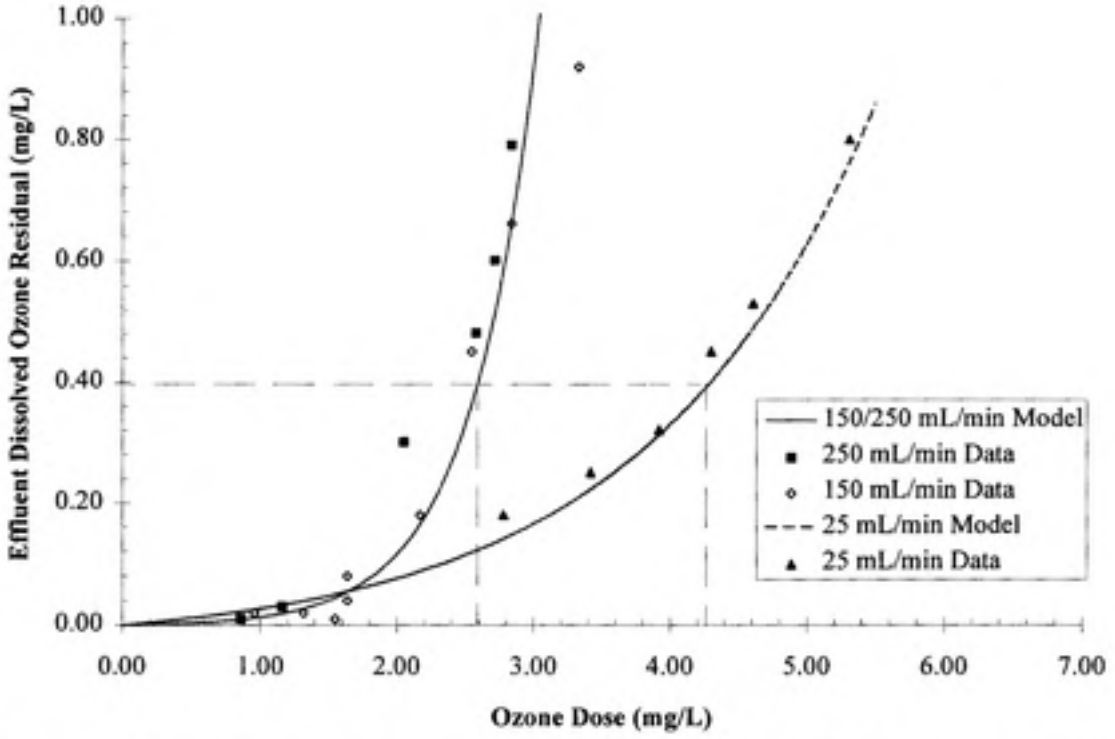

FIGURE 4.11 (A) EFFLUENT OZONE RESIDUALS FOR LIQUID FLOW RATES OF 150/250 AND 25 mL/min

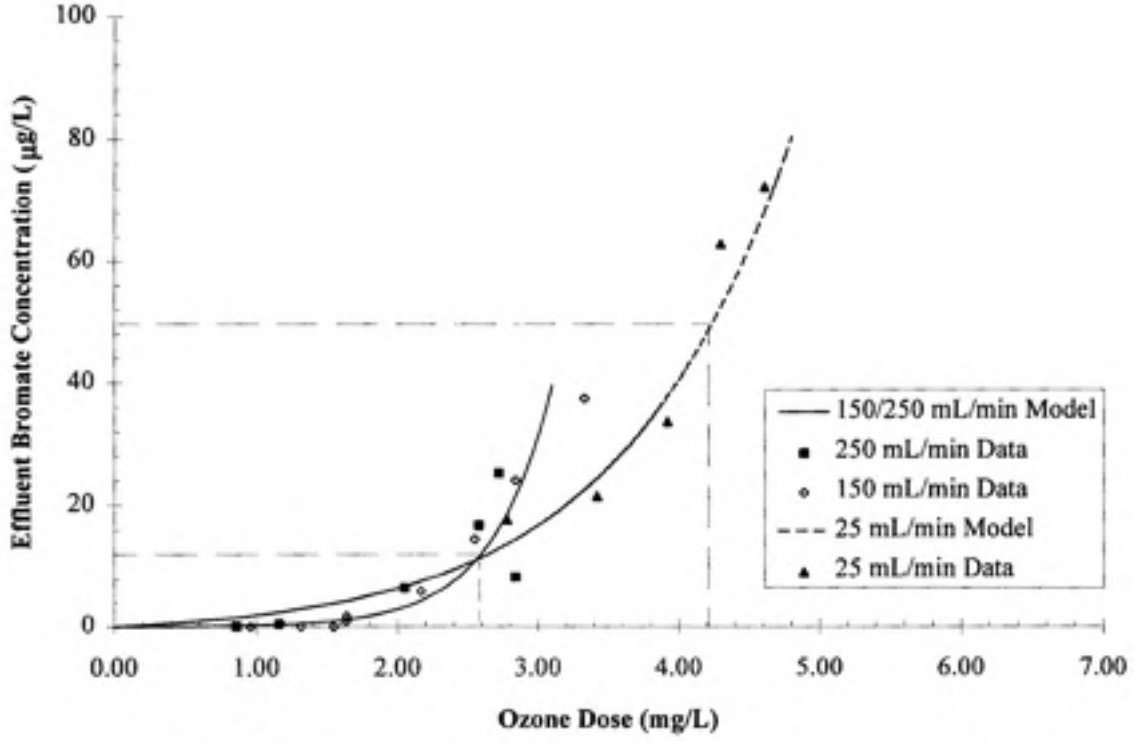

FIGURE 4.11 (B) BROMATE FORMATION FOR LIQUID FLOW RATES OF 150/250 AND 25 mL/min (pH 7.0, 2.5 mg/L TOC, 300 µg/L Br^-, 1 mM carbonate)

4.7 Effect of Ammonia Addition

The addition of ammonia has been proposed as a method of controlling bromate formation (von Gunten and Hoigne, 1994). It has been postulated that ammonia reacts with hypobromous acid to form monobromamine which ties up the hypobromite ion to delay bromate formation. However, the behavior of ammonia is pH-dependent, due to the dissociation of the ammonium ion and hypobromous acid at the pH values associated with water treatment. Several experiments were run to investigate the effectiveness of ammonia addition at two pH's, 7.0 and 8.3. Influent Br^- concentrations and carbonate concentrations were 300 µg/L and 1 mM, respectively. The TOC concentration was 2.5 mg/L and the molar ratio of N:Br was 1:1. The results for pH 7.0 and 8.3 are displayed in Figures 4.12a and b and 4.13a and b, respectively.

At pH 7.0, there appears to be no effect of ammonia addition on dissolved ozone residual or bromate formation, as shown in Figure 4.12. A statistical analysis of the results for both the ozone residuals and bromate concentrations revealed that there was no significant difference between the data with and without the addition of ammonia at the α=0.05 level. Therefore, the results are shown with one common exponential model.

For pH 8.3, at all ozone doses measured, the addition of ammonia resulted in an increased effluent dissolved ozone residual, as shown in Figure 4.13a. Pulse radiolysis research has observed that ammonia will react with hydroxyl radicals; thus, ammonia acts as a radical scavenger (Westerhoff et al., 1994), thereby decelerating ozone decomposition and increasing residual ozone concentrations. In Figures 4.13a and b, the exponential model curves are provided only for the results without the addition of ammonia. The results for the addition of ammonia do not show an exponential trend.

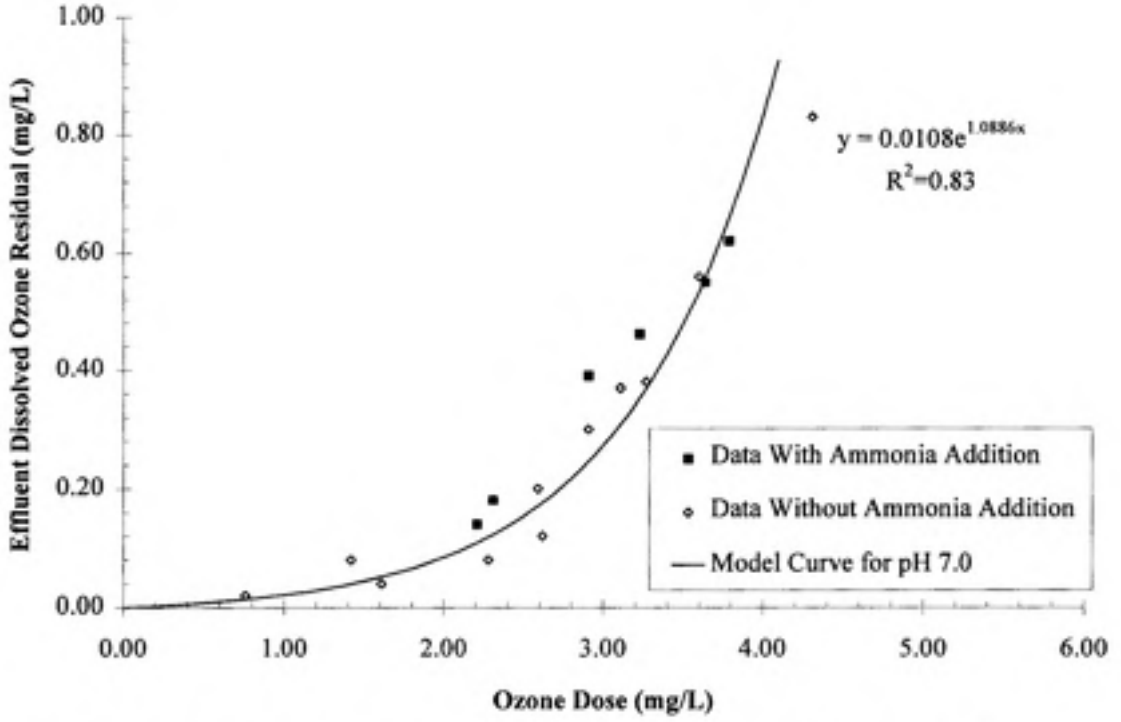

FIGURE 4.12 (A) IMPACT OF AMMONIA ADDITION ON EFFLUENT OZONE RESIDUAL AT PH 7.0

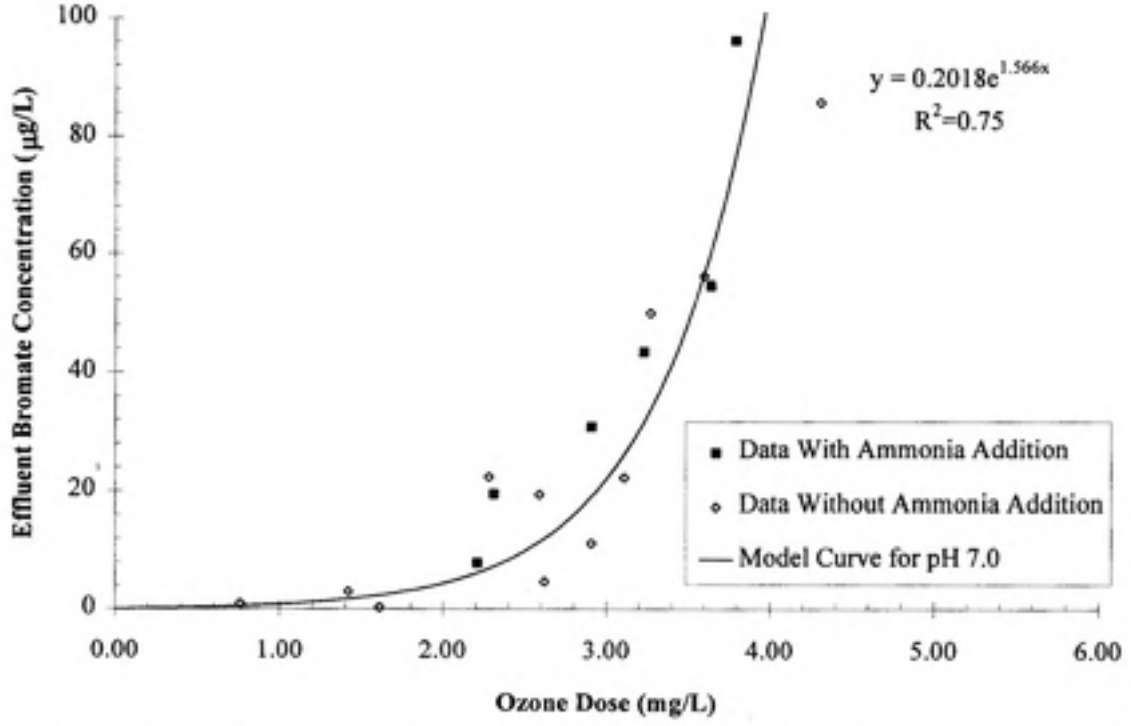

FIGURE 4.12 (B) IMPACT OF AMMONIA ADDITION ON BROMATE FORMATION AT PH 7.0
(pH 7.0, 2.5 mg/L TOC, 300 µg/L Br^-, 1 mM carbonate)

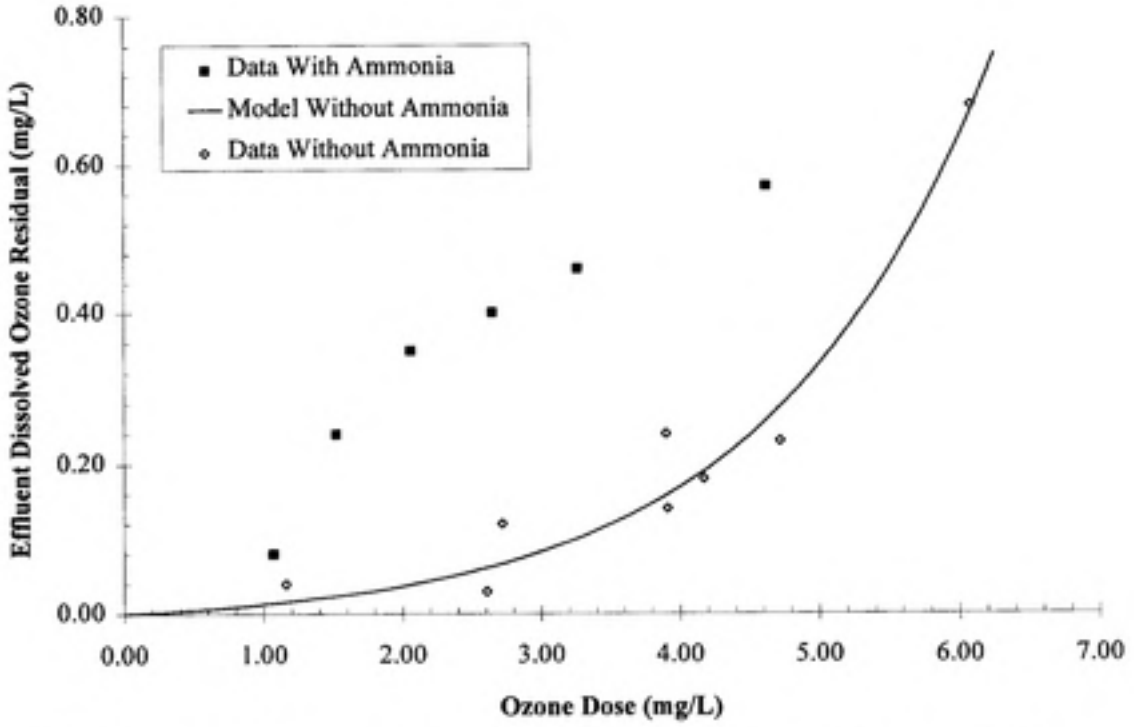

FIGURE 4.13 (A) EFFLUENT OZONE RESIDUAL WITH AMMONIA ADDITION AT PH 8.3

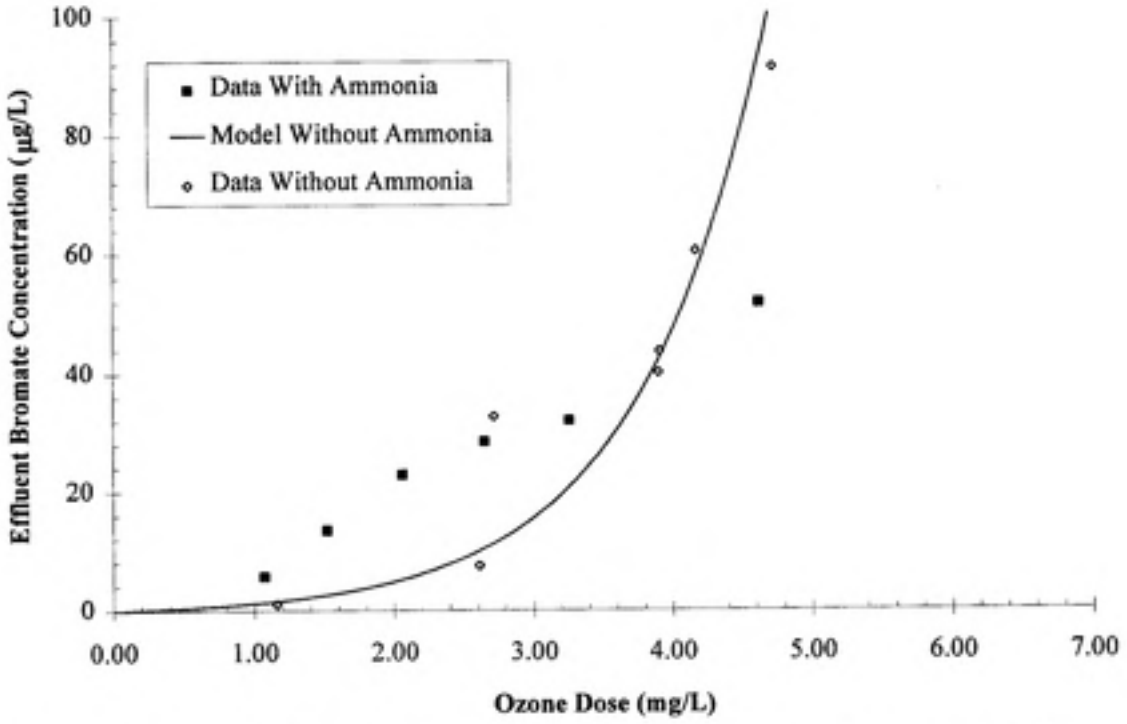

FIGURE 4.13 (B) BROMATE FORMATION WITH AMMONIA ADDITION AT PH 8.3
(pH 8.3, 2.5 mg/L TOC, 300 µg/L Br^-, 1 mM carbonate)

The corresponding formation of bromate was found to decrease with the addition of ammonia. This is illustrated further in Table 4.15 for two different target ozone residuals. Because lower ozone doses are required to achieve each target ozone residual in the presence of ammonia, less bromate is produced. Table 4.15 shows that the apparent decrease in bromate production due to ammonia addition is especially pronounced at the higher dissolved ozone residual.

TABLE 4.15 BROMATE FORMATION AT PH 8.3 WITH AMMONIA ADDITION

Ammonia Addition*	Target Ozone Residual 0.2 mg/L		Target Ozone Residual 0.4 mg/L	
	Required Ozone Dose (mg/L)	Corresponding Bromate Conc. (µg/L)	Required Ozone Dose (mg/L)	Corresponding Bromate Conc. (µg/L)
With	1.4	11	2.7	29
Without	4.1	34	5.2	>100

* Values in table for "With Ammonia" obtained from reading Figures 4.13a and b

These results contradict those of Harrington (1994) who performed a limited CMFR investigation with ammonia addition at pH 8.5; Harrington reported no effect from the addition of ammonia on dissolved ozone residual or bromate production. Siddiqui and Amy (1993) observed that the higher the pH value, the greater was the effect of ammonia addition on lowering bromate production. While these experiments (Siddiqui and Amy, 1993) were conducted on a batch basis, they are consistent with the findings of this research. Other researchers (Krasner et al., 1993; Glaze et al., 1993) have found conflicting results with ammonia addition under various reactor conditions, molar ratios of N:Br^-, and pH values.

4.8 Post-Reactor Formation of Bromate

The effects of ozone decay in the reactor effluent and the corresponding formation of bromate during the dissipation of the ozone residual were investigated. After the ozonated solution exited the reactor, the dissipation of the ozone residual was examined to simulate post-reactor conditions in practice. In practice, after contacting the water with ozone, the water is often passed through a series of reactor chambers without additional ozone being applied before the water is subsequently dosed with hydrogen peroxide which is used to destroy any ozone residual. Therefore, the water is "held" with the effluent dissolved ozone residual before entering the next treatment process in the plant.

These experiments were done under baseline conditions for duplicate samples. After steady-state ozonation in the continuous-flow reactor (fifty minutes), a 100-mL sample taken from the reactor was immediately purged with N_2 gas for ten minutes and then stored for the measurement of bromate. Two additional 100-mL samples were stored in 100-mL stoppered volumetric flasks to follow the rate of ozone decay and the corresponding formation of bromate. One sample was held for ten minutes and then was purged with N_2 gas; the other sample was held for twenty minutes before purging with N_2 gas. Aliquots of each sample were taken for ozone residual measurement just before each sample was purged with N_2 gas.

Figures 4.14a and b show the decrease in ozone residual with time and the resulting formation of bromate during the period of ozone decay for duplicate samples. Figure 4.14a shows that after ten minutes, the effluent ozone residual of 0.4 mg/L was almost completely dissipated for both samples. Less than 1 µg/L of bromate was formed during dissipation of the ozone residual.

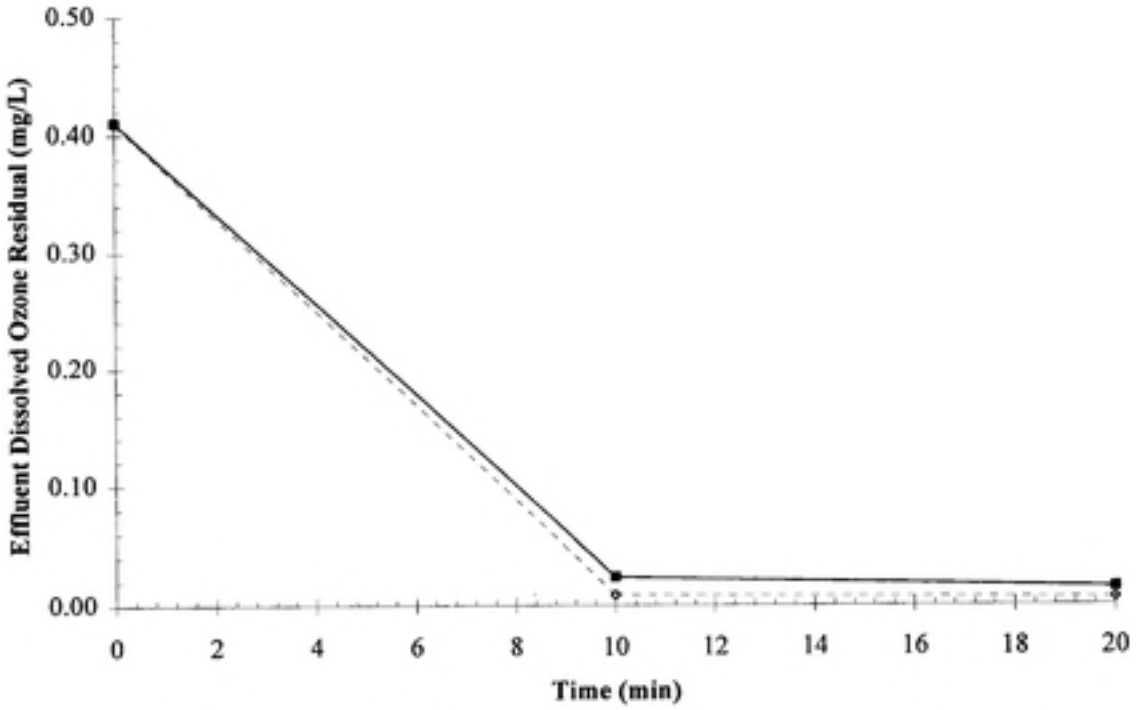

FIGURE 4.14 (A) BATCH DECAY OF EFFLUENT OZONE RESIDUAL WITH TIME

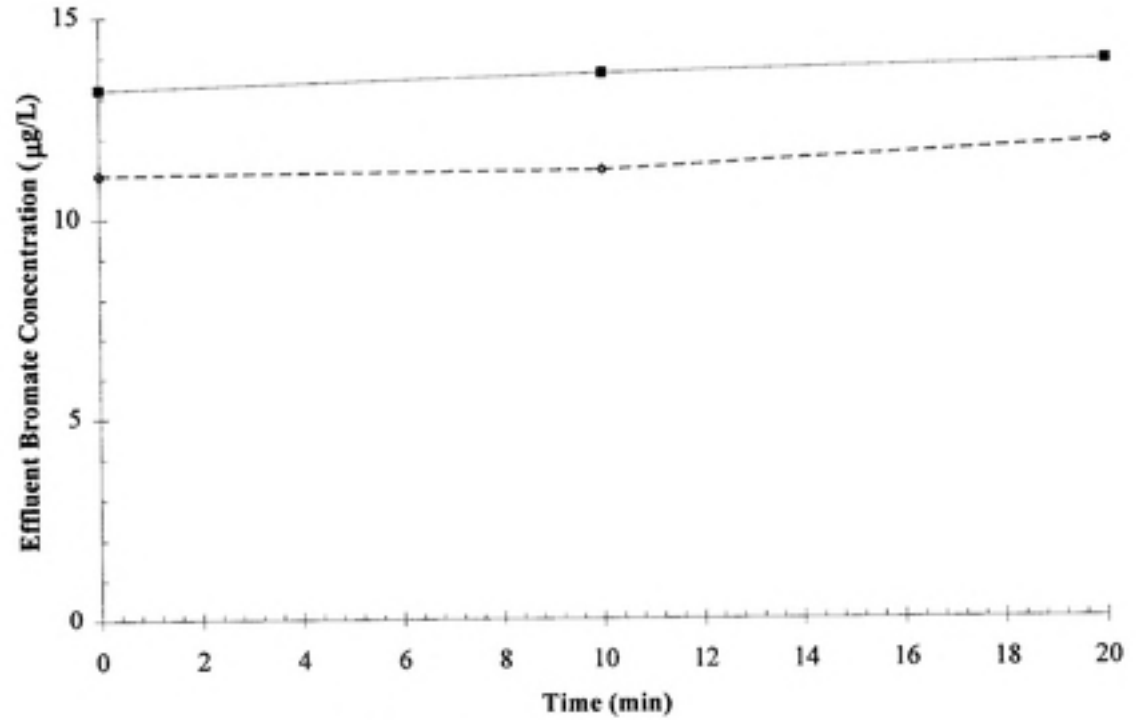

FIGURE 4.14 (B) FORMATION OF BROMATE DURING BATCH DECAY OF OZONE
(pH 7.0, 2.5 mg/L TOC, 300 µg/L Br^-, 1 mM carbonate)

The effect of hydrogen peroxide addition on the dissolved ozone residual exiting the reactor and the corresponding formation of bromate were examined. As stated earlier, hydrogen peroxide is often used in practice to destroy the ozone residual prior to downstream treatment processes. Four different experiments were run to achieve various effluent ozone residuals. After steady-state ozonation in the continuous-flow reactor, one 100-mL sample from the reactor was immediately purged with N_2 gas for ten minutes and then stored for subsequent bromate analysis. Another 100-mL sample was added to a 100-mL volumetric flask with a concentration of hydrogen peroxide equal to 0.5 times the expected ozone residual on a mass basis. The sample with hydrogen peroxide was allowed to react for 10 minutes before purging with N_2 gas. Because the dissolved ozone residual was not immediately known at the time of sample collection, the hydrogen peroxide target of 0.5 times the ozone residual was not always achieved.

Table 4.16 presents the results of these four experiments and Figure 4.15 shows the results graphically. The results show that, with the exception of the second sample, there is not a significant change in the concentration of bromate due to the addition of hydrogen peroxide and the subsequent reaction of ozone and hydrogen peroxide. As discussed earlier in this section, an ozone residual of 0.4 mg/L almost completely dissipated in ten minutes without hydrogen peroxide addition, producing less than 1 µg/L additional bromate. Although it cannot be determined if the hydrogen peroxide enhanced decay of the ozone residual, the addition of hydrogen peroxide apparently did not enhance the formation of bromate during this period of ozone decay. Other researchers have found conflicting results with respect to hydrogen peroxide addition; some have reported an increase in bromate formation with the continued application of hydrogen peroxide to the reactor influent (Daniel and Meyerhofer, 1993; Krasner et al., 1993) and others have noted decreases in bromate formation (Kruithof and Meijers, 1993).

TABLE 4.16 RESULTS OF H_2O_2 ADDITION ON BROMATE FORMATION

Initial Ozone Conc. (mg/L)	H_2O_2 Conc. (mg/L)	H_2O_2/O_3 ratio	Ozone Conc. after 10 min (mg/L)	Initial Bromate Conc. (µg/L)	Final Bromate Conc. (µg/L)
0.2	0.05	0.28	0.03	18	15
0.4	0.20	0.47	0.01	65	47
0.5	0.15	0.29	0.01	40	44
0.7	0.30	0.45	0.00	98	103

Note: The hydrogen peroxide stock and standard solutions used in this research were not standardized by the DPD standardization method; knowledge of this method was acquired after experimental work was completed.

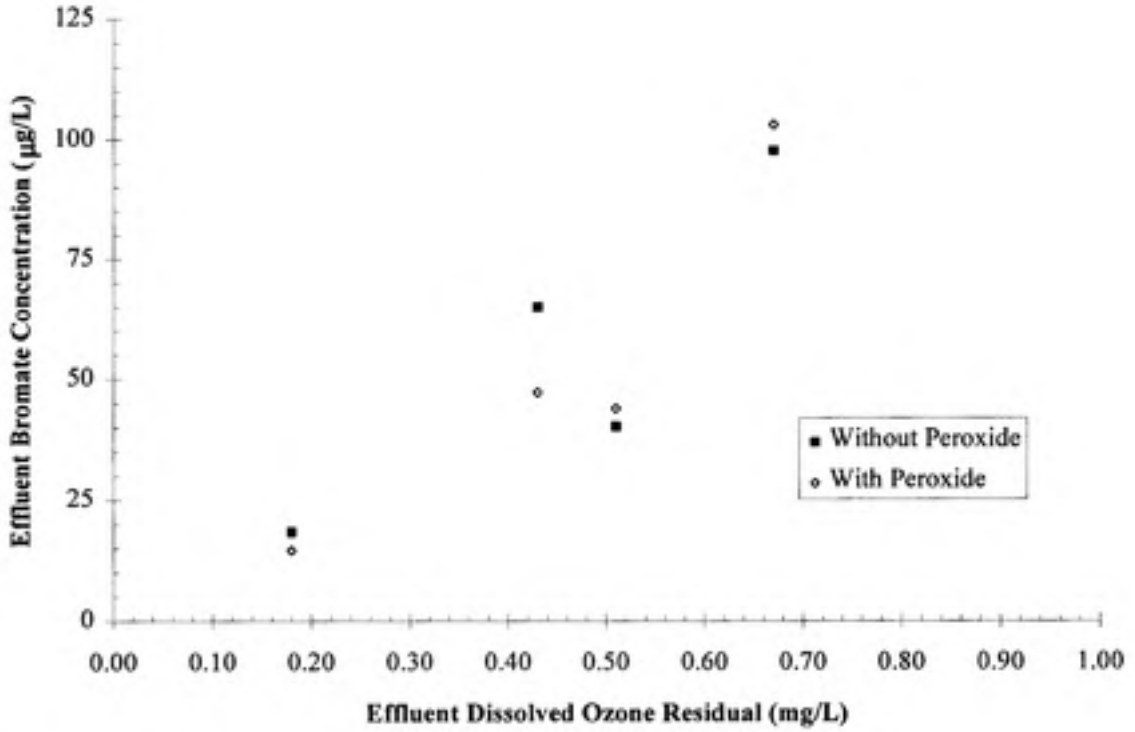

FIGURE 4.15 EFFECT OF H_2O_2 ADDITION ON BROMATE FORMATION
(pH 7.0, 2.5 mg/L TOC, 300 µg/L Br^-, 1 mM carbonate)

4.9 Summary of Research Findings and Implications for Water Treatment Practice

The USEPA is expected to regulate bromate in drinking water at the PQL of 10 µg/L (USEPA, 1994); this MCL is expected to decrease as the practical detection limit for bromate is lowered. The WHO recommends a level of 25 µg/L (WHO, 1993). The results of this study show that, under various water quality and treatment conditions, it will be difficult to meet the MCL. This is especially true when the requisite ozone dose to produce an ozone residual sufficient to meet CT disinfection requirements is applied. Therefore, when ozone is used as a disinfectant, there is a balance that must be achieved between disinfection CT requirements and the formation of bromate, especially at high bromide concentrations and high pH values.

The USEPA has established disinfection and filtration criteria in the Surface Water Treatment Rule (SWTR) (1989). The total log removal/inactivation requirements for uncontaminated surface water supplies is 3.0-log (99.9%) removal and/or inactivation for *Giardia* and 4.0-log (99.99%) removal and/or inactivation for viruses. For a properly operated conventional treatment plant, the removal credit received is 2.5 and 2.0-logs of *Giardia* and viruses, respectively. Therefore, 0.5 and 2.0-logs of inactivation of *Giardia* and viruses, respectively, must be achieved from chemical disinfection (e.g., ozonation).

The influent water in this research had a water temperature of 23-26°C; thus, from the SWTR Guidance Manual (USEPA, 1989), the CT for 2.0-log inactivation of viruses by ozone is 0.15 mg-min/L at 25°C and the CT for 0.5-log inactivation of *Giardia* cysts by ozone is 0.08 mg-min/L at 25°C. Therefore, the controlling disinfection criterion under these conditions is the 2.0-log inactivation of viruses at 0.15 mg-min/L.

However, these conditions describe a best-case scenario. For example, colder water temperatures, such as 0.5°C, require up to six times the CT as compared to the CT for ozone required at 25°C. Also, the above calculations are for waters treated by coagulation, sedimentation, and filtration; higher CT values apply for waters that are not filtered. Additionally, recent concern about *Cryptosporidium* has the waterworks industry considering a CT requirement of five to ten times the CT required for *Giardia*

inactivation in order to inactivate *Cryptosporidium*. Hence, there are several situations in practice which would necessitate increased CT requirements to achieve effective water treatment.

Based on the above discussion, Tables 4.17-20 summarize some of the important implications of this research; the target ozone residuals considered cover a variety of water quality and treatment scenarios found in practice. The conditions for each example are listed below, where all but the last condition are for theoretical hydraulic residence times (HRTs) of ten minutes:

① pH 7.0, 2.5 mg/L TOC, 1 mM Carbonate, 300 µg/L Br^-

② pH 7.0, 2.5 mg/L TOC, 1 mM Carbonate, 100 µg/L Br^-

③ pH 7.0, 2.5 mg/L TOC, 1 mM Carbonate, 50 µg/L Br^-

④ pH 6.5, 2.5 mg/L TOC, 1 mM Carbonate, 300 µg/L Br^-

⑤ pH 6.0, 2.5 mg/L TOC, 1 mM Carbonate, 300 µg/L Br^-

⑥ pH 7.0, 5.0 mg/L TOC, 1 mM Carbonate, 300 µg/L Br^-

⑦ pH 7.0, 2.5 mg/L TOC, 0 mM Carbonate, 300 µg/L Br^-

⑧ pH 7.0, 2.5 mg/L TOC, 1 mM Carbonate, 300 µg/L Br^-, HRT=2.0 min.

Four scenarios for CT credit are examined below. The CT values are taken from the SWTR Guidance Manual (USEPA, 1989). For 0.5-log *Cryptosporidium* inactivation, the CT required for the inactivation of *Giardia* was multiplied by a factor of five. The scenarios include:

* T=25°C, 2-log viruses/0.5-log *Giardia*; controlling CT=0.15 mg-min/L
* T=25°C, 2-log viruses/0.5-log *Giardia*/0.5-log *Cryptosporidium*; controlling CT=0.4 mg-min/L
* T=0.5°C, 2-log viruses/0.5-log *Giardia*; controlling CT=0.9 mg-min/L
* T=0.5°C, 2-log viruses/0.5-log *Giardia*/0.5-log *Cryptosporidium*; controlling CT=2.4 mg-min/L

The required ozone doses and corresponding bromate concentrations were obtained from the equations of the exponential model curves found for each set of conditions. For each scenario, the controlling CT was used to calculate the target ozone residual, C, based on the hydraulic residence time, T, for each condition examined. (The hydraulic residence time used in the CT calculation corresponds to the T_{10}, where T_{10} is $0.1054xT_{Theo}$ for the bench-scale CMFR). Thus, for an ideal reactor with a $T_{10}=T_{theo}$, the target residuals would be lower, as would the required ozone dose and bromate production.) The target ozone residual was then used to calculate the required ozone dose, based on the exponential model equation. Once the required ozone dose to achieve disinfection credit was determined, the corresponding bromate formation was calculated using the corresponding model equations.

Tables 4.17-4.20 show the results of the calculations for the four different scenarios considered. It is important to remember, however, that the results obtained here are reactor-specific (one CMFR) and may differ from concentrations formed in other types of reactors under identical water quality and treatment conditions. Another important note is that the experimental results and model curves were obtained under warm water conditions of 23-26°C. The bromate concentrations obtained for the cold water scenarios of 0.5°C are only extrapolations. Disinfection, like all rate processes is temperature-dependent and the formation of bromate at lower temperatures would be different than those obtained at 23-26°C. Therefore, using the results from 23-26°C for the 0.5°C inactivation scenarios is only for purposes of illustration and the concentrations shown are likely to be conservative estimations of the actual levels of bromate that would be formed at 0.5°C.

TABLE 4.17 BROMATE FORMATION AT 25°C WITH A REQUIRED CT=0.15 mg-min/L

Water Quality Characteristics*	Target Ozone Residual (mg/L)	Required Ozone Dose (mg/L)	Bromate Concentration (µg/L)
①	0.14	2.5	7.8
②	0.14	2.1	1.5
③	0.14	2.2	1.0
④	0.14	2.5	2.7
⑤	0.14	2.1	4.5
⑥	0.14	5.8	9.0
⑦	0.14	2.9	1.3
⑧	0.71	2.7	18

* See Text

TABLE 4.18 BROMATE FORMATION AT 25°C WITH A REQUIRED CT=0.4 mg-min/L

Water Quality Characteristics*	Target Ozone Residual (mg/L)	Required Ozone Dose (mg/L)	Bromate Concentration (µg/L)
①	0.38	3.4	32
②	0.38	3.2	6.8
③	0.38	3.0	4.7
④	0.38	3.0	12
⑤	0.38	3.1	12
⑥	0.38	6.9	25
⑦	0.38	4.1	7.0
⑧	1.90	3.2	58

* See Text

TABLE 4.19 BROMATE FORMATION AT 0.5°C WITH A REQUIRED CT=0.9 mg-min/L

Water Quality Characteristics*	Target Ozone Residual (mg/L)	Required Ozone Dose (mg/L)	Bromate Concentration (µg/L)
①	0.85	4.1	101
②	0.85	4.2	23
③	0.85	3.8	17
④	0.85	3.5	38
⑤	0.85	3.9	27
⑥	0.85	7.9	57
⑦	0.85	5.1	29
⑧	4.30	3.6	152

* See Text

TABLE 4.20 BROMATE FORMATION AT 0.5°C WITH A REQUIRED CT=2.4 mg-min/L

Water Quality Characteristics*	Target Ozone Residual (mg/L)	Required Ozone Dose (mg/L)	Bromate Concentration (µg/L)
①	2.3	5.0	>200
②	2.3	5.4	101
③	2.3	4.6	80
④	2.3	4.1	162
⑤	2.3	4.8	70
⑥	2.3	9.0	156
⑦	2.3	6.2	159
⑧	11	4.1	>200

* See Text

In what would be considered a worst-case scenario, T=0.5°C with provisions for *Cryptosporidium* inactivation (Table 4.20, CT=2.4 mg-min/L), all of the cases exceed the USEPA's proposed MCL for bromate of 10 µg/L. The WHO's 25 µg/L level is also exceeded in all cases. Therefore, from the results in Table 4.20, it seems clear the proposed levels of bromate will be exceeded under a wide variety of water quality parameters and operating conditions when disinfection of *Cryptosporidium* is required.

In the other cold water scenario, when *Cryptosporidium* inactivation was not considered (see Table 4.19), most of the examples produced bromate concentrations above the WHO's suggested level. The two cases, two and three, which produced bromate concentrations below 25 µg/L are the cases with low bromide concentrations at 100 µg/L and 50 µg/L, respectively. Again, it is important to remember that the bromate concentrations shown for the cold water scenarios are calculated from exponential models which were obtained from experimental results under warmer water temperatures of 23°C-26°C.

For the scenarios examined with warm water conditions, the bromate levels produced are of less concern with respect to proposed regulations and recommended criteria. When inactivation for *Cryptosporidium* is not considered (see Table 4.17), only one case, case eight at 18 µg/L of bromate, exceeded the USEPA's 10 µg/L MCL. Table 4.18 shows that only two cases produce bromate at levels above the WHO's

recommended level when inactivation of *Cryptosporidium* is considered. The two cases, cases one and eight, which were above the 25 µg/L level, are cases with either a high concentration of influent bromide (300 µg/L) or a low HRT (2.0 minutes). In all cases, example eight produced the highest bromate concentration. This research suggests that compliance with the proposed USEPA MCL and WHO recommended levels is most sensitive to the HRT of the ozonation reactor. Although the USEPA would like to set the MCL at the 10^{-4} cancer risk level of 5 µg/L, as discussed earlier, the MCL of 10 µg/L is based on the practical quantitation level of bromate. Therefore, if the detection limit for bromate were lowered, e.g., to the cancer risk level of 5 µg/L, this research indicates that even under the best-case scenario, with warm water temperatures and no provisions for *Cryptosporidium* inactivation (see Table 4.17), it would be difficult to meet this lowered MCL.

Another set of calculations was performed using the experimental results and corresponding exponential model equations to determine the maximum dissolved ozone residuals and transferred ozone doses at which the USEPA's proposed MCL of 10 µg/L and the WHO's recommended level of 25 µg/L were exceeded. The same eight cases used in the previous analysis were used here. For each example, either the MCL of 10 µg/L or the WHO recommended level of 25 µg/L bromate was used to calculate the required ozone dose at which these concentrations of bromate are produced. Then, the resulting dissolved ozone residual was calculated based on the calculated ozone dose. Once the corresponding ozone residual was calculated, the CT_{10} that could be achieved with that ozone residual was determined. Again, the hydraulic residence time used in the CT calculation corresponds to the T_{10} in this study, where T_{10} is $0.1054 \times T_{Theo}$ for the bench-scale ozone reactor (CMFR). Table 4.21 displays the results of these calculations.

The results show that, for the bench-scale reactor, the acceptable CT_{10} ranged from 0.01-0.18 mg-min/L for the USEPA's 10 µg/L MCL and 0.02-1.2 mg-min/L for the 25 µg/L WHO suggested level. Excluding the low HRT case (example eight), dissolved ozone residuals could not be greater than 0.2-0.6 mg/L without exceeding the USEPA MCL. For the WHO limit, acceptable ozone residuals ranged from 0.1 to 1.1 mg/L. The

TABLE 4.21 REQUIRED OZONE DOSES AND DISSOLVED OZONE RESIDUALS AT WHICH THE 10 µg/L AND 25 µg/L REGULATORY LEVELS FOR BROMATE WOULD BE EXCEEDED

		USEPA = 10 µg/L			WHO = 25 µg/L		
Water Quality* Characteristic	T_{10}** (min)	Required O_3 Dose (mg/L)	Required O_3 Residual (mg/L)	CT_{10} (mg-min/L)	Required O_3 Dose (mg/L)	Required O_3 Residual (mg/L)	CT_{10} (mg-min/L)
①	1.05	2.6	0.2	0.2	3.2	0.3	0.3
②	1.05	3.6	0.5	0.5	4.3	0.9	1.0
③	1.05	3.5	0.6	0.6	4.0	1.1	1.2
④	1.05	3.0	0.3	0.4	3.3	0.6	0.7
⑤	1.05	2.9	0.3	0.3	3.8	0.8	0.8
⑥	1.05	5.9	0.2	0.2	6.9	0.4	0.4
⑦	1.05	4.3	0.5	0.5	5.0	0.8	0.8
⑧	0.21	1.6	0.1	0.01	1.8	0.1	0.02

* See Text

** Corresponding to $T_{10}/T_{theoretical} = 0.1054$

highest acceptable dissolved ozone residuals were for case three, where the water had an influent bromide concentration of only 50 µg/L.

Finally, the bromate results obtained from the models for the variable pH and influent Br^- concentration experiments were used to create Figures 4.16 and 4.17, where bromate formation as a function of CT_{10} and either pH or influent Br^- concentration is illustrated. The range of CT_{10} values, 0.30 to 3.0 mg-min/L, were used as target CT's that are representative of those which might be encountered in practice. The ozone doses required to achieve the CT_{10}'s were calculated based on a T_{10} of 1.05 minutes ($T_{10}=0.1054 \times T_{Theo}$, where T_{Theo} is ten minutes for the CMFR). Knowing the required dissolved ozone residuals for the target CT_{10}'s allowed for calculation of the ozone doses from the model equations for each pH or bromide scenario. Then, using the ozone dose, the corresponding bromate concentrations were calculated from the bromate model equations. The plots are specific to the CMFR with 2.5 mg/L TOC, 1 mM carbonate, a liquid flow rate of 50 mL/min (HRT=10 minutes), a gas flow rate of 395 mL/min, and a water temperature of 23-26°C. Both figures are truncated at 50 µg/L bromate which is used here as the maximum bromate concentration of interest.

In Figure 4.16, beyond a CT_{10} of 0.3 mg-min/L the 10 µg/L MCL is exceeded for all of the pH values. Only the pH 6.0 and 6.5 values do not exceed the proposed USEPA MCL at a CT_{10} of 0.3 mg-min/L. As bromide concentration decreases in Figure 4.17, a higher CT_{10} can be achieved before bromate levels greater than 10 µg/L are exceeded. Therefore, disinfection credit plays an important role in the balancing act between bromate formation and disinfection when ozone is the disinfectant.

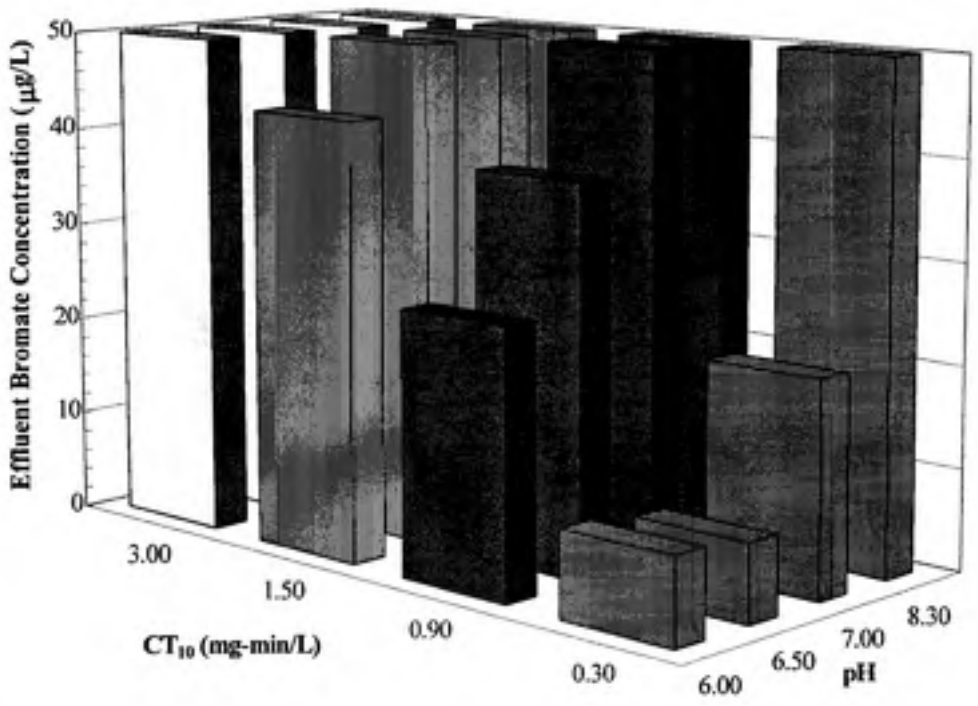

FIGURE 4.16 BROMATE FORMATION AS A FUNCTION OF CT_{10} AND pH WITH 300 µg/L INFLUENT Br^- CONCENTRATION

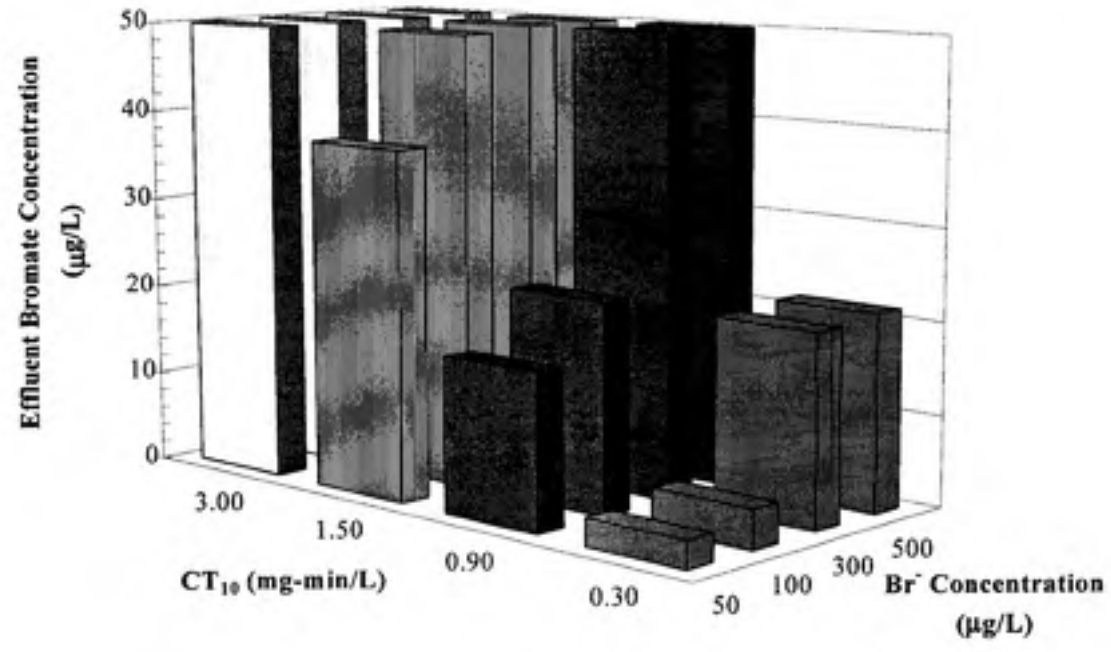

FIGURE 4.17 BROMATE FORMATION AS A FUNCTION OF CT_{10} AND Br^- CONCENTRATION AT pH 7.0

CHAPTER 5

CONCLUSIONS AND RECOMMENDATIONS

5.1 CONCLUSIONS

The goal of this research was to evaluate conditions for the formation and control of bromate in a bench-scale, dynamic, continuous-flow, completely-mixed reactor by varying several water quality parameters. Therefore, the results and conclusions are specific to this reactor configuration and to water quality conditions investigated. The results indicate that for any transferred ozone dose, as pH increased the effluent dissolved ozone residual increased. This is due to the increased rate of ozone decomposition at higher pH values. The results also indicate that although the exponential models for each set of pH results were not statistically different, as pH increased, the formation of bromate increased. The increased bromate formation at higher pH's is due to the increased ozone doses required to reach a specified ozone residual at elevated pH's.

For various influent bromide concentrations, as ozone dose was increased, the effluent dissolved ozone residual increased, independent of the influent bromide concentration. Bromate formation was found to be enhanced with increasing influent bromide concentration. These results agree with theory which indicates that the concentration of hypobromite, which leads to the formation of bromate, should increase with increases in influent bromide ion concentration.

The required ozone doses to achieve measurable ozone residuals increased with an increase in TOC concentration. Organic carbon exerts an ozone demand which promotes the consumption of ozone and as organic carbon concentration increases, more ozone is required to achieve a dissolved ozone residual. As TOC concentrations increased, formation of bromate decreased. For a constant ozone dose, solutions with lower organic carbon concentrations exert less of an ozone demand. Therefore, there is more ozone available to react with the bromide ion to form bromate.

In the presence of inorganic carbon, ozone residuals increased for any applied ozone dose, compared to water in the absence of carbonate species. This is due to the

scavenging of hydroxyl radicals by the carbonate species which decelerates ozone decomposition and promotes the persistence of a higher effluent dissolved ozone residual. Although it has been suggested that carbonate species act as hydroxyl radical scavengers to slow down the formation of bromate, these results show that bromate production is enhanced by the presence of the carbonate species. The carbonate radicals produced from scavenging the hydroxyl radicals may play a role in bromate production. In contrast, the addition of t-butanol, also a hydroxyl radical scavenger, provided for increased dissolved ozone residuals and decreased bromate concentrations.

The addition of ammonia at pH 7.0 did not seem to affect either the effluent dissolved ozone residual or bromate formation. Yet, dissolved ozone residuals increased and bromate formation decreased with the addition of ammonia at pH 8.3.

The influence of mass transfer variations showed that for each applied ozone dose, residual ozone concentrations increased, as liquid flow rate increased. The results indicate that bromate formation decreased with the increase in liquid flow rate. As the gas flow rate decreased, the influent ozone gas concentrations and partial pressures increased; this provided for an increase in the effluent dissolved ozone residual. Also, a decrease in the gas flow rate caused a decrease in bromate formation.

The batch ozone decay in the reactor effluent resulted in almost complete dissipation of the effluent ozone residual in ten minutes and the formation of less than 1 µg/L. It could not be determined if the addition hydrogen peroxide to the reactor effluent to increase the rate of ozone decay enhanced the decay of the ozone residual, but the addition of hydrogen peroxide did not impact the formation of bromate.

With the USEPA's proposed MCL for bromate at 10 µg/L (1994), and the WHO's suggested level of 25 µg/L (1993), along with CT disinfection requirements which are increasing due to the need to provide for inactivation of *Cryptosporidium*, the results of this research show that there is a balance that must be achieved between disinfection CT requirements and the formation of bromate when ozone is used as the disinfectant. In most cases, waters with low pH (e.g., 6.0) and low influent bromide concentrations (e.g., 50 µg/L) produced bromate at levels below the MCL of 10 µg/L with 0.5-log inactivation

of *Cryptosporidium* and *Giardia* and 2.0-log inactivation of viruses in warm water temperatures (23-26°C). Also, it was found that a variety of other water quality and treatment scenarios encountered in practice could maintain bromate levels within the WHO's level of 25 µg/L and still achieve the same degree of disinfection (0.5-log inactivation of *Cryptosporidium* and *Giardia*, 2.0-log inactivation of viruses), but only at warm water temperatures of 25°C. When the pH is increased above 7.0, and the influent bromide concentration is increased beyond 100 µg/L, bromate is formed at levels above the USEPA and WHO level, when attempting to provide for inactivation of *Cryptosporidium* at these higher temperatures.

5.2 Recommendations

Ultimately, it would be desirable to develop a mathematical model to predict bromate formation based on the water quality parameters and reactor conditions investigated in this research. This would demonstrate and clarify which water quality parameters and reactor conditions influence the formation of bromate to the greatest degree.

Although bromate formation was found in this study to be dependent on a number of water quality parameters, this research was conducted on only one source of organic matter. A more comprehensive study on various types of natural organic material from a variety of sources would be desirable due to the different chemical properties of natural organic matter. Because bromate formation at lower pH and influent Br^- levels showed decreased bromate formation, research should be focused at these lower levels to find the optimal pH and influent Br^- concentration to achieve acceptable levels of bromate formation. Research should also be directed at clarifying the different results for the influence of ammonia addition on bromate formation at various pH levels.

A more comprehensive understanding of the respective roles of hydrogen peroxide, bromide, and ozone on bromate formation is warranted. Exploration of hydrogen peroxide dose and pH should be conducted to elucidate the role of molecular ozone and hydroxyl radicals on bromate formation. In order to identify more realistically

the conditions for bromate formation, bench-scale ozonation reactors should contain contactor configurations which behave comparable to those in practice. Because the provisions for *Cryptosporidium* inactivation are expected to increase bromate concentrations above the regulated levels, the balance between CT disinfection requirements for *Cryptosporidium* and bromate formation under different water quality and temperature conditions should be studied closely, particularly if the practical quantification level (PQL) is lowered. If the PQL were lowered to the 10^{-4} or 10^{-5} cancer risk levels, corresponding to bromate concentrations of 5 µg/L and 0.5 µg/L, respectively, additional research on the formation and control of bromate would be critical.

REFERENCES

APHA, AWWA, WEF. Standard Methods for the Examination of Water and Wastewater. 17th Edition. APHA, AWWA, WEF. Washington, D.C. (1989).

APHA, AWWA, WEF. Standard Methods for the Examination of Water and Wastewater. 16th Edition. APHA, AWWA, WEF. Washington, D.C. (1985).

Aieta, E. M. et al. Advanced Oxidation Processes for Treating Groundwater Contaminated with TCE and PCE: Pilot-Scale Evaluations. J. Am. Water Works Assoc. 80:5:64 (1988).

Amy, G., Siddiqui, M., Zhai, W., DeBroux, H., Odum, W. National Survey of Bromide in Drinking Water Sources and Impacts on Disinfection By-Products Formations. AWWA. AWWARF in press (1993).

Bader, H. and Hoigne, J. Determination of ozone in Water By the Indigo Method. Water Research. 15:449 (1981).

Buxton, G.V. and Elliot, A.J. Rate Constant for Reaction of Hydroxyl Radicals with Bicarbonate Ions. Radiation Phys. Chem. 27:241 (1986)

Croue, J.P., Koudjonou, B.K. and Legube, B. Parameters Affecting the Formation of Bromate Ion During Ozonation. J. Ozone Science Engineering. ?:18:1 (1996).

CRC Handbook of Chemistry & Physics. 76th Edition. CRC Press, New York, New York, (1995-1996).

Daniel, P. and Meyerhofer, P. Ozone and Bromide Ion: Treatability Issues. 11th Ozone World Congress, San Francisco, California, 1993.

Glaze, W.H., Weinberg, H.S. and Cavanagh, J.E. Evaluating the Formation of Brominated DBPs During Ozonation. J. Am. Water Works Assoc. 85:1:96 (1993).

Gordon,G., Bubnis, B., and Kuo, C-y. A Flow Injection , Non-Ion Chromatographic Method for Measuring Low-Level Bromate Ion in Ozone Treated Waters. J. Ozone Science Engineering. 16:1:79 (1994).

Haag, W.R. and Hoigne, J. Kinetics and Products of the Reactions of Ozone with Various Forms of Chlorine and Bromine in Water. J. Ozone Science and Engineering. 6:103 (1984).

Haag, W.R. and Hoigne, J. Ozonation of Bromide-Containing Waters: Kinetics of Formation of Hypobromous Acid and Bromate. Environmental Science and Technology. 17:5:261 (1983).

Harrington, G.W. Characteristics of Natural Organic Matter and Their Influence on Alum Coagulation. Ph.D. Dissertation: University of North Carolina at Chapel Hill, (1997).

Harrington, L.J. Measurement, Formation, and Control of Bromate in Ozonated Waters. Masters Technical Report: University of North Carolina at Chapel Hill, (1994).

Hautmann, D.P. and Bolyard, M. Analysis of Oxyhalide Disinfection By-Products and Other Anions of Interest in Drinking Water by Ion Chromatography. J. Chromatography. 602:65 (1992).

Hoigne, J. The Chemistry of Ozone in Water. Process Technologies for Water Treatment. Edited by Samuel Stucki. Plenum Publishing Corporation. 1988.

Hull, C.S., Singer, P.C., Saravanan, K. and Miller, C.T. Ozone Mass Transfer and Reaction: Completely Mixed Systems. In Proc. of Annual Conf. of the Am. Water Works Assoc. American Water Works Association: Vancouver, B.C. (1992).

Kleinbaum, D.G., Kupper, L.L., and Muller, K.E. Applied Regression Analysis and Other Multivariable Methods. Duxbury Press: Belmont, CA., (1978).

Krasner, S.W., Glaze, W.H., Weinberg, H.S., Daniel, P.A. and Najm, I.N. Formation and Control of Bromate During Ozonation of Waters Containing Bromide. J. Am. Water Works Assoc. 85:1:73 (1993).

Krasner, S.W., McGuire, J.H., Jacangelo, J.G., Patania, H.L., Reagan, K.M. and Aieta, E.M. The Occurrence of Disinfection By-Products in U.S. Drinking Water. J. Am. Water Works Assoc. 81:8:41 (1989).

Kruithof, J.C. and Meijers, R.T. Presence and Formation of Bromate Ion in Dutch Drinking Water Treatment. IWSA Workshop, Paris, 1993.

Kurokawa, Y., Aoki, S., Matsushima, Y., Takamura, N., Imazawa, T. and Hayashi, Y. Dose-Response Studies on the Carcinogenicity of Potassium Bromate in F344 Rats After Long-Term Oral Administration. J. National Cancer Inst. 77:4:977 (1986).

Lawler, D.F. and Singer, P.C. Analyzing Disinfection Kinetics and Reactor Design: A Conceptual Approach Versus the SWTR. J. Am. Water Works Assoc. 67:11:? (1993).

Najm, I.N. and Krasner, S.W. Effects on Bromide and NOM on By-Product Formation. J. Am. Water Works Assoc. 87:1:106 (1995).

Roustan, M., Duguet, J.P., Laine, Do-Quang, Z. and Mallevialle, J. Bromate Ion Formation: Impact of Ozone Contactor Hydraulics and Operating Conditions. J. Ozone Science Eng. ?:18:87 (1996).

Shukiary, H.M., Miltner, R.J., and Summers, R.S. Bromide's Effect on DBP Formation, Speciation, and Control: Part 1, Ozonation. J. Am. Water Works Assoc. 86:6:72 (1994).

Siddiqui, M.S. and Amy, G.L. Factors Affecting DBP Formation During Ozone-Bromide Reactions. J. Am. Water Works Assoc. 85:1:63 (1993).

Siddiqui, M.S., Amy, G.L. and Ozekin, K. Bromate Formation During Ozonation: Effect of NH_3/Br^- Ratio. 12th Ozone World Congress, Lillee, France. (1995).

Siddiqui, M.S., Amy, G.L. and Rice, R.G. Bromate Ion Formation: A Critical Review. J. Am. Water Works Assoc. 87:10:58 (1995).

Singer, P.C. Assessing Ozonation Research Needs in Drinking Water. J. Am. Water Works Assoc. 82:5:86 (1990).

Singer, P.C. Control of Disinfection By-Products in Drinking Water. J. of Environmental Engineering. 120:4:727 (1994).

Snoeyink. V.L. and Jenkins, D. Water Chemistry. John Wiley and Sons: New York, N.Y. (1980).

Song, R., Westerhoff, P., Minear, R., and Amy, G. Bromate Minimization During Ozonation. J. Am. Water Works Assoc. 89:6:69 (1997).

Staehelin, J. and Hoigne, J. Decomposition of Ozone in Water in the Presence of Organic Solutes Acting as Promoters and Inhibitors of Radical Chain Processes. Environmental Science and Technology. 19:12:1206 (1985).

Staehelin, J. and Hoigne, J. Decomposition of Ozone in Water: Rate of Initiation by Hydroxide Ions and Hydrogen Peroxide. Environmental Science and Technology. 16:10:676 (1982).

Sutton, H.C. and Downes, M.T. Reactions of HO_2 Radical in Aqueous Solution with Bromine and Related Compounds. Jour. Chem. Soc. Faraday. Trans. I. 68:1498 (1965).

Taube, Henry. Reactions in Solutions Containing O_3, H_2O_2, H^+ and Br^-. The Specific Rate of the Reaction $O_3 + Br^- \rightarrow$. J. Amer. Chem. Soc. 64:2468 (1942).

USEPA. 40 CFR Parts 141&142--National Primary Drinking Water Regulations: Disinfectants/Disinfection By-Products; Proposed Rule. Federal Register. 59:145:38668 (1994).

USEPA. Guidance Manual for Compliance With the Surface Water Treatment Requirements for Public Water Systems (Draft). (1989).

USEPA. 40 CFR Parts 141&142--National Primary Drinking Water Regulations: Surface Water Treatment Requirements; Proposed Rule. Federal Register. 59:145:38832 (1994).

USEPA. Method 300.0: Determination of Inorganic Anions by Ion Chromatography. Office of Research and Development: Environmental Samples. (1993).

USEPA. Excerpt from the DBP/ICR Analytical Methods Manual (Preliminary). DBP/ICR Manual (Draft). (1995).

Vander Der Jagt, H., Noij, Th.H.M., and Ooms, P.C.A. Analysis and Identification of Bromate Ion in Water by Ion Chromatography and Multiple Detection at the Low-ppb Level. IWSA Workshop. Paris, 1993.

von Gunten, U. and Hoigne, J. Bromate Formation During Ozonation of Bromide-Containing Waters: Interaction of Ozone and Hydroxyl Radical Reactions. Environmental Science and Technology. 28:7:1234 (1994).

von Gunten, U., Bruchet, A. and Costentin, E. Bromate Formation in Advanced Oxidation Processes. J. Am. Water Works Assoc. 88:6:53 (1996).

von Gunten, U. and Hoigne, J. Factors Controlling the Formation of Bromate During Ozonation of Bromide-Containing Waters. J. Water SRT. 41:5:299 (1992).

Wajon, J.E., and Morris, J.C. Rates of Formation of N-Bromo Amines in Aqueous Solutions. Inorg. Chem. 21:12:4258 (1982)

Weinberg, H.S. Pre-Concentration Techniques for Bromate Analysis in Ozonated Waters. J. Chromatography. 671:141 (1994)

Weinberg, H.S. and Yamada, H. IC/Spectrophotometric Method. Submitted to Analytical Chemistry for publication (1997).

Westerhoff, P.G. et al. Kinetic Modeling of Bromate Formation in Ozonated Waters: Molecular Ozone Versus HO· Radical Pathways. In Proc. of Annual Conf. of the Am. Water Works Assoc. New York, New York (1994).

World Health Organization. Guidelines for Drinking Water Quality. WHO. Geneva, Switzerland (1993).

Yamada, H. By-Products of Ozonation of Low Bromide Waters and Reduction of the By-Products by Activated Carbon. 11th Ozone World Congress, San Francisco, California, 1993.

Yates. R.S. and Stenstrom, M.K. Bromate Production in Ozone Contactors. In Proc. of Annual Conf. of the Am. Water Works Assoc. AWWA: San Antonio, TX. (1993).

Zehavi, D. and Rabani, J. The Oxidation of Aqueous Bromide Ions by Hydroxyl Radicals: A Pulse Radiolytic Investigation. J. Physical Chemistry. 76:3:312 (1972).

APPENDIX A

MISCELLANEOUS CONCERNS

This appendix contains miscellaneous information, figures, and tables pertaining to the research.

A.1 STEADY-STATE ASSUMPTION

As stated in the text, it was assumed that after three hydraulic residence times the reactor was at steady state. Figures A.1-3 show the absorbance readings for the influent and effluent gas-phase ozone concentrations and the effluent liquid-phase ozone concentration as they approach steady-state.

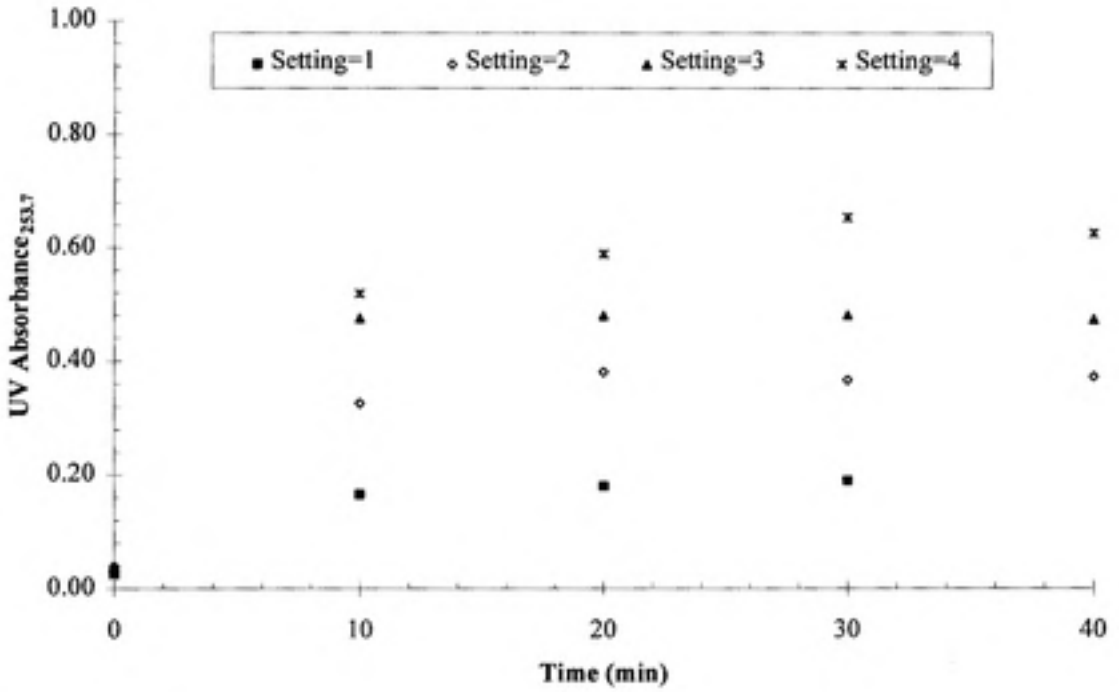

FIGURE A.1 EXAMPLE OF INFLUENT GAS-PHASE OZONE CONCENTRATION APPROACHING STEADY-STATE

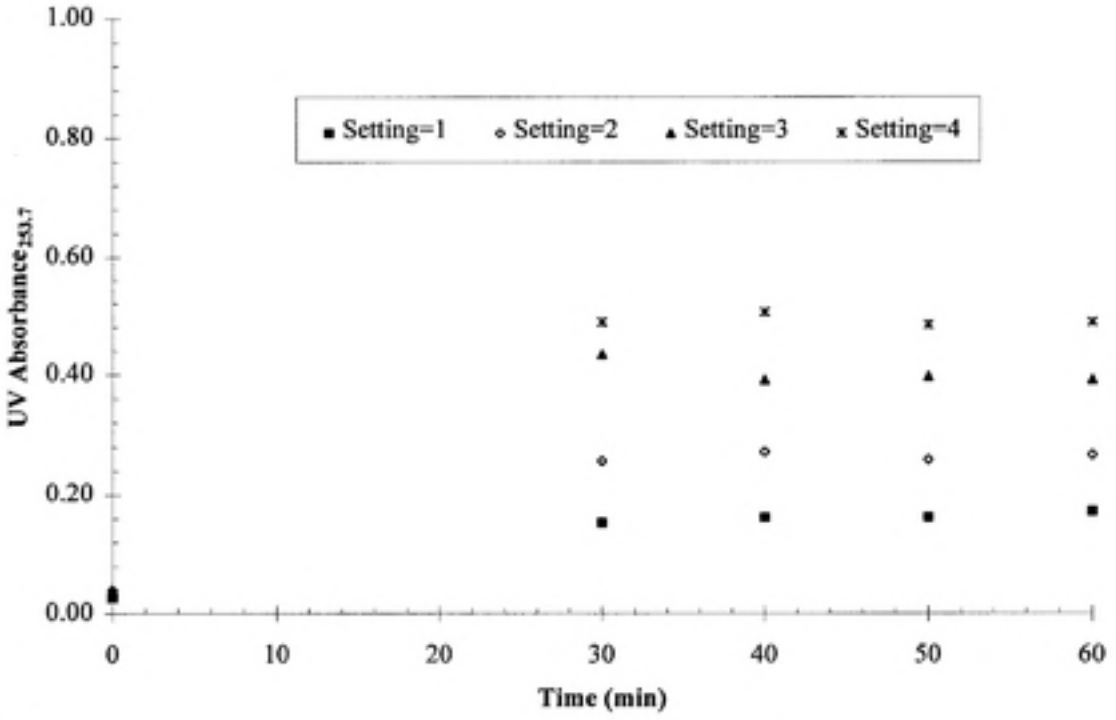

FIGURE A.2 EXAMPLE OF EFFLUENT GAS-PHASE OZONE CONC. APPROACHING STEADY-STATE

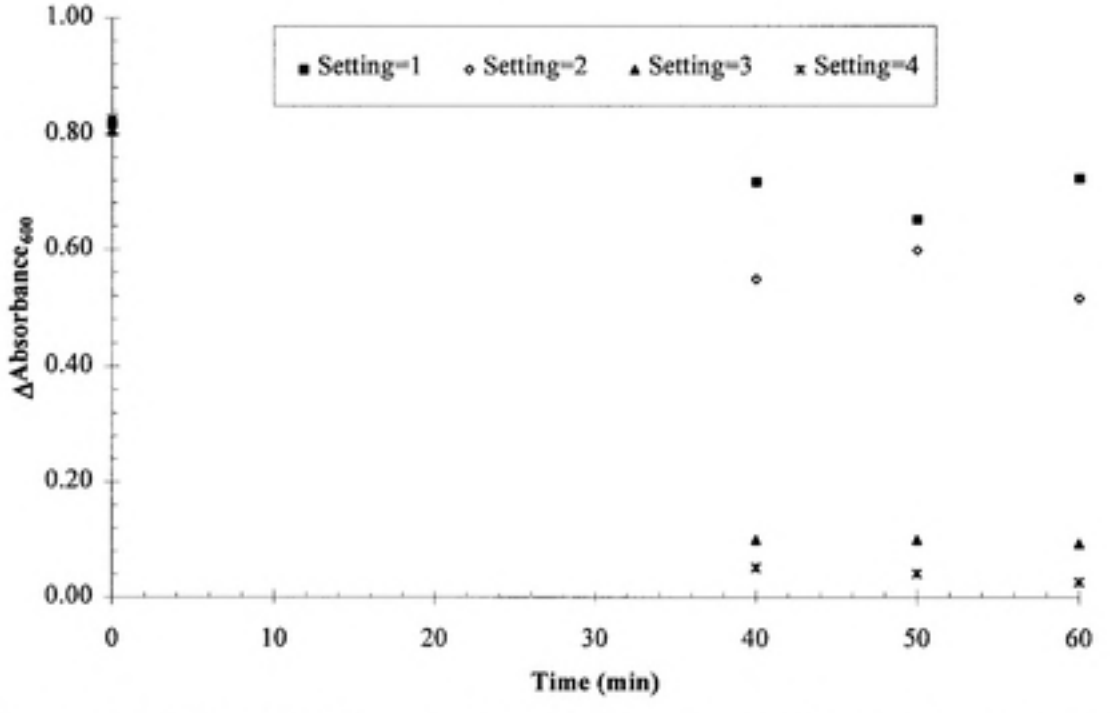

FIGURE A.3 EXAMPLE OF EFFLUENT LIQUID-PHASE OZONE CONCENTRATION APPROACHING STEADY-STATE

A.2 Indigo Calibration Curve

Although liquid-phase ozone concentrations were calculated using Beer's Law, several calibration curves were made to check the indigo reagents. To obtain the calibration curve, a stock solution of ozone was prepared by ozonating a pH 3.0 solution of OFDW for one hour. Then the concentration of the ozone stock solution was obtained by adding a known sample volume to a beaker containing approximately 1.0 g of potassium iodide (KI), per Standard Method 422 (APHA, AWWA, WEF, 1985). The pH of the solution was lowered to below pH 2.0 with concentrated H_2SO_4 and then the sample was titrated with 0.01 M Na_2SO_3 using starch as the indicator (APHA, AWWA, WEF, 1985). After the concentration of the solution was calculated, aliquots of the ozone stock solution were added to several 100-mL volumetric flasks with indigo reagent II to obtain various ozone concentrations. The volumetric flasks were filled to the line with OFDW and the absorbance at 600 nm was then measured. Figure A.4 is an example calibration curve. The values on the x-axis are calculated from the sodium thiosulfate titration of the ozone stock solution.

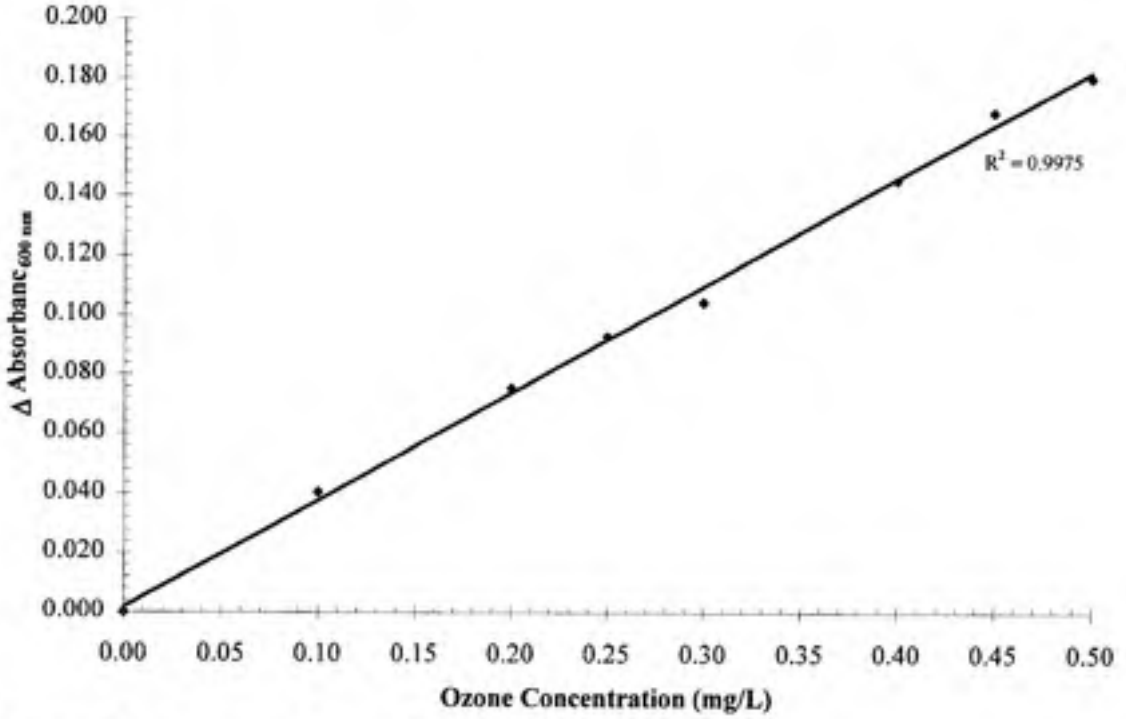

Figure A.3 Example Indigo Calibration Curve

APPENDIX B

EXAMPLE ION CHROMATOGRAPH PROGRAMS

Included are example program methods used for analyzing bromate. Bromcala.met is the method used to analyze the samples and Tara.met is the method used to analyze the calibration standards. Both methods were used in the direct injection procedure.

DIONEX METHOD PARAMETERS - BROMCALA.MET

Method Comment:
Column ID:
Analyst ID:

System Parameters

System Name: Anion Chromatography	
Number of Detectors	1
Run Time (minutes)	23.00
Sampling Rate (seconds)	0.20
Detector 1 Type	CDM-2
Detector 1 real time plot scale maximum (uS)	1.00
minimum	-1.00
Save Data File	Yes
Data File Name: C:\DX\METHOD\04089700.DXX	

-- DETECTOR 1 PARAMETERS --

Report Options

Create ASCII Report File	Yes
Print Report	Yes
Print All Components	No
Print Components Found	No
Print Missing Components	No
Print All Peaks	Yes
Print Unknown Peaks	No
Print Chromatogram	Yes
Autoscale Chromatogram Maximum	No
Autoscale Chromatogram Minimum	No
Fill Peaks with Color	No
Draw Grid Lines on Chromatogram	No
Show Component Fraction Numbers	No
Label with Peak Number	Yes
Label with Retention Times on Chromatogram	No
Label with Component Name	No
Format File Name: C:\DX\METHOD\default.prf	

Integration Parameters

Starting Peak Width (seconds)	20.0
Peak Threshold	16.000
Peak Area Reject	10000
Area Reject for Reference Peaks	1000

Data Events

Time	Description
0.00	Stop peak detection
1.00	Force baseline at start of all peaks
1.20	Start peak detection
2.31	Halve bunching factor

Component Table -- Last Modified: 09:05 on Tue, 08 Apr 1997

Component # 1 Bromate Retention Time 3.31
Reference Comp. Bromate Window Size 0.50 min.
Amount = K0 + K1*Area
K0 = -6.58190E+000
K1 = 6.54903E-005

Level	Amount	Area	Height
1	0.00000E+000	562233	127160
2	1.00000E+001	148595	16861
3	1.50000E+001	216581	24612
4	2.50000E+001	458561	42733
5	5.00000E+001	706489	80017
6	1.00000E+002	1580366	159593
7	2.00000E+002	3107102	307488
8	2.50000E+002	3949225	401828

Timed Events File: C:\DX\METHOD\AS9A.TE

Step	Time	Description
Init		CDM-2 AutoOffset Off
Init		CDM-2 Recorder Mark OFF
Init		CDM-2 Temp. Comp. = 1.7 / Deg C
Init		CDM-2 Recorder Range = 1.00 uS
Init		CDM-2 Cell ON
Init		ACI Autosmp OFF
Init		ACI TTL 1 OFF
Init		ACI AC 1 OFF
Init		ACI AC 2 OFF
Init		GPM Start
Init		GPM Hold Gradient Clock
Init		GPM Reset ON
1	0.0	CDM-2 Recorder Range = 3.00 uS
1	0.0	ACI Autosmp ON
2	2.0	CDM-2 AutoOffset ON
2	2.0	ACI Autosmp OFF
2	2.0	Start Sampling
2	2.0	GPM Run Gradient Clock
2	2.0	GPM Reset OFF
3	9.0	CDM-2 Cell OFF
3	9.0	GPM Hold Gradient Clock
3	9.0	GPM Reset ON

Lo Pressure Limit = 0
Hi Pressure Limit = 3200
Eluent 1 -
Eluent 2 -
Eluent 3 -
Eluent 4 -
V5 Off - load
V5 On - inject
V6 Off - load
V6 On - inject

Time	Flow	%1	%2	%3	%4	V5	V6	Comment
0.0	1.5	20	0	80	0	0	0	
0.1	1.5	20	0	80	0	1	0	
5.0	1.5	20	0	80	0	0	0	
9.0	1.5	20	0	80	0	0	0	

Calibration Parameters

Number Of Levels for Calibration	8
Force Calibration Curve Through Origin	No
Calibration Fit Type	Linear
Replace Or Average Calibrations	Average
External or Internal Calibration	External
Calculate Unknowns by Area or Height	Area
Default Sample Volume	1.0
Default Dilution Factor	1.0
Default Response Factor for Unknown Peaks	0.0
Calibration Standard Volume	1.0
Internal Standard Amount in Samples	1.0
Amount Units	ug/L

DIONEX METHOD PARAMETERS - BROMCALA.MET

Method Comment:
Column ID:
Analyst ID:

System Parameters

System Name: Anion Chromatography

Number of Detectors	1
Run Time (minutes)	23.00
Sampling Rate (seconds)	0.20
Detector 1 Type	CDM-2
Detector 1 real time plot scale maximum (uS)	1.00
minimum	-1.00
Save Data File	Yes

Data File Name: C:\DX\METHOD\04089700.DXX

-- DETECTOR 1 PARAMETERS --

Report Options

Create ASCII Report File	Yes
Print Report	Yes
Print All Components	No
Print Components Found	No
Print Missing Components	No
Print All Peaks	Yes
Print Unknown Peaks	No
Print Chromatogram	Yes
Autoscale Chromatogram Maximum	No
Autoscale Chromatogram Minimum	No
Fill Peaks with Color	No
Draw Grid Lines on Chromatogram	No
Show Component Fraction Numbers	No
Label with Peak Number	Yes
Label with Retention Times on Chromatogram	No
Label with Component Name	No

Format File Name: C:\DX\METHOD\default.prf

Integration Parameters

Starting Peak Width (seconds)	20.0
Peak Threshold	16.000
Peak Area Reject	10000
Area Reject for Reference Peaks	1000

Data Events

Time	Description
0.00	Stop peak detection
1.00	Force baseline at start of all peaks
1.20	Start peak detection
2.31	Halve bunching factor

Component Table -- Last Modified: 15:34 on Mon, 07 Apr 1997

Component # 1 BROMATE Retention Time 2.89
Reference Comp. none Window Size 0.50 min.
Amount = K0 + K1*Area
K0 = 1.19635E+002
K1 = -6.98520E-006

Level	Amount	Area	Height
1	0.00000E+000	6319737	682664
2	1.00000E+001	3966527	562420
3	1.50000E+001	402822	88138
4	2.50000E+001	15461006	2404795
5	5.00000E+001	4821745	715513
6	1.00000E+002	1308391	157791
7	1.50000E+002	1754457	349539
8	2.00000E+002	1947044	369072
9	2.50000E+002	3633111	462678

Timed Events File: C:\DX\METHOD\AS9AB.TE

Step	Time	Description
Init		CDM-2 AutoOffset Off
Init		CDM-2 Recorder Mark OFF
Init		CDM-2 Temp. Comp. = 1.7 / Deg C
Init		CDM-2 Recorder Range = 1.00 uS
Init		CDM-2 Cell ON
Init		ACI Autosmp OFF
Init		ACI TTL 1 OFF
Init		ACI AC 1 OFF
Init		ACI AC 2 OFF
Init		GPM Start
Init		GPM Hold Gradient Clock
Init		GPM Reset ON
1	0.0	CDM-2 Recorder Range = 3.00 uS
1	0.0	ACI Autosmp ON
2	2.0	CDM-2 AutoOffset ON
2	2.0	ACI Autosmp OFF
2	2.0	Start Sampling
2	2.0	GPM Run Gradient Clock
2	2.0	GPM Reset OFF

Lo Pressure Limit = 0
Hi Pressure Limit = 3200
Eluent 1 -
Eluent 2 -
Eluent 3 -
Eluent 4 -
V5 Off - load
V5 On - inject
V6 Off - load
V6 On - inject

Time	Flow	%1	%2	%3	%4	V5	V6	Comment
0.0	1.5	20	0	80	0	0	0	
0.1	1.5	20	0	80	0	1	0	
6.0	1.5	20	0	80	0	1	0	
8.0	1.5	100	0	0	0	0	0	
12.0	1.5	100	0	0	0	0	0	
17.0	1.5	20	0	80	0	0	0	
23.0	1.5	20	0	80	0	0	0	

Calibration Parameters

Number Of Levels for Calibration	9
Force Calibration Curve Through Origin	No
Calibration Fit Type	Linear
Replace Or Average Calibrations	Average
External or Internal Calibration	External
Calculate Unknowns by Area or Height	Area
Default Sample Volume	1.0
Default Dilution Factor	1.0
Default Response Factor for Unknown Peaks	0.0
Calibration Standard Volume	1.0
Internal Standard Amount in Samples	1.0
Amount Units	ug/L

APPENDIX C

METHOD DEVELOPMENT/EVALUATIONS FOR ION CHROMATOGRAPHY

Many of the reagents and techniques applied in the research were carefully chosen to optimize ion chromatography analysis. This appendix contains the criteria and explanations for the final selections.

C.1 OZONE QUENCHING AGENT

It was suspected that as long as an ozone residual persists, the formation of bromate continues. Therefore, to quantify bromate concentrations in the reactor, the ozone residual should be quenched immediately after coming out of the reactor. Also, the quenching agent must not react with bromate. The bromate peak detection must also not be affected. Indigo was used for quenching ozone residuals in the liquid phase, but if indigo was used in ion chromatography it could cause complications. Therefore, bromate samples were sparged with nitrogen gas to quench the ozone residuals. Several quenching times were investigated and ten minutes was found to be the optimal quenching time for all ozone residuals. This technique is well documented by Haag and Hoigne (1983) and did not affect bromate concentrations, as shown in Table C.1 below.

TABLE C.1 EFFECT OF SAMPLE SPARGING ON BROMATE CONCENTRATION

Sample	Peak Area
50 µg/L Sparged-A	711268
50 µg/L Sparged-B	680352
50 µg/L Unsparged-A	680352
50 µg/L Unsparged-B	647970

C.2 METHOD DETECTION LIMIT FOR THE DIRECT INJECTION PROCEDURE

The direct injection procedure method detection limit (MDL) was calculated by injecting 10 replicates of 10 µg/L of bromate in a mixture of OFDW water with a TOC concentration of 2.5 mg/L and 8 replicates of 10 µg/L of bromate in OFDW water only.

The peak areas and the equivalent bromate concentration for the replicates are listed in Tables C.2 and C.3.

TABLE C.2 METHOD DETECTION LIMIT RESULTS FOR DIRECT INJECTION PROCEDURE (OFDW ONLY)

Sample	Peak Area	Bromate Concentration (µg/L)
10 µg/L-A	124744	11.57
10 µg/L-B	130108	11.91
10 µg/L-C	117600	11.11
10 µg/L-D	100050	10.00
10 µg/L-E	132324	12.05
10 µg/L-F	110540	10.67
10 µg/L-G	110816	10.68
10 µg/L-H	113920	10.88

TABLE C.3 METHOD DETECTION LIMIT RESULTS FOR DIRECT INJECTION PROCEDURE (TOC MIXTURE)

Sample	Peak Area	Bromate Concentration (µg/L)
10 µg/L-A	180776	11.99
10 µg/L-B	98692	6.83
10 µg/L-C	126722	8.59
10 µg/L-D	185036	12.26
10 µg/L-E	97892	6.78
10 µg/L-F	114744	7.84
10 µg/L-G	106107	7.30
10 µg/L-H	123676	8.40
10 µg/L-I	118637	8.08
10 µg/L-J	157400	10.52

The following equation from the Environmental Protection Agency's DBP/ICR (Preliminary) Analytical Methods Manual (1995) was applied to obtain the MDL:

$$MDL = t \times s \qquad \text{Eqn.C.1}$$

where t = student t value for n-1 degrees of freedom (n = number of replicates) at the 99% confidence level; $t_{n=10}$=2.821; $t_{n=8}$=2.998.

s = standard deviation of the replicates.

The direct injection MDL was determined to be 2.08 µg/L in the OFDW water only matrix and 5.81 µg/L in the TOC and OFDW water matrix. All calibration curves for the direct injection procedure were prepared with 10 µg/L as the lowest calibration standard.

To ensure that the use of calibration standards made in OFDW were appropriate to use in obtaining bromate concentrations from the synthetic water samples, samples obtained for bromate analysis were also spiked with known concentrations of bromate. Table C.4 provides some examples of the spike recoveries found in this research. All spike recoveries in this research primarily ranged between 80% and 120%.

TABLE C.4 BROMATE SPIKE RECOVERIES FOR DIRECT INJECTION IC PROCEDURE

Sample	Sample Conc. (µg/L)	Target Spike Conc. (µg/L)	Spike + Sample Conc. (µg/L)	% Recovery
1	2.4	50	45.9	88
2	2.6	50	51.8	98
3	14.4	50	63.9	99
4	23.2	50	72.6	99
5	24.9	50	81.9	114
6	21.0	50	78.3	115
7	23.2	50	74.9	103
8	13.5	50	52.1	78
9	13.3	50	50.5	75
10	<0.2	50	49.1	99
11	<0.2	50	50.2	100
12	17.9	50	58.9	82
13	0.84	50	45.2	89
14	18.2	50	69.2	102
15	21.1	50	65.5	89
16	18.6	50	66.4	96
17	17.4	50	55.7	77

C.3 Preparation of Calibration Standards

As stated in Chapter 3, each sample was manually filtered through a 0.45 µm filter cartridge and two AgCl cartridges in series before analysis on the IC. Because the calibration standards were prepared in OFDW water only, the standards did not contain any impurities which would require any pre-treatment before analysis. A calibration curve was prepared with standards that were pre-treated with a filter and AgCl cartridges; the pre-treatment did not affect the bromate concentration or bromate detection, as shown in Table C.5. Therefore, the calibration standards were prepared without passing them through a 0.45 µm filter or AgCl cartridges before analysis on the IC.

Table C.5 Effect of Pre-Treatment on Calibration Standards for IC Analysis

Sample	With Pre-Treatment	Without Pre-Treatment
	Peak Area	Peak Area
10 µg/L	115340	142044
15 µg/L	202864	198760
25 µg/L	391732	324180
50 µg/L	720968	667772
100 µg/L	1588152	1608136
150 µg/L	2295926	2383858
200 µg/L	3111428	3115858
250 µg/L	3765928	3758694

APPENDIX D

DATA

Below is a complete set of the results from this research. A few sample calculations are provided for clarification. Unless noted, the gas and liquid flowrates are 395 mL/min and 50 mL/min, respectively. The results for the hydrogen peroxide addition are located in Chapter 4.

CONDITIONS: pH=7.0, 2.5 mg/L as C, 300 µg/L Br^-, 1 mM Carbonate

Transferred Ozone Dose (mg/L)	Cg,in (mg/L)	Cg,out (mg/L)	P_{O3} (atm)	Transfer Efficiency (%)	Ozone Residual (mg/L)	Bromate (µg/L)
0.76	0.62	0.53	0.0003	14.52	0.02	0.83
1.42	1.20	1.02	0.0006	15.00	0.08	2.96
1.61	0.65	0.45	0.0003	30.77	0.04	0.22
2.28	1.24	0.95	0.0006	23.39	0.08	22.34
2.62	1.29	0.96	0.0006	25.58	0.12	4.75
2.59	2.01	1.68	0.0009	16.42	0.20	19.40
2.91	2.74	2.37	0.0013	13.50	0.30	11.20
3.11	1.99	1.61	0.0009	19.10	0.37	22.21
3.27	2.96	2.55	0.0014	13.85	0.38	49.85
3.60	3.69	3.24	0.0017	12.20	0.56	56.16
4.31	4.90	4.35	0.0023	11.22	0.83	85.47

The partial pressure of ozone was calculated in the following way:

$$P_{O_3}\,(\text{atm}) = \left(C_{g,in} \times 22.4\ \text{L} \times \left(\frac{1\text{mole}}{48000\ \text{mg}}\right)\right) \times 1\ \text{atm} \qquad \text{Eqn.D.1}$$

The transfer efficiency was calculated in the following manner:

$$\text{Transfer Efficiency} = \left(\frac{C_{g,in} - C_{g,out}}{C_{g,in}}\right) \times 100\% \qquad \text{Eqn.D.2}$$

CONDITIONS: pH=6.0, 2.5 mg/L as C, 300 µg/L Br^-, 1 mM Carbonate

Transferred Ozone Dose (mg/L)	Cg,in (mg/L)	Cg,out (mg/L)	P_{O3} (atm)	Transfer Efficiency (%)	Ozone Residual (mg/L)	Bromate (µg/L)
1.67	0.71	0.50	0.0002	29.58	0.06	0.31
1.92	1.38	1.14	0.0005	17.39	0.12	6.43
1.98	1.13	0.87	0.0004	23.01	0.13	5.91
1.98	1.23	0.98	0.0005	20.33	0.13	7.64
2.38	2.10	1.79	0.0008	14.76	0.28	16.23
3.03	3.17	2.78	0.0013	12.30	0.44	17.14
3.41	3.85	3.42	0.0016	11.17	0.56	18.51
3.74	4.30	3.82	0.0018	11.16	0.79	20.61
4.35	6.22	5.67	0.0026	8.84	1.08	24.31

CONDITIONS: pH=6.5, 2.5 mg/L as C, 300 µg/L Br^-, 1 mM Carbonate

Transferred Ozone Dose (mg/L)	Cg,in (mg/L)	Cg,out (mg/L)	P_{O3} (atm)	Transfer Efficiency (%)	Ozone Residual (mg/L)	Bromate (µg/L)
1.76	0.92	0.70	0.0003	23.91	0.04	0.38
2.59	1.34	1.01	0.0005	24.63	0.19	3.29
2.62	1.42	1.09	0.0005	23.24	0.20	4.07
2.78	2.09	1.74	0.0008	16.75	0.24	12.53
3.12	2.51	2.12	0.0010	15.54	0.46	12.87
3.26	2.86	2.45	0.0011	14.34	0.50	16.03
3.45	4.50	4.07	0.0019	9.56	0.60	45.98
3.73	5.36	4.89	0.0023	8.77	0.71	50.85

CONDITIONS: pH=7.5, 2.5 mg/L as C, 300 µg/L Br^-, 1 mM Carbonate

Transferred Ozone Dose (mg/L)	Cg,in (mg/L)	Cg,out (mg/L)	P_{O3} (atm)	Transfer Efficiency (%)	Ozone Residual (mg/L)	Bromate (µg/L)
1.83	0.82	0.59	0.0003	28.05	0.08	2.64
2.61	1.94	1.61	0.0008	17.01	0.24	17.89
2.95	2.41	2.04	0.0010	15.35	0.27	37.98
3.67	3.37	2.91	0.0014	13.65	0.40	83.98
3.85	3.49	3.00	0.0014	14.04	0.47	61.99
4.55	4.62	4.05	0.0019	12.34	0.55	114.37
5.05	5.13	4.49	0.0021	12.48	0.85	117.54

CONDITIONS: pH=8.3, 2.5 mg/L as C, 300 µg/L Br^-, 1 mM Carbonate

Transferred Ozone Dose (mg/L)	Cg,in (mg/L)	Cg,out (mg/L)	P_{O3} (atm)	Transfer Efficiency (%)	Ozone Residual (mg/L)	Bromate (µg/L)
1.16	0.75	0.60	0.0003	20.00	0.04	1.09
2.61	1.41	1.08	0.0005	23.40	0.03	7.50
2.72	1.86	1.52	0.0007	18.28	0.12	32.82
3.90	2.94	2.47	0.0012	15.99	0.24	40.21
3.91	2.34	1.85	0.0009	20.94	0.14	43.77
4.17	2.63	2.10	0.0010	20.15	0.18	60.60
4.72	2.55	1.95	0.0009	23.53	0.23	91.60
6.08	5.47	4.70	0.0022	14.08	0.68	226.32

CONDITIONS: pH=7.0, 2.5 mg/L as C, 50 µg/L Br^-, 1 mM Carbonate

Transferred Ozone Dose (mg/L)	Cg,in (mg/L)	Cg,out (mg/L)	P_{O3} (atm)	Transfer Efficiency (%)	Ozone Residual (mg/L)	Bromate (µg/L)
1.83	1.30	1.07	0.0006	17.94	0.09	<0.20
2.12	1.29	1.02	0.0006	20.93	0.12	0.46
2.31	2.18	1.88	0.0010	13.76	0.21	3.05
2.76	1.85	1.50	0.0009	18.92	0.24	1.92
3.03	2.69	2.30	0.0013	14.50	0.40	5.78
3.26	3.23	2.78	0.0015	13.93	0.47	6.11

CONDITIONS: pH=7.0, 2.5 mg/L as C, 100 µg/L Br^-, 1 mM Carbonate

Transferred Ozone Dose (mg/L)	Cg,in (mg/L)	Cg,out (mg/L)	P_{O3} (atm)	Transfer Efficiency (%)	Ozone Residual (mg/L)	Bromate (µg/L)
1.64	0.99	0.78	0.0005	21.21	0.11	0.81
2.43	1.34	1.04	0.0006	22.39	0.16	2.10
2.46	1.68	1.37	0.0008	18.45	0.21	3.30
3.10	1.98	1.59	0.0009	19.70	0.29	6.67
3.45	3.02	2.59	0.0014	14.24	0.54	7.63
3.66	3.40	2.94	0.0016	13.53	0.54	11.06

CONDITIONS: pH=7.0, 2.5 mg/L as C, 500 µg/L Br^-, 1 mM Carbonate

Transferred Ozone Dose (mg/L)	Cg,in (mg/L)	Cg,out (mg/L)	P_{O3} (atm)	Transfer Efficiency (%)	Ozone Residual (mg/L)	Bromate (µg/L)
2.15	0.95	0.68	0.0004	28.42	0.12	5.02
2.56	1.39	1.06	0.0006	23.74	0.16	10.31
2.48	1.88	1.57	0.0009	16.49	0.22	21.51
3.03	2.22	1.84	0.0010	17.12	0.36	26.79
3.51	2.57	2.12	0.0012	17.51	0.43	29.19
3.67	2.89	2.43	0.0013	15.92	0.53	51.04

CONDITIONS: pH=7.0, 0.0 mg/L as C, 300 µg/L Br^-, 1 mM Carbonate

Transferred Ozone Dose (mg/L)	Cg,in (mg/L)	Cg,out (mg/L)	P_{O3} (atm)	Transfer Efficiency (%)	Ozone Residual (mg/L)	Bromate (µg/L)
0.63	1.45	1.37	0.0006	5.52	0.29	19.85
0.82	1.78	1.67	0.0009	6.54	0.34	24.70
1.14	2.14	2.00	0.0009	6.54	0.45	37.27
1.43	2.40	2.22	0.0010	7.50	0.48	43.43
1.58	2.73	2.56	0.0012	6.23	0.54	74.14
1.84	4.02	3.78	0.0018	5.97	0.63	124.79

CONDITIONS: pH=7.0, 5.0 mg/L as C, 300 µg/L Br^-, 1 mM Carbonate

Transferred Ozone Dose (mg/L)	Cg,in (mg/L)	Cg,out (mg/L)	P_{O3} (atm)	Transfer Efficiency (%)	Ozone Residual (mg/L)	Bromate (µg/L)
4.55	1.53	0.95	0.0004	37.91	0.02	0.78
4.89	2.43	1.81	0.0008	25.51	0.10	0.84
5.15	3.39	2.74	0.0013	19.17	0.16	13.62
6.95	6.03	5.15	0.0024	14.59	0.51	46.81
7.49	7.70	6.75	0.0032	12.34	0.64	61.34
8.21	9.62	8.58	0.0040	10.81	0.89	97.11

CONDITIONS: pH=7.0, 2.5 mg/L as C, 300 µg/L Br^-, 0 mM Carbonate

Transferred Ozone Dose (mg/L)	Cg,in (mg/L)	Cg,out (mg/L)	P_{O3} (atm)	Transfer Efficiency (%)	Ozone Residual (mg/L)	Bromate (µg/L)
2.34	0.77	0.47	0.0004	38.96	0.04	0.21
3.34	1.57	1.14	0.0007	27.39	0.24	2.14
3.35	1.79	1.37	0.0008	23.46	0.26	2.56
3.48	2.61	2.17	0.0012	16.86	0.31	3.63
3.68	3.16	2.69	0.0015	14.87	0.36	6.55
3.60	2.90	2.49	0.0014	14.14	0.37	8.99
4.90	4.99	4.37	0.0023	12.42	0.55	17.42
5.25	6.60	6.02	0.0031	8.79	0.74	22.12

CONDITIONS: pH=7.0, 2.5 mg/L as C, 300 µg/L Br^-, 2 mM Carbonate

Transferred Ozone Dose (mg/L)	Cg,in (mg/L)	Cg,out (mg/L)	P_{O3} (atm)	Transfer Efficiency (%)	Ozone Residual (mg/L)	Bromate (µg/L)
1.90	1.07	0.83	0.0009	22.43	0.06	1.72
2.27	1.46	1.17	0.0010	19.86	0.21	17.27
2.40	1.69	1.38	0.0010	18.34	0.22	16.58
2.66	2.20	1.86	0.0011	15.45	0.26	29.62
2.94	2.78	2.42	0.0012	12.95	0.36	29.02
3.29	2.99	2.58	0.0013	13.71	0.41	40.61
3.73	4.41	3.94	0.0015	10.66	0.57	65.88
4.49	5.91	5.34	0.0017	9.64	0.81	123.13

CONDITIONS: pH=7.0, 2.5 mg/L as C, 300 µg/L Br^-, 1 mM Carbonate + t-Butanol (5:1)

Transferred Ozone Dose (mg/L)	Cg,in (mg/L)	Cg,out (mg/L)	P_{O3} (atm)	Transfer Efficiency (%)	Ozone Residual (mg/L)	Bromate (µg/L)
1.99	1.15	0.90	0.0005	21.74	0.13	<0.20
2.19	1.30	1.02	0.0006	21.54	0.28	<0.20
2.46	1.90	1.59	0.0009	16.32	0.47	<0.20
3.06	2.62	2.23	0.0012	14.89	0.47	<0.20
3.47	2.86	2.42	0.0013	15.38	0.65	<0.20
3.66	3.89	3.42	0.0018	12.08	0.72	0.43

CONDITIONS: pH=7.0, 2.5 mg/L as C, 300 µg/L Br^-, 1 mM Carbonate, Q_g=100 mL/min

Transferred Ozone Dose (mg/L)	Cg,in (mg/L)	Cg,out (mg/L)	P_{O3} (atm)	Transfer Efficiency (%)	Ozone Residual (mg/L)	Bromate (µg/L)
1.06	2.05	1.52	0.0010	25.85	0.43	12.62
1.63	2.97	2.15	0.0014	27.61	0.49	23.58
2.01	3.79	2.79	0.0018	26.39	0.61	26.33
2.00	3.60	2.58	0.0017	28.33	0.70	27.88
2.24	4.83	3.65	0.0023	24.43	0.82	43.96
2.53	4.10	2.86	0.0019	30.24	0.87	50.47
3.04	5.82	4.30	0.0027	26.12	1.24	57.81

CONDITIONS: pH=7.0, 2.5 mg/L as C, 300 µg/L Br^-, 1 mM Carbonate, Q_L=25 mL/min

Transferred Ozone Dose (mg/L)	Cg,in (mg/L)	Cg,out (mg/L)	P_{O3} (atm)	Transfer Efficiency (%)	Ozone Residual (mg/L)	Bromate (µg/L)
2.78	1.28	1.10	0.0006	14.06	0.18	17.63
3.42	1.66	1.44	0.0008	13.25	0.25	21.47
3.92	2.08	1.91	0.0010	8.17	0.32	33.63
4.30	2.55	2.28	0.0012	10.59	0.45	63.00
4.61	3.11	2.82	0.0015	9.32	0.53	72.45
5.31	5.25	4.91	0.0025	6.48	0.80	124.81

CONDITIONS: pH=7.0, 2.5 mg/L as C, 300 µg/L Br^-, 1 mM Carbonate, Q_L=150 mL/min

Transferred Ozone Dose (mg/L)	Cg,in (mg/L)	Cg,out (mg/L)	P_{O3} (atm)	Transfer Efficiency (%)	Ozone Residual (mg/L)	Bromate (µg/L)
0.96	0.90	0.54	0.0004	40.00	0.02	<0.20
1.55	1.49	0.90	0.0007	39.60	0.01	<0.20
1.32	1.58	1.08	0.0007	31.65	0.02	<0.20
1.64	2.20	1.57	0.0010	28.64	0.08	1.71
1.64	2.33	1.71	0.0011	26.61	0.04	1.01
2.17	2.94	2.12	0.0014	27.89	0.18	5.92
2.55	4.63	3.66	0.0022	20.95	0.45	14.50
2.84	6.34	5.26	0.0030	17.03	0.66	24.03
3.33	8.69	7.42	0.0041	14.61	0.92	37.42

CONDITIONS: pH=7.0, 2.5 mg/L as C, 300 µg/L Br^-, 1 mM Carbonate, Q_L=250 mL/min

Transferred Ozone Dose (mg/L)	Cg,in (mg/L)	Cg,out (mg/L)	P_{O3} (atm)	Transfer Efficiency (%)	Ozone Residual (mg/L)	Bromate (µg/L)
0.86	1.27	0.73	0.0006	42.52	0.01	<0.20
1.16	2.90	2.17	0.0014	25.17	0.03	0.47
2.05	5.34	4.04	0.0025	24.34	0.30	6.47
2.58	6.93	5.30	0.0032	23.52	0.48	16.72
2.72	9.34	7.15	0.0044	23.45	0.60	25.22
2.84	9.74	7.94	0.0045	18.48	0.79	8.25

CONDITIONS: pH=7.0, 2.5 mg/L as C, 300 µg/L Br^-, 1 mM Carbonate + Ammonia (1:1)

Transferred Ozone Dose (mg/L)	Cg,in (mg/L)	Cg,out (mg/L)	P_{O3} (atm)	Transfer Efficiency (%)	Ozone Residual (mg/L)	Bromate (µg/L)
2.21	1.82	1.54	0.0007	15.38	0.14	7.89
2.31	2.20	1.83	0.0009	16.82	0.18	19.45
2.91	3.04	2.67	0.0012	12.17	0.39	30.75
3.23	3.61	3.20	0.0015	11.36	0.46	43.31
3.64	4.39	3.93	0.0018	10.48	0.55	54.55
3.79	5.3	4.82	0.0022	9.06	0.62	95.99

CONDITIONS: pH=8.3, 2.5 mg/L as C, 300 µg/L Br^-, 1 mM Carbonate + Ammonia (1:1)

Transferred Ozone Dose (mg/L)	Cg,in (mg/L)	Cg,out (mg/L)	P_{O3} (atm)	Transfer Efficiency (%)	Ozone Residual (mg/L)	Bromate (µg/L)
1.07	1.46	1.32	0.0006	9.59	0.08	5.74
1.52	1.78	1.52	0.0007	14.61	0.24	13.52
2.06	2.47	2.21	0.0010	10.53	0.35	22.97
2.65	2.85	2.51	0.0012	11.93	0.40	28.54
3.26	3.46	3.05	0.0014	11.85	0.46	32.11
4.62	4.46	3.88	0.0018	13.00	0.57	51.89

CONDITIONS: pH=6.0, 2.5 mg/L as C, 300 µg/L Br^-, 1 mM Carbonate--Batch Decay

Sample 1:		
Time (min)	**Ozone Residual (mg/L)**	**Bromate (µg/L)**
0	0.411	11.08
10	0.024	11.21
20	0.015	11.90
30	0.009	-
47	0.003	-
Sample 2:		
Time (min)	**Ozone Residual (mg/L)**	**Bromate (µg/L)**
0	0.410	13.20
10	0.009	13.60
20	0.006	13.90
30	0.003	-
40	0.000	-

- Did not measure bromate

APPENDIX E

CALCULATIONS FOR STATISTICAL ANALYSIS

As stated in the text and shown in the figures, several of the data sets appeared to overlap with one another. Therefore, a statistical analysis of coincidence was done at the α=0.05 level to test for coincident lines, or lines with equal slopes and equal intercepts. The two straight lines were compared using one single regression equation. First, because the results were illustrated in an exponential form, the ozone residuals and bromate concentrations were transformed into their natural log form where the equation of the line then changed to:

$$\mathrm{Ln}(Y) = \mathrm{Ln}(a) + bX \qquad \text{Eqn.E.1}$$

where the values of Y are either the effluent ozone residual or the bromate concentration and X represents the ozone dose. The two models that were being compared were put into the following forms:

$$Y = \beta_0 + \beta_1 X + \beta_2 Z + \beta_3 XZ + E \qquad \text{Eqn.E.2}$$

and

$$Y = \beta_0 + \beta_1 X + E \qquad \text{Eqn.E.3}$$

where if the hypothesis H_o:β_2=β_3=0 is true then the first model reduces to the second model and then the two lines are coincident. Then a multiple-partial F test was utilized because of the subset of regression coefficients. The equation for the F-test is:

$$F(XZ, Z|X) = \frac{\left[\text{regression SS } (X, Z, XZ) - \text{regression SS } (X)\right] / 2}{\text{MS residual } (X, Z, XZ)} \qquad \text{Eqn.E.4}$$

where in this case X = Ln (ozone residual or bromate concentration)

Z = 0 or 1 dummy variable

XZ = product of two terms to show interaction and the significance of its addition

Then ANOVA (Analysis of Variance) results from Excel's regression analysis were used to complete the F-tests with the following results, as shown in Table E.1, for the listed pairs of results examined.

TABLE E.1 F-STATISTICS FOR TEST OF COINCIDENCE

Ozone Residual		
Pair	**Calculated F-Statistic**	**F-Statistic at α=0.05 level**
pH 6.0 and 6.5	5.13	3.68
pH 6.0 and 8.3	1.15	3.81
pH 6.5 and 7.0	1.88	3.68
pH 7.0 and 7.5	5.74	3.74
50 and 100 µg/L Br^-	2.12	4.46
300 and 500 µg/L Br^-	0.51	3.81
Ql=150 and 250 mL/min	1.19	3.98
1.0 and 2.0 mM Carbonate	0.57	3.68
0.0 and 2.0 mM Carbonate	7.14	3.89
With/Without t-Butanol	13.0	2.13
With/Without Ammonia at pH=7.0	1.62	3.81
Bromate		
Pair	**Calculated F-Statistic**	**F-Statistic at α=0.05 level**
pH 6.0 and 6.5	0.45	3.68
pH 6.0 and 8.3	1.35	3.81
pH 6.5 and 7.0	1.92	3.68
pH 7.0 and 7.5	1.30	3.74
50 and 100 µg/L Br^-	6.28	4.46
300 and 500 µg/L Br^-	0.19	3.81
100 and 300 µg/L Br^-	4.44	3.81
Ql=150 and 250 mL/min	2.29	3.98
1.0 and 2.0 mM Carbonate	0.29	3.68
0.0 and 2.0 mM Carbonate	24.7	3.89
With/Without Ammonia at pH=7.0	0.65	3.81

Most of the pairs examined for both the bromate concentrations and ozone residuals were found to be less than the F-statistic at the α=0.05 level. Thus, the results within each pair show a strong coincidence (Kleinbaum et al., 1978).